NASA-CR-176234
19860001110

A Reproduced Copy

OF

N86-10577

Reproduced for NASA

by the

NASA Scientific and Technical Information Facility

OLD DOMINION UNIVERSITY RESEARCH FOUNDATION

DEPARTMENT OF CIVIL ENGINEERING
SCHOOL OF ENGINEERING
OLD DOMINION UNIVERSITY
NORFOLK, VIRGINIA

PASSIVE DAMPING CONCEPTS FOR SLENDER COLUMNS IN SPACE STRUCTURES

By

Zia Razzaq, Principal Investigator

and

Rajendra K. Ekhelikar, Graduate Research Assistant

Progress Report
For the period February 1, 1985 to July 1, 1985

Prepared for the
National Aeronautics and Space Administration
Langley Research Center
Hampton, Virginia 23665

Under
Research Grant NAG-1-336
Harold G. Bush, Technical Monitor
SDD-Structural Concepts Branch

May 1985

N86-10577#

DEPARTMENT OF CIVIL ENGINEERING
SCHOOL OF ENGINEERING
OLD DOMINION UNIVERSITY
NORFOLK, VIRGINIA

PASSIVE DAMPING CONCEPTS FOR SLENDER COLUMNS IN SPACE STRUCTURES

By

Zia Razzaq, Principal Investigator

and

Rajendra K. Ekhelikar, Graduate Research Assistant

Progress Report
For the period February 1, 1985 to July 1, 1985

Prepared for the
National Aeronautics and Space Administration
Langley Research Center
Hampton, Virginia 23665

Under
Research Grant NAG-1-336
Harold G. Bush, Technical Monitor
SDD-Structural Concepts Branch

Submitted by the
Old Dominion University Research Foundation
P.O. Box 6369
Norfolk, Virginia 23508

May 1985

ACKNOWLEDGEMENT

The support, encouragement, and thought-provoking ideas of Mr. Harold G. Bush and Dr. Martin M. Mikulas, Jr. of SDD-Structural Concepts Branch, NASA Langley Research Center are sincerely appreciated.

Thanks are also due to Mr. Robert Miserentino and his technical staff, especially to Mr. Al Insley for the help in setting up the instrumentation for the vibration apparatus.

PASSIVE DAMPING CONCEPTS FOR SLENDER COLUMNS IN SPACE STRUCTURES

By

Zia Razzaq[1] and Rajendra K. Ekhelikar[2]

ABSTRACT

An experimental and theoretical study of three different passive damping concepts is conducted for a slender member with partial rotational end restraints. Over a hundred full-scale natural vibration experiments were conducted to evaluate the effectiveness of mass-string, polyethylene tubing, and chain damping concepts. The damping properties obtained from the experiments were used in the approximate analyses based on the partial differential equation of motion for the problem. The comparison of the experimental and the theoretical deflection-time relations shows that the velocity-dependent damping model used in the theory is adequate. From the experimental results, the effect of end connection friction and induced axial forces on damping is identified. The definition of an efficiency index is proposed based on the damping ratio and the mass of a given passive damping device. Using this definition, the efficiencies of the three damping devices are compared. The polethylene tubing concept resulted into a low damping efficiency. Although the chain damping concept provides a significant amount of damping and a rapid decay of member vibration, its mass-based efficiency inuex is much lower than that of the string-mass concept.

[1]Associate Professor, Department of Civil Engineering, Old Dominion University, Norfolk, Virginia 23508.

[2]Graduate Research Assistant, Department of Civil Engineering, Old Dominion University, Norfolk, Virginia 23508.

TABLE OF CONTENTS

TABLE OF CONTENTS - Continued

LIST OF TABLES

LIST OF FIGURES

LIST OF FIGURES - Continued

LIST OF FIGURES - Continued

LIST OF FIGURES - Continued

1. INTRODUCTION

1.1 Preliminary Remarks

Members with large slenderness may be used to form large space structures for use in NASA's related space missions. Tubular members with slenderness ratios of the order of a thousand may be needed due to the optimization constraints imposed by efficient packaging and deployment requirements. A desirable feature of the overall response of a space frame would be its ability to transfer the global energy very rapidly, due to an imposed perturbation, to the individual members which may then dissipate the energy locally. If this can be achieved, the individual members may be expected to act as possible "energy sinks" for the system. Thus, a fundamental problem which one is faced with is that of the identification of potential damping concepts which may be used to absorb passively all or a large portion of the member energy.

Two types of damping approaches are used currently by engineers for absorbing vibration of energy in various kinds of structures (4). These are classified as "active" or "passive" damping systems. A damping system is active if there is an external energy supply to reduce to an admissible level the vibration characteristics at chosen points of a structure, within a given band of frequency or an interval of time for a predicted class of excitation. Active systems can generate local forces, which are related to distant motion variables or external command signals. Passive systems can dissipate energy, or temporarily store it and then return it. Passive damping elements generate active or dissipating forces, which are related to local motion variables.

Active damping systems are used where the operating conditions vary so widely that variations in the strategy of control are frequently called for.

Among the advantages of passive damping systems are their simplicity, contained weight, low cost, and high reliability.

This research report presents the outcome of an experimental investigation of three different passive damping concepts for a slender member with partial rotational end restraints. Theoretical results based on approximate analyses are also presented and compared to those obtained experimentally. Partial restraints are used since a member in a real space structure seldom possesses pinned end or fixed end conditions. The end connections and the adjoining members in a space structure provide partial rotational restraints.

1.2 Literature Review

A review of the existing literature indicates that a rather limited amount of research has been conducted in the past on passive damping of slender members.

Reference 7 describes how a support structure for antennas and solar panels can also be used for damping mechanical vibrations. Figure 1(a) shows the damping support consisting of two thin-walled aluminum tubes, one of which can slide within the other under vibration loads. Silicone grease was used as the vibration-damping medium in between the two tubes. Figure 1(b) shows a coil spring attached to the outer tube to transmit the static loads imposed on the structure. Under vibration, the coil moves with the outer tube thereby employing viscous drag of the silicone grease to effect damping.

Razzaq, Voland, Rush, and Mikulus (1) presented an experimental and theoretical study of the natural vibration of a passively damped uniform slender tubular member with partial rotational end restraints as shown in

Figure 2. A damping concept consisting of a string-mass assembly was explored in a few tests, in addition to the structural damping present in the member. Lead shots were used as masses. Tests were conducted with no lead shots; with one or three lead shots at member midheight; and with three equidistant lead shots. Lateral vibration tests were conducted in the absence of any externally applied axial load. The three-lead configurations both provided considerably greater damping than the single lead shot damper.

In the experiments reported in Reference 1, the effect of end connection friction was not quantified. Also, there was some axial compression of unknown magnitude as indicated by the experimental frequencies (average = .42 Hz) which were generally somewhat lower than the expected theoretical frequencies (average = 3.58 Hz). Due to these factors, and possibly the attendant three-dimensional effects, the reported damping ratios were higher than those found in the present investigation.

In Reference 2 there is a brief outline of the outcome of viscoelastic passive damping tests conducted on skeletal space structures. Two huge trusses were erected on the ground for vibration testing. Figure 3 shows a 60 ft. high truss subjected to 1 Hz vibration. Aluminum tubing is being used as horizontal members of the test structures. The diagonals of one are constructed of plexiglass and the other of Lexan. Damping Modules on the diagonals contain viscoelastic material for passive application and result in an increase of 3.8% to 6% damping. Extensive studies have been conducted in the past on the application of viscoelastic damping materials for plate and shell-like structures (6).

In this research report, a study of three different passive damping concepts for slender tubular members is presented.

1.3 Problem Statement

Figure 2 shows schematically a slender member of length L with a hollow circular cross section. The outer diameter of the section is D_0, the wall thickness is t_0, and the material of the member is mild steel. The steel member is used since very slender graphite composite tubes which may be used in space structures are not yet available. The member ends are provided with connections which possess partial rotational restraint characteristics. No axial or lateral movement of the member ends is permitted.

The problem is to identify potential passive damping concepts to absorb the energy of natural flexural vibration of the member, and to study the comparative effectiveness of each concept. The vibration is induced by plucking and releasing the member at its midheight.

1.4 Objective and Scope

The following are the main objectives of this study.

1. Identification of potential passive damping concpets for slender structural members. Specifically, the following damping concepts are investigated:
   a. Mass-String
   b. Polyethylene Tubing
   c. Chain
2. Evaluate the suitability of theoretical analyses by comparison to the experimental results.
3. Evaluate the damping efficiencies of the various damping devices.

1.5 Assumptions and Conditions

The following assumptions and conditions have been adopted in this study:

1. The deflections are small.
2. The material of the member is linearly elastic.
3. Only planar vibration of the member is considered.
4. Damping force is opposite but proportional to the velocity at any location along the length of the member.
5. The member is tested under 1-g conditions at normal room temperature.
6. The effect of secondary induced forces such as the variable axial tension or compression developed in the member during vibration is considered to be small and, therefore, neglected in the theoretical analysis.

2. THEORETICAL BACKGROUND

2.1 Governing Equations

The differential equation of equilibrium governing natural vibration of a flexural member (Reference 9) can be written as:

$$EI \frac{\partial^4 w}{\partial x^4} + \rho \frac{\partial^2 w}{\partial t^2} + C \frac{\partial w}{\partial t} = 0 \qquad (1)$$

in which

E = Young's modulus of the member material,

I = Moment of inertia of the member section,

ρ = Mass per unit length of the member,

C = Damping coefficient,

w(x,t) = Lateral member displacement.

Equation 1 may be used for the analysis of the member shown in Figure 2 as long as the induced flexural vibrations are small and assuming that the passive damping devices will provide viscous damping. The validity of the latter assumption is investigated using the experimental data and explained in Chapter 3.

The boundary and initial conditions for the problem in Figure 2 are given in Reference 1 and are summarized here:

$$w(o,t) = 0 \qquad (2)$$

$$w(L,t) = 0 \qquad (3)$$

$$EI \frac{\partial^2 w}{\partial x^2}(o,t) = K \frac{\partial w}{\partial x}(o,t) \qquad (4)$$

$$EI \frac{\partial^2 w}{\partial x^2}(L,t) = -K \frac{\partial w}{\partial x}(L,t) \qquad (5)$$

$$\frac{\partial w}{\partial t}(x,o) = 0 \qquad (6)$$

$$w(x,o) = \emptyset\,(K,EI,L,x) \qquad (7)$$

Equation 2 to 5 represent the boundary conditions whereas Equation 6 and 7 are the initial conditions. Equation 7 expresses the condition that at zero time, the member deflected shape is dependent upon K, EI, L, and x.

2.2 Semi-Analytic Solution

Based on the separation of variables approach, the solution to Equation 1 may be expressed as:

$$w(x,t) = W(x)\,T(t) \qquad (8)$$

Substituting this equation into Equation 1 results in the following two ordinary differential equations:

$$\frac{d^4 W}{dx^4} - \lambda W = 0 \qquad (9)$$

$$\frac{d^2 T}{dt^2} + \frac{C}{\rho}\frac{dT}{dt} + \omega^2 T = 0 \qquad (10)$$

in which λ is a parameter to be determined, and ω is the undamped cir-

:ular frequency given by:

$$\omega = \sqrt{\frac{EI\lambda}{\rho}} \tag{11}$$

In Reference 1 the following expression for $W(x)$ is adopted:

$$W(x) = A_1 \left[\sin\frac{\pi x}{L} + \frac{KL}{4\pi EI}\left(1 - \cos\frac{2\pi x}{L}\right)\right] \tag{12}$$

If the mid-height displacement of the member is Δ_0, then Equation 12 gives:

$$A_1 = \frac{\Delta_0}{1 + \frac{KL}{2\pi EI}} \tag{13}$$

Invoking Galerkin's orthogonality criterion, the following expression for λ is obtained (Reference 1):

$$\lambda = \frac{(\pi)^4}{(L)^4}\ \frac{12(\pi EI)^2 + 80EIKL + 12(KL)^2}{12(\pi EI)^2 + 32EIKL + 2.25\ (KL)^2} \tag{14}$$

The critical damping factor is given by (Reference 9):

$$C_c = 2\ \sqrt{EI\rho\lambda} \tag{15}$$

The damping coefficient C in Equation 10 is given by:

$$C = \zeta\, C_c \tag{16}$$

in which ζ, the damping ratio, is obtained using the logarithmic decrement method (5). The closed-form solution of Equation 10 for an underdamped system is (9):

$$T(t) = e^{-ct/2\rho}\,[F_1 \cos \beta t + F_2 \sin \beta t] \tag{17}$$

where F_1 and F_2 are constants of integration and β is given by:

$$\beta = 0.5 \sqrt{4\omega^2 - (c/\rho)^2} \tag{18}$$

Using Equations 6 and 8 one obtains:

$$\frac{dT(0)}{dt} = 0 \tag{19}$$

which gives

$$F_2 = \frac{F_1\, C}{\rho\ \beta} \tag{20}$$

when substituted into Equation 16. From Equations 12, 17 and 20 one obtains:

$$w(x,t) = A_c \left[\sin \frac{\pi x}{L} + \frac{KL}{4\pi EI}\,(1 - \cos \frac{2\pi x}{L})\right] e^{-\frac{Ct}{2\rho}} \left[\cos \beta t + \frac{C}{\rho\beta} \sin \beta t\right] \tag{21}$$

in which A_c is a constant, and is found to be equal to A_1 since the initial deflection at $x = 0.5L$ is Δ_0. Equation 21 can be used for a direct computation of the member lateral deflections as a function of time and the various input parameters.

3.3 Finite-Difference Solution

Using central finite-difference expressions with second order truncation errors (Reference 8), Equation 1 can be written as follows (Reference 1):

$$\frac{EI}{h^4}\left[w(x_{i-2}, t_j) - 4w(x_{i-1}, t_j) + 6w(x_i, t_j) - 4w(x_{i+1}, t_j) + w(x_{i+2}, t_j)\right] + \frac{\rho}{(\Delta t)^2}\left[w(x_i, t_{j+1}) - 2w(x_i, t_j) + w(x_i, t_{j-1})\right] + \frac{C}{\Delta t}\left[w(x_i, t_{j+1}) - w(x_i, t_j)\right] = 0 \qquad (22)$$

The above equation can be abbreviated as follows:

$$\frac{EI}{h^4}\left[w_{i-2,j} - 4w_{i-1,j} + 6w_{i,j} - 4w_{i+1,j} + w_{i+2,j}\right] + \frac{\rho}{(\Delta t)^2}\left[w_{i,j+1} - 2w_{i,j} + w_{i,j-1}\right]$$

$$+ \frac{C}{\Delta t}[w_{i,j+1} - w_{i,j}] = 0 \qquad (23)$$

in which

h = panel length along the x axis of the member,

Δt = small time interval,

x_i = ih for each i = 1,2,3.... M,

t_j = j(Δt) for each j 0,1,2,3,..., j_{max},

m = number of equidistant nodes over [0,1],

j_{max} = maximum desired j values.

Similarly, the boundary conditions 2 to 5 in the difference form becomes:

$$w_{o,j} = 0 \qquad (24)$$

$$w_{m,j} = 0 \qquad (25)$$

$$\frac{EI}{h} + \frac{K}{2} \quad w_{-1,j} + \frac{EI}{h} - \frac{K}{2} \quad w_{1,j} = 0 \qquad (26)$$

$$\frac{EI}{h} + \frac{K}{2} \quad w_{M-1,j} + \frac{EI}{h} + \frac{K}{2} \quad w_{M-1,j} = 0 \qquad (27)$$

Applying Equation 23 at i = 1,2,3 ... (M-1) and invoking Equations 24 to 27 leads to the following matrix equation:

$$\{w_{i,j+1}\} = c_1 [r] \{w_{i,j}\} + c_2 \{w_{i,j-1}\} \qquad (28)$$

in which

$$c_1 = \frac{-1}{b_3 + b_4} \tag{29}$$

$$c_2 = b_3\, c_1 \tag{30}$$

$$b_3 = \frac{\rho}{(\Delta t)^2} \tag{31}$$

$$b_1 = \frac{EI}{h^4} \tag{32}$$

$$b_5 = \frac{\frac{EI}{h} - \frac{K}{2}}{\frac{EI}{h} + \frac{K}{2}} \tag{33}$$

$$b_4 = \frac{C}{\Delta t} \tag{34}$$

where $[\Gamma]$ is the following symmetrical square matrix of order M-1:

$$[\Gamma] = \begin{bmatrix} \gamma_1 & \gamma_2 & \gamma_3 & 0 & 0 & 0 & \cdot & \cdot \\ & \gamma_4 & \gamma_3 & \gamma_3 & 0 & 0 & \cdot & \cdot \\ & & \gamma_4 & \gamma_2 & \gamma_3 & 0 & \cdot & \cdot \\ & & & \cdot & \cdot & \cdot & \cdot & \cdot \\ & & & & \cdot & \cdot & \cdot & \cdot \\ \text{Symmetric} & & & & & \gamma_4 & \gamma_2 & \gamma_3 \\ & & & & & & \gamma_4 & \gamma_2 \\ & & & & & & & \gamma_1 \end{bmatrix} \tag{35}$$

in which

$$\gamma_1 = 6b_1 - 2b_3 - b_4 - b_1 b_5 \tag{36}$$

$$\gamma_2 = 6b_1 - 2b_3 - b_4 \tag{37}$$

$$\gamma_3 = -4b_1 \tag{38}$$

$$\gamma_4 = b_1 \tag{39}$$

Equation 28 can be used to calculate the deflection if $\{w_{i,j+1}\}$ and $\{w_{i-1,j}\}$ are known. To avoid a negative time interval owing to the use of central finite-difference scheme when starting the recursion indicated in this equation, the following special forward start-up difference equation for $w_{i,1}$ is derived in Reference 1:

$$w_{i,1} = b_6\phi_{i-2} - 4b_6\phi_{i-1} + (6b_6 + 1)\,\phi_i - 4b_6\phi_{i+1} + b_6\phi_{i+2} \tag{40}$$

in which

$$b_6 = -\frac{(\Delta t)^2 EI}{2h^4\,\rho}$$

The initial static deflected shape in Equation 7 may be determined using any one of the several classical structural analysis, an approximate deflected shape (Reference 1) for the member due to a midheight displacement Δ_0 at $t=0$ is taken in the following form:

$$w_{i,0} = W(x) \tag{41}$$

$W(x)$ is given by Equation 12.

The following steps summarize the procedure for determining the approximate deflection time response of the member:

1. Define input data: L, K, ρ, E, I, M, ΔT, and j_{max}.
2. Calculate the constants b_1, b_3, b_4, b_5, c_1, c_2, using Equations 29-34; γ_1 to γ_4 using Equations 36-39; and formualte $[\Gamma]$ using Equation 35.
3. Calculate λ using Equation 14.
4. Calculate the critical damping factor C_{cr} using Equation 15, and the damping coefficient C using Equation 16.
5. Set $j = 0$ and $t = 0$.
6. Specify the midspan deflection Δ_0 and generate the initial deflection vector $\{w_{i,0}\}$ using Equation 41.
7. Set $j = 1$, $t = \Delta t$, and calculate $\{w_{i,1}\}$ using Equation 40.
8. Increment j by 1.
9. Set $t = j(\Delta t)$.
10. Calculate $\{w_{i,j}\}$ using Equation 28.
11. If $j < j_{max}$, go to 9.
12. Stop.

In the above procedure, Δt was taken as 0.001 sec. based on a preliminary time-convergence study. Also, dividing the member into 11 equal panels (M=12) was found to be appropriate for the numerical study present-

ed in the following section, as well as, for comparisons to the experimental data given in Chapter 3.

2.4 Numerical Results

For the deflection-time analysis of the member shown in Figure 2, computer programs were written based on the procedures given in Section 2.2 and 2.3, respectively. In this section, a numerical study based on these computer programs is presented with the following input data: $L = 12$ ft.; $D_0 = 0.5$ in.; $t_0 = 0\ 065$ in.; $K = 2{,}230$ lb-in/rad; $\rho = 651 \times 10^{-7}$ lb-sec^2/in^2; $E = 30 \times 10^6$ psi; and $\Delta_0 = 0.366$ in. This data corresponds to the vibration tests described in Chapter 3.

Figure 4 shows deflection-time plots obtained using the semi-analytic and the finite-difference methods with the above mentioned input data and $\zeta = 0.006$. The undamped natural frequency using the finite-difference approach was observed to be 3.53 Hz whereas that obtained from the semi-analytic approach was 3.73 Hz. Table 1 shows a comparison of the deflection-time envelope ordinates obtained from Figure 4 based on the two methods for $t = 1$ to 6 seconds. A comparison of both positive and negative envelope ordinates is made. In this table, Δ_{FD} and Δ_{SA} represent the ordinates of the envelopes based on the finite-difference, and the semi-analytic procedures, respectively. The ratios Δ_{FD}/Δ_{SA} are also given in the table. As evident from the table, the ratio Δ_{FD}/Δ_{SA} increases as time increases. The maximum deviation between the two methods is found to be about 2.50 percent, at $t = 6$ seconds.

Figures 5 and 6 show the envelopes for various values of ζ in the range from 0.0 to 1.0 and obtained by the finite-difference and the semi-analytic procedures, respectively. A comparison of the curves in Figures 5

and 6 shows that the maximum difference between the results of the two methods is of the same order of magnitude as discussed above for Figure 4. In addition, it was observed that this difference diminished gradually with an increase in ζ. Computer Programs and their sample outputs are given in Appendix A.

3. EXPERIMENTAL STUDY

3.1 Specimen and End Fixtures

The experimental study consisted of conducting natural vibration tests on a tubular steel member. The tests were performed both with and without passive damping devices. The member ends were provided with specially designed base plates which in turn were bolted to external fixed supports. The connections between the member ends and the base plates provided partial rotational restraint. The tubular member was 12 ft. long with $D_0 = 0.5$ in, and $t_0 = 0.065$ in.

Figure 2 shows schematically the member tested. The member end connection details are shown in Figure 7. Each end connection was a two piece assembly. One piece was a steel blade 1-1/2 in. long with a 3/16 x 1/2 in. cross section welded to a steel base plate. The outer piece was a steel clevis designed to fit snugly overall but 1/4 in. of the blade and fastened to it by screws fitted through two drilled holes. The exposed 1/4 in. of the blade, thin in one direction (3/16 in.) but thick in the other (1/2 in.) provided partial rotational restraint in one plane of vibration and considerably greater rotational restraint in the orthogonal plane. This design provided the member a preferred direction of vibration, that is, about the weaker axis of the blade. The top end of the clevis was a 1 in. threaded rod which screwed by a distance $S = 5/8$ in. into the specimen. Since the primary purpose of the experimental investigation was to study the effect on ζ of each passive damping device under consideration, the connection friction was reduced considerably by means of a "jam nut" screwed on to the threaded clevis rod and butted against each member end, as shown in Figure 7. The jam nuts were used for all of the tests reported in this section except for an initial set of tests which were conducted for the purpose of

comparison. The upper base plate was bolted to a heavy bracket which in turn was bolted to a backstop, and the lower base plate was bolted to the floor directly beneath the upper one.

3.2 Specimen Initial Imperfection

The tubular member used in the experimental part of this study had an initial imperfection. The member deviation at right angles to the plumb line was measured using a theodolite placed at a distance of 7.2 ft. from the member. Table 2 summarizes the specimen initial imperfections measured at 1 ft. intervals. The second and the third columns in this table present the measured deviation of the member centerline relative to the plumb line in the plane of vibration and in the orthogonal plane. As seen from the deviation at 12 ft. from the top of the member, the member was out-of-plumb by an absolute amount of 0.10 in. in each plane. The fourth and fifth columns of Table 2 represent the actual imperfections in the two planes calculated from the deviation measurements. Figures 11(a) and 11(b) show graphically the data give in Table 2. In these figures, the curved solid lines from A to B represent the actual member centerline. The plumb lines are represented by the chain lines BA' and BA", and the straight dashed lines from A to B are used to define the actual imperfection at 1 ft. intervals. For proper visualization of the spatial imperfection, the probe location is also identified in these figures. The maximum imperfection values in the two planes were found to be 0.070 in. and 0.378 in., respectively. Such small imperfection is not expected to affect the natural frequency of the member.

3.3 Test Procedure and Instrumentation

The end restraint rotational stiffness K about the minor axis was evaluated experimentally for both top and the bottom end connections using the procedure given in Reference 1. Twelve experiments were conducted on each end connection and the moment-rotation relations obtained. Figure 8 shows a typical moment-rotation relationship for the bottom end connection. All such relationships were found to be linear. The average value of K was found to be 2,230 lb-in/rad. Similar tests were conducted to obtain major axis end restraint rotational stiffness. Figure 9 shows a typical major axis moment-rotation relationship for the bottom end connection. The average major axis rotational connection stiffness was found to be 7,280 lb-in/rad. Since the slender member under investigation is vibrated about the major axis, the applicable K value for the results presented later in this research report is 2,230 lb-in/rad.

The instrumentation used in the test consisted of a proximity probe, vibration instrumentation, and a deflection-time curve plotter. Figure 10 shows the proximity probe mounted on a bracket at member midheight in the plane of vibration. To induce natural vibration, the specimen was pulled away from the proximity probe by 0.366 in. with the help of a nylon string and then released by burning the string with a match stick.

The midheight deflection versus time curves were obtained automatically by means of an on-line plotter. Damping ratios were computed from each deflection-time plot using the logarithmic decrement method (9). Each test was repeated three time to obtain a good average value for the damping ratio. The details of the instrumentation and the initial setup are explained in Appendix B.

3.4 String-Mass Damping Concept

In Reference 1, vibration tests were conducted on an imperfect tubular steel member with partial rotational end restraints. A passive damping concept consisting of a string-mass assembly was explored in a few of the tests, in addition to the structural damping present in the system. Lead shots were suspended inside the tubular member by means of a nylon string. In addition to the baseline tests with no lead shots, experiments were conducted with one and three lead shots suspended inside tne member. The tests were conducted without any jam nuts at the member ends. The test results reported in Reference 1, therefore, represented the combined effects of the connection friction, the string-mass dampers, inherent structural damping, and other influences on the indicated damping characteristics of the member. The other influences included the presence of the initial imperfection, small induced axial forces, and three-dimensional movement of the member due to a spiral-like motion emanating from the threaded end connections in the absence of jam nuts. In the experiments reported herein, the installation of jam nuts was seen to result in a considerable reduction of the three-dimensional member movement.

As a part of the present research, the string-mass concept was studied extensively both with and without jam nuts to identify the effects of the connection friction and the number of lead shots on the member damping.

Besides the baseline experiments on the member without any damping devices, tests were conducted with a total of twelve different string-mass configurations shown in Figures 12 and 13. Figures 12(a) through 12(h) show 1, 2, 3, 5, 7, 9, 15 and 21 lead shots suspended inside the member by a nylon string. The lead shots were attached to a nylon string with a 0.2 cm. clear spacing between them. The gap between the lead shots allowed flexible movement of the configurations during vibration. Figures 13(a) through

13(c) show 2, 3, and 21 lead shots suspended equidistantly inside the member with spacings of L/3, L/4, and L/22, respectively. The lead shots were mounted symmetrically about the member midheight and the nylon string did not extend beyond the lower most lead shot. Each lead shot has an average diameter of 0.254 cm. and weighed 0.47 gm. The nylon string weighed 0.01417 gms. per ft. As shown in Figure 14, the nylon string was tied to an internal screw which in turn was screwed into the top threaded clevis rod.

3.4.1 Performance of String-Mass Concept with Lead Shots at Midheight

A series of natural vibration tests were conducted on the member shown in Figure 2 and provided with the string-mass configurations shown in Figure 12 both in the absence and presence of jam nuts. In addition to the baseline natural vibration tests in the absence of passive dampers, the experimental results for the eight string-mass configurations shown in Figure 12 without jam nuts are summarized in Table 3. Each configuration was tested three times to obtain a good average. Tests 1-3, 4-6, 7-9, ... were performed with 0, 1, 2, ... number of lead shots, respectively, as indicated in the first two columns of Table 3. The experimental plots of the midheight deflection, Δ, versus time, t, for Tests 1, 4, 7, 10, 13, 16, 19, 22, and 25 are shown in Figures 15 through 23, respectively. These are representative plots for Tests 1-27. The values of the experimental natural frequency, f_e, and the damping ratio, ζ, as well as their averages for these tests are given in columns 3-6 of Table 3 and were computed using the deflection-time plots. The average f_e values for the various tests ranged from 3.84 to 3.98 Hz. The average ζ values increased substantially with an increase in the number of lead shots and ranged from 0.00243 to 0.00693.

Table 4 summarizes the experimental results for Tests 28-54 in the presence of jam nuts and correspond, respectively, to Tests 1-27 as far as

their string-mass configurations are concerned. Representative Δ-t plots for the tests referred to in Table 4 are given in Figures 24-32. The average f_e values for the various tests ranged from 3.74 to 3.91 Hz. The average ζ values ranged from 0.00103 to 0.00615 with the upper limit corresponding to 21 lead shots.

In the experiments with 21 lead shots, the value of ζ was found to vary slightly with time. This variation diminished as a decreasing number of lead shots was used.

3.4.2 Effect of Connection Friction on Damping Ratios

Figure 33 shows the relationships between the damping ratio, ζ, and the number of lead shots, n, both with and without jam nuts. The two curves shown in this figure are plotted using the data given in the second and the sixth columns of each Tables 3 and 4. The solid curve for the tests with jam nuts and the dashed curve for those without are fairly parallel to each other indicating a nearly constant effect on ζ of the connection friction and other possibly less dominant influences described earlier in this research report. The average constant difference between the ζ values of the two curves is 0.0012. Also, the shape of the ζ-n curves in Figure 33 shows a rapid initial increase in ζ. The rate of increase in ζ decreases gradually with an increase in n.

3.4.3 Performance of String-Mass Concept with Equidistant Lead Shots

In order to study the influence of the location of lead shots on damping, a series of vibration tests were conducted on the member provided with the string-mass configurations with equidistant lead shots in Figure 13. The end connection jam nuts were used in all the tests.

Table 5 summarizes the experimental results for Test 55-63 for 2, 3,

and 21 lead shots spaced equidistantly. Representative Δ-t plots for these tests are given in Figures 34-36. The respective average f_e values were found to be 3.93, 3.89, and 3.98 Hz. The corresponding average ζ values were 0.00228, 0.00258, and 0.00462.

3.4.4 Effect of Location of Lead Shots on Damping Ratio

A comparison of the damping ratios for the 2 and 3 lead shot tests given in Table 4 to those in Table 5 indicate that they are practically the same. This conclusion, however, does not hold for the 21 lead shot tests as evidenced by the significant reduction of ζ from 0.00615 for the midheight location to 0.00462 for the equidistant case. Figure 37 shows a comparison of the corresponding Δ-t plots. From these results, it is concluded that the midheight location for the lead shots provides better passive damping than the lead shots spaced equidistantly.

3.5 Effect of Induced Axial Force on Member Frequency and Damping Ratio

An axial tensile or compressive force can be induced in the member by turning it about the longitudinal axis (x axis in Figure 2) in the clockwise or counterclockwise directions, respectively. A series of member vibration tests were conducted with induced axial forces and in the absence of any damping device. Jam nuts were used in all the tests. Table 6 summarizes the results for Tests 64-75 for four different values of axial force, P. The values of P recorded in this table were not measured experimentally but were determined indirectly by solving Equation 28 of Reference for P in terms of the natural frequency f, and other parameters as follows:

$$P = \frac{1}{\mu_1} (\mu_2 - 4 f^2 L^2 \rho \mu_3) \qquad (42)$$

n which

$$\mu_1 = 12(\pi EI)^2 + 32EIKL + 3(KL)^2 \tag{43}$$

$$\mu_2 = \frac{\pi^2 EI}{L^2}\left[12(\pi EI)^2 + 80\,EIKL + 12(KL)^2\right] \tag{44}$$

$$\mu_3 = 12(\pi EI)^2 + 32\,EIKL + 9/4\,(KL)^2 \tag{45}$$

The undamped natural frequency for each test can be obtained using the following expression (Reference 9):

$$f = \frac{f_e}{1-\zeta^2} \tag{46}$$

The average fe and ζ values given in the last two columns of Table 6 were used to find f through Equation 54. The P values were then computed using Equation 42 and entered in the second column of Table 6. The negative and the positive signs for P in this table are used for tensile and compressive forces, respectively. For Tests 64-66, the member was rotated in a clockwise direction until it could no longer be rotated further manually. The computed P was found to be a tensile force of -155.0 lb. Similarly, other amounts of member rotations resulted in axial forces of -19.8, -4.5, and +10.8 lb., respectively, for Tests 67-69, 70-72, and 73-75, as indicated in Table 6.

As expected the average member frequency f_e increases from 3.83 Hz to

6.64 Hz as the tensile force is increased from -4.5 lb. to -155.0 lb., whereas damping ratio ζ experiences some reduction, as indicated in Table 6. Similarly, the average f_e decreases, attaining a value of 3.42 Hz when an axial compressive force of +10.8 lb. is induced, with a significant increase in ζ, as given in Table 6. The representative Δ-t plots for the tests are given in Figures 38-41.

Tests 70-72 resulting in P = -4.5 lb. deserve special attention. In these tests, the member was adjusted by axial rotations with a view to obtain a zero axial force. This was attempted using an experimental trial and error procedure as follows. When a small axial compressive force was induced, the member appeared slightly bent by visual observations. On the other hand, when a small axial tensile force was induced, the member frequency showed a corresponding slight increase measured from a Δ-t plot. For a "zero" point, that is, for no expected axial force, the approximate position of the member between the compressive and the tensile states was determined by trial and error. The vibration tests were then calculated with the assumption that the axial force would be nearly zero. The computed axial force as presented in Table 6, however, turned out to be -4.5 lb. The presence of this force may be attributed largely to the approximate nature of the trial and error procedure as well as the unavoidable tension induced in the member during vibration since the member ends are not allowed to move axially. From these results, it is concluded that such small amounts of unavoidable axial forces were present in all of the tests conducted in this research.

3.6 Polyethylene Tubing Damping Concept

A series of natural vibration tests were conducted on the member shown in Figure 2 and provided with various types of polyethylene tubing over its entire length. All the tests were conducted with jam nuts. The following three tubing arrangements were inserted in the member:

(a) A low stiffness polyethylene tube with an outer diameter of 0.33 in., a wall thickness of 0.04 in., and weighing 0.0254 lb/ft.

(b) A stiff polyethylene tube with an outer diameter of 0.33 in., a wall thickness of 0.04 in., and weighing 0.0140 lb/ft.

(c) A low stiffness polyethylene tube with an outer diameter of 0.25 in., a wall thickness of 0.04 in., and weighing 0.00875 lb/ft inserted in the stiff polyethylene tube (b) and the resulting assembly inserted into the member.

Table 7 summarizes the experimental results for Tests 76-81 based on the above mentioned polyethylene tubing concepts. The deflection time plots for Tests 76, 79, and 82 are shown in Figures 42-44, respectively. The maximum ζ was found to be 0.0022 for the tubing arrangement (a) and is nearly the same as for Tests 34-36 (Table 4) which were conducted with two lead shots at member midheight. Clearly, the polyethylene tubing concept is far less effective than the string-mass concept in providing passive damping.

3.7 Chain Damping Concept

A "bright zinc chain" was suspended inside the tubular member by a nylon string to absorb the vibration energy through collisions as well as frictional forces between the chain links. Figure 45 shows the photograph of a portion of the chain used for the experiments. The chain weighed 0.05 lb/ft and its major lateral dimension was approximately equal to the inner

diameter of the tubular member. Chains of 1, 2, 3, 5, 7, 9, and 10 ft. lengths were tested. Each chain was situated symmetrically about the member midheight. Natural vibration tests were conducted in the presence of end jam nuts.

Table 8 summarizes the experimental frequencies for Tests 85-105 for chain lengths ranging from 1 to 10 ft. Deflection-time plots for Tests 85, 88, 91, 94, 97, 100, and 103 are given in Figures 46-52, respectively. A noteworthy characteristic of the chain damping approach is that the damping ratio ζ obtained from it increases considerably with time as the chain length is increased, unlike the mass-string or polyethylene tube concepts in which ζ remains constant. Table 9 presents the ζ values for Tests 85-105 at average times of 0 to 6 seconds with one second intervals. The corresponding average ζ values for various chain lengths are given in Table 10. The data given in Table 10 is also shown graphically in Figure 53 indicating the time dependence of ζ in the form of curves relating ζ to the average time, t_a. From this figure, it is clear that ζ increases rapidly both with an increase in the chain length as well as the time of vibration. The best results are obtained for the 10 ft. long chain for which ζ increases almost exponentially with time. The average damping ratio, ζ_{av}, versus the chain length relationship is shown in Figure 54. The ζ_{av} values used in this plot were obtained by taking the averages of ζ values given in Table 10 for the average times from 0 to 6 seconds for each chain length.

4. COMPARISON OF RESULTS AND DAMPING EFFICIENCIES

1 Theory Versus Experiment

Two different theoretical solutions, namely, the semi-analytic and the inite-difference procedures, for predicting the natural vioration response f the member shown in Figure 2 were outlined in Chapter 2. Experimental esults for the string-mass, polyethylene tubing, and chain damping concepts or a total of 105 tests were presented in Chapter 3. In this section, a omparison of the experimental results is made to the theoretical ones for ests 52, 76, and 103 corresponding to the maximum ζ values obtained for he three concepts, respectively, which were conducted in the presence of the jam nuts.

Figures 55-57 show the comparison of the experimental and the semi-analytic deflection-time (Δ-t) plots for Tests 52, 76, and 103, respectively. for the three concepts. The natural frequency from the semi-analytic procedure was found to be 3.73 Hz. Figure 55 shows the Δ-t plots for Test 52 corresponding to 21 lead shots at the member midheight. Two ζ values equal to 0.0085 and 0.00615 obtained from the experimental Δ-t plot for the first, and all of the subsequent cycles, respectively, were fed into the semi-analytic procedure. A higher first ζ value is needed for a proper accommodation of the initial nonlinear part of the Δ-t relationship. The experimental natural frequency was found to be 3.78 Hz. Similarly, Figure 56 for Test 76 shows the comparison of the Δ-t plots for the polyethylene tubing concept (a), with ζ = 0.0096, and 0.00220, respectively, for the first, and all of the subsequent cycles. The experimental natural frequency was found to be 3.96 Hz. Figure 57 for Test 103 shows the comparison of the Δ-t plots for the chain damping concept. The experimental frequency was found to be 4.01 Hz. As mentioned in Chapter 3, the ζ

lues for the chain damping concept varied considerably with time. Thus, ir a proper comparison of the experimental and the theoretical Δ-t plots, ie following variable parabolic ζ expression was developed using the verage ζ values at 0, 3, and 6 seconds, for the 10 ft. chain as given in able 10.

$$\zeta = 0.001289\ t^2 - 0.002270\ t + 0.008570 \qquad (47)$$

Strictly speaking, Equation 21 in Section II is applicable only when the damping coefficient C, related directly to ζ via Equation 16, is a constant. Obviously, Equation 47 leads to a time dependent C expression. However, Equation 21 was used directly with the C expression based on Equation 47 to obtain the theoretical Δ-t curve shown in Figure 57 and was found to be in fairly good agreement with the experimental curve. This may be attributed principally to the fact that the variation in ζ with t is not really drastic at least during the first 3 seconds; it varies from 0.00852 to 0.01320. The subsequent variation in ζ is more rapid, from 0.01320 to 0.04090 in 3 additional seconds, however, it did not also result in to a very significant deviation of the theoretical Δ-t plot relative to the experimental one except in the region of the fairly low-amplitude vibration toward the tail end of the Δ-t relationship.

Figures 58-60 show the comparison of the experimental and the finite-difference Δ-t plots for Tests 52, 76, and 103, respectively, for the three concepts. The natural frequency from the finite-difference procedure was found to be 3.53 Hz. As seen from these figures, the experimental and the finite-difference Δ-t plots are in good agreement. The same ζ values were used for the finite-difference curves as were used in the semi-analytic

ocedure, including Equation 47 for chain damping. It should be pointed it that a time-dependent ζ can readily and accurately be accounted for in ie finite-difference solution owing to its discretized nature relative to

.2 Efficiency of Various Damping Concepts

The main purpose of a passive damping device is to damp out the deflections of a member in minimum possible time. A damping device would be onsidered efficient if it would achieve this goal with a minimum of its own ass. Any kind of a measure of the efficiency of a damping concept, thereore, should involve a damping property and the mass of the passive damping evice. For evaluating the relative merit of the passive damping concepts, he following definition of an "efficiency index" is proposed herein:

$$\eta = \frac{\zeta - \zeta_0}{m_d} \tag{48}$$

In which ζ and m_d are the damping ratio, and the mass of the passive damping device, respectively, and ζ_0 is the damping ratio in the absence of any passive damping device. The subtraction of ζ_0 from ζ eliminates the effect of the inherent structural damping so that only the effect of damping due to the damping device itself is reflected in the efficiency index.

Table 11 presents the computed efficiencies of the various damping concepts considered in this investigation. The test numbers, the details of the damping devices, the weight w_d of the passive damping device, the average z, and the efficiency index η based on Equation 48 are given in

this table. The mass of the passive damping device is computed using the following expression:

$$m_d = \frac{W_d}{g} \tag{49}$$

in which $g = 32.2$ ft/sec^2. The baseline ζ_0 value is taken as 0.00243 as obtained from Tests 1-3 for computing n values for the string-mass concept without jam nuts. For the remaining tests for all three concepts in the presence of jam nuts, ζ_0 is taken as 0.00103 as obtained from Tests 28-30. Also, for the chain damping concept, the average ζ values given in Table 11 represent the average of the average damping ratios over 0-6 seconds range for each chain length given in Table 10.

A glance at the n values in Table 11 shows that it varies from 0.12 for the tubing concepts (a) and (c) to 19.44 for the string-mass concept with two equidistant lead shots. All other efficiency index values for the three concepts lie between these two extremes. For the string-mass concept with lead shots at midheight and without jam nuts, n varies between 6.67 and 17.11, while that with jam nuts varies between 7.59 and 19.28. For equidistant lead shots, $n = 5.31$ to 19.44. For the polyethylene tubing concept, $n = 0.12$ to 0.20. For the chain damping concept $n = 0.56$ to 1.21. Figure 61 shows the experimental relationships between n and the number of lead shots for the string-mass concept, and the chain length for the chain damping concept. The lower horizontal axis of this figure gives the chain length while the upper one defines the number of lead shots, n. The upper two relationships are for the string-mass concept with and without jam nuts. The three data points for the equidistant lead shots are also

shown in this figure. The relationship for the chain damping concept is shown below the string-mass concept curves. As evident from Figure 61, the maximum n value is obtained for two equidistant lead shots. Also, two lead shots give the peak points on each of the n-n relationships both with and without jam nuts. As the number of lead shots is increased beyond two, the n value decreases almost continuously. Although the chain damping A-t relationships show a rapid decay of member vibration (see Figure 60) as compared to, for example, the 21 lead shot case (Figure 58), the mass-dependent definition of the efficiency index used herein makes the chain damping concept appear less attractive. Another interesting point of observation is that the presence of significant end connection friction generally reduces the efficiency index of the string-mass damping concept. This can be seen clearly from Figure 61 in which the n-n relationship for the string-mass concept with jam nuts is generally above that for the one without jam nuts.

5. CONCLUSIONS AND FUTURE RESEARCH

5.1 Conclusions

The following principal conclusions are drawn from this research on a partially restrained slender tubular member subjected to natural vibration:

1. The semi-analytic and the finite-difference solutions are in reasonable agreement with the experimental results.
2. The effect of end connection friction on damping ratio is nearly constant for various masses of the passive damping devices.
3. The presence of an axial compressive force in the member increases the apparent damping ratio while a tensile force decreases it.
4. For the string-mass concept, the damping ratio increases gradually at a decreasing rate as the number of lead shots is increased.
5. Equidistant lead shots result in lower damping ratios as compared to the lead shots at member midheight except for the two lead shot case.
6. The polyethylene tubing concept does not provide any significant damping.
7. For the chain damping concept, the damping ratio increases very rapidly with an increase in the chain length as well as with time.
8. Although the chain damping concept provides a significant amount of damping and a rapid decay of member vibration, its mass-based efficiency index is much lower than that of the string-mass concept.
9. An efficiency index for measuring the damping performance of the various passive damping devices is proposed and shows that the string-mass concept is more efficient than the chain damping and the polyethylene damping concepts.

5.2 Future and On-Going Research

In the present investigation, three different types of passive damping concepts were studied. Other passive damping concepts should be explored with a view to maximize the damping efficiency index as proposed herein. These may include electrostatic damping, suspended chambers with oil and discs, and other hybrid concepts. Experimental work on some of these concepts is in progress.

NOMENCLATURE

c	Damping Coefficient
c_{cr}	Critical damping coefficient
E	Young's modulus
F	Undamped natural frequency
F_e	Damped natural frequency
g	Acceleration due to gravity
h	Panel length along the length of the member
I	Moment of inertia of the member section
K	Rotational stiffness
L	Length of the member
M_d	Mass of the passive damping device
n	Number of lead shots
P	Axial force
t	Time
W_d	Weight of the damping device
w	Lateral member displacement
Δ_{FD}	Deflection ordinate based on the finite-difference procedure
Δ_o	Initial member deflection
Δ_{SA}	Deflection ordinate based on the Semi-analytical procedure.
Δ_t	Small time increment
ζ	Damping ratio
ζ_o	Damping ratio without damping device
η	Efficiency index
ρ	Mass per unit length of the member

REFERENCES

1. Razzaq, Z. Voland, R.T.; Bush, H.G.; and Mikulas, Jr. M.M.: Stability, Vibration, and Passive Damping of Partially Restrained Imperfect Columns. NASA Technical Memorandum 85697, October 1983.

2. Martin Marietta Space test article: Vibration Damping Studied for Weapons. "Aviation Week & Space Technology," A McGraw-Hill Publication, New York, July 2, 1984.

3. Timoshenko, S.P.; and Gere, J.M.: Theory of Elastic Stability. 2nd Edition, McGraw-Hill Book Company, New York, 1961.

4. Muszynska, A.: A Survey of Vibration Control Methods. Article in Man Under Vibration - Suffering and Protection, edited by G. Bianchi, K. V., Frolov, and A. Oledzki, Proceedings of the International CISM-IFTOMM-WHO Symposium, Udine, Italy, April 3-6, 1979, pp. 287-314.

5. Biggs, J.M., Introduction to Structural Dynamics, McGraw Hill Book Co., New York, N.Y., 1964.

6. Damping Control for Design Flexibility, ASME Short Course Program, The American Society of Mechanical Engineers, March 21-24, 1983, Norfolk, Virginia.

7. NASA Tech Brief "Light-Weight Load Support Serve as Vibration Damper." Source: W.E.; Layman, JPL-661, Category No. 05, May 1965.

8. Gerald, C.F.; and Wheatley, P.O.: Applied Numerical Analysis. Third Edition, Addison-Wesley Publishing Company, Sydney, 1970.

9. Craig, Jr., Roy R.: Structural Dynamics, An Introduction to Computer Methods. John Wiley & Sons, New York, 1983.

TABLES

'able 1. Comparison of Deflection-Time Envelope Ordinates ($\zeta = 0.006$)

Time, t seconds	Positive deflection envelope			Negative deflection envelope		
	Δ_{FD}, inches	Δ_{SA}, inches	Δ_{FD}/Δ_{SA}	Δ_{FD}, inches	Δ_{SA}, inches	Δ_{FD}/Δ_{SA}
1	0.314	0.314	0.999	0.310	0.311	0.995
2	0.284	0.287	0.988	0.272	0.275	0.986
3	0.243	0.249	0.985	0.242	0.246	0.983
4	0.212	0.216	0.981	0.205	0.210	0.978
5	0.181	0.185	0.978	0.176	0.180	0.976
6	0.156	0.160	0.975	0.154	0.159	0.975

able 2. Specimen Initial Imperfection

Distance from top of member, feet	Deviation, in inches		Actual imperfection, in inches	
	In plane of vibration	In orthogonal plane	In plane of vibration	In Orthogonal plane
0	0.000	0.000	0.000	0.000
1	0.000	0.050	0.008	0.108
2	0.000	0.150	0.023	0.216
3	0.010	0.250	0.075	0.275
4	0.020	0.310	0.070	0.333
5	0.020	0.420	0.068	0.361
6	0.020	0.410	0.070	0.360
7	0.010	0.420	0.061	0.378
8	0.010	0.400	0.053	0.276
9	0.000	0.350	0.045	0.250
10	-0.060	0.300	0.016	0.130
11	-0.100	0.200	0.008	0.047
12	-0.100	0.100	0.000	0.000

ıble 3. Experimental Results for String-Mass Concept with Lead Shots at Midheight without Jam Nuts

Test No.	Number of Lead shots	Frequency f_e, Hertz	Damping ratio, ζ	Average f_e, Hertz	Average ζ
1	0	3.98	0.00252	3.97	0.00243
2		3.95	0.00256		
3		4.00	0.00221		
4	1	3.95	0.00273	3.93	0.00278
5		3.92	0.00240		
6		3.92	0.00321		
7	2	3.87	0.00294	3.92	0.00353
8		3.98	0.00344		
9		3.93	0.00428		
10	3	3.96	0.00394	3.98	0.00395
11		3.98	0.00407		
12		3.99	0.00386		
13	5	3.92	0.00439	3.93	0.00429
14		3.96	0.00432		
15		3.91	0.00418		
16	7	3.78	0.00479	3.87	0.00466
17		3.91	0.00461		
18		3.92	0.00459		
19	9	3.92	0.00487	3.84	0.00519
20		3.80	0.00539		
21		3.82	0.00522		
22	15	4.12	0.00574	3.94	0.00601
23		3.90	0.00592		
24		3.80	0.00637		
25	21	3.98	0.00668	3.84	0.00693
26		3.82	0.00683		
27		3.73	0.00730		

able 4. Experimental Results for String-Mass Concept with Lead Shots at Midheight with Jam Nuts

Test No.	Number of Lead shots	Frequency f_e, Hertz	Damping ratio, ζ	Average f_e, Hertz	Average ζ
28	0	3.57	0.00110	3.74	0.00103
29		3.85	0.00100		
30		3.82	0.00100		
31	1	3.83	0.00140	3.81	0.00145
32		3.83	0.00133		
33		3.79	0.00165		
34	2	3.81	0.00220	3.74	0.00227
35		3.92	0.00248		
36		3.51	0.00215		
37	3	3.91	0.00265	3.91	0.00263
38		3.89	0.00245		
39		3.93	0.00280		
40	5	3.81	0.00275	3.83	0.00281
41		3.84	0.00285		
42		3.84	0.00285		
43	7	3.76	0.00344	3.80	0.00336
44		3.90	0.00324		
45		3.76	0.00340		
46	9	3.99	0.00423	3.80	0.00419
47		3.80	0.00442		
48		3.63	0.00392		
49	15	4.00	0.00536	3.90	0.00543
50		3.72	0.00537		
51		3.98	0.00558		
52	21	3.78	0.00596	3.79	0.00615
53		3.81	0.00610		
54		3.78	0.00640		

Table 5. Experimental Results for String Mass Concept with Equidistant Lead Shots and with Jam Nuts

Test No.	Number of lead shots	Frequency f_e, Hertz	Damping ratio, ζ	Average f_e, Hertz	Average ζ
55	2	3.96	0.00206	3.93	0.00228
56		3.94	0.00238		
57		3.90	0.00241		
58	3	3.83	0.00267	3.89	0.00258
59		3.91	0.00261		
60		3.93	0.00248		
61	21	3.98	0.00473	3.98	0.00462
62		4.01	0.00451		
63		3.96	0.00462		

Table 6. Effect of Axial Force on Member Frequency and Damping Ratio

Test No.	Axial Force, P lb.	Frequency f_e, Hertz	Damping ratio, ζ	Average f_e, Hertz	Average ζ
64	-155.0	6.78	0.00106	6.64	0.00083
65		6.37	0.00060		
66		6.78	0.00083		
67	-19.8	4.21	0.00104	4.20	0.00104
68		4.18	0.00103		
69		4.21	0.00107		
70	-4.5	3.83	0.00110	3.83	0.00105
71		3.85	0.00105		
72		3.82	0.00100		
73	+10.8	3.41	0.00517	3.42	0.00526
74		3.43	0.00564		
75		3.41	0.00499		

Table 7. Experimental Results for Polyethylene Tubing Concept with Jam Nuts

Test No.	Tubing Arrangement	Frequency f_e, Hertz	Damping ratio, ζ	Average f_e, Hertz	Average ζ
76	(a)	3.96	0.00239	3.95	0.00220
77		3.92	0.00208		
78		3.96	0.00213		
79	(b)	4.01	0.00238	3.93	0.00205
80		3.74	0.00195		
81		3.98	0.00183		
82	(c)	3.72	0.00199	3.68	0.00207
83		3.66	0.00202		
84		3.64	0.00221		

Table 8. Experimental Frequencies for Chain Damping Concept with Jam Nuts

Test No.	Chain length, feet	Frequency f_e, Hertz	Average f_e, Hertz
85	1	3.98	3.92
86		3.90	
87		3.89	
88	2	4.15	4.15
89		4.12	
90		4.17	
91	3	3.95	3.91
92		3.93	
93		3.85	
94	5	4.02	4.00
95		4.00	
96		4.00	
97	7	4.00	4.01
98		4.03	
99		4.01	
100	9	3.97	3.93
101		3.97	
102		3.87	
103	10	4.01	4.01
104		4.01	
105		4.01	

Table 9. Experimental Damping Ratios for Chain Damping Concept with Jam Nuts

Test No.	Damping ratio, ζ						
	0 sec	1 sec	2 sec	3 sec	4 sec	5 sec	6 sec
85	0.00312	0.00268	0.00241	0.00283	0.00291	0.00331	0.00341
86	0.00301	0.00271	0.00269	0.00277	0.00287	0.00299	0.00349
87	0.00295	0.00298	0.00240	0.00270	0.00292	0.00300	0.00348
88	0.00320	0.00309	0.00317	0.00355	0.00419	0.00432	0.00441
89	0.00317	0.00312	0.00318	0.00349	0.00429	0.00429	0.00429
90	0.00298	0.00332	0.00330	0.00358	0.00424	0.00432	0.00456
91	0.00391	0.00419	0.00409	0.00423	0.00479	0.00539	0.00618
92	0.00401	0.00423	0.00408	0.00418	0.00492	0.00542	0.00629
93	0.00416	0.00421	0.00416	0.00416	0.00475	0.00539	0.00613
94	0.00448	0.00471	0.00477	0.00512	0.00579	0.00639	0.00810
95	0.00471	0.00461	0.00481	0.00503	0.00583	0.00621	0.00801
96	0.00464	0.00498	0.00509	0.00512	0.00584	0.00665	0.00792
97	0.00539	0.00567	0.00601	0.00659	0.00701	0.00866	0.01130
98	0.00562	0.00522	0.00613	0.00671	0.00712	0.00849	0.01090
99	0.00574	0.00534	0.00583	0.00663	0.00717	0.00883	0.01100
100	0.00688	0.00659	0.00741	0.00912	0.01170	0.01731	0.02390
101	0.00689	0.00658	0.00753	0.00891	0.01230	0.01693	0.02370
102	0.00721	0.00713	0.00756	0.00907	0.01430	0.01745	0.02530
103	0.00879	0.00912	0.01020	0.01320	0.02310	0.02790	0.04170
104	0.00891	0.00911	0.01060	0.01330	0.02290	0.02830	0.04110
105	0.00786	0.00877	0.01130	0.01000	0.02030	0.02990	0.03990

Table. 10. Experimental Average Damping Ratios for Chain Damping Concept with Jam Nuts

Chain length, feet	average damping ratio, ζ						
	0 sec	1 sec	2 sec	3 sec	4 sec	5 sec	6 sec
1	0.00303	0.00279	0 00250	0.00260	0.00290	0.00310	0.00346
2	0.00312	0.00317	0.00325	0.00354	0.00424	0.00431	0.00442
3	0.00403	0.00421	0.00411	0.00419	0.00482	0.00540	0.00620
5	0.00461	0.00476	0.00489	0.00509	0.00582	0.00641	0.00801
7	0.00558	0.00541	0.00599	0.00664	0.00710	0.00866	0.01100
9	0.00699	0.00676	0.00750	0.00903	0.01276	0.01723	0.02423
10	0.00852	0.00900	0.01070	0.01320	0.02210	0.02870	0.04090

Table 11. Efficiencies of Various Damping Concepts.

Test Nos.	Details of damping devices		W_d lb.	Average ζ	Efficiency index, n lb-sec^2/ft
1-3	Number of lead shots at midheight, without jam nuts	0	0.00000	0.00243	—
4-6		1	0.00103	0.00278	10.94
7-9		2	0.00207	0.00353	17.11
10-12		3	0.00310	0.00395	15.78
13-15		5	0.00517	0.00429	11.58
16-18		7	0.00723	0.00466	9.93
19-21		9	0.00930	0.00519	9.55
22-24		15	0.01550	0.00601	7.43
25-27		21	0.02170	0.00693	6.67
28-30	Number of lead shots at midheight, with jam nuts	0	0.00000	0.00103	—
31-33		1	0.00103	0.00145	13.12
34-36		2	0.00207	0.00227	19.28
37-39		3	0.00310	0.00263	16.61
40-42		5	0.00517	0.00281	11.08
43-45		7	0.00723	0.00336	10.37
46-48		9	0.00930	0.00419	10.93
49-51		15	0.01550	0.00543	9.11
52-54		21	0.02170	0.00615	7.59
55-57	Number of Equi-distant read shots with jam nuts	2	0.00207	0.00228	19.44
58-60		3	0.00310	0.00258	16.10
61-63		21	0.02170	0.00462	5.31
76-78	Polyethylene tubing concept	(a)	0.30480	0.00220	0.12
79-81		(b)	0.16800	0.00205	0.20
82-84		(c)	0.27300	0.00207	0.12
85-87	Chain length, ft.	1	0.05000	0.00291	1.21
88-90		2	0.10000	0.00372	0.86
91-93		3	0.15000	0.00471	0.79
94-96		5	0.25000	0.00565	0.71
97-99		7	0.35000	0.00719	0.56
100-102		9	0.45000	0.01200	0.79
103-105		10	0.50000	0.01900	1.15

FIGURES

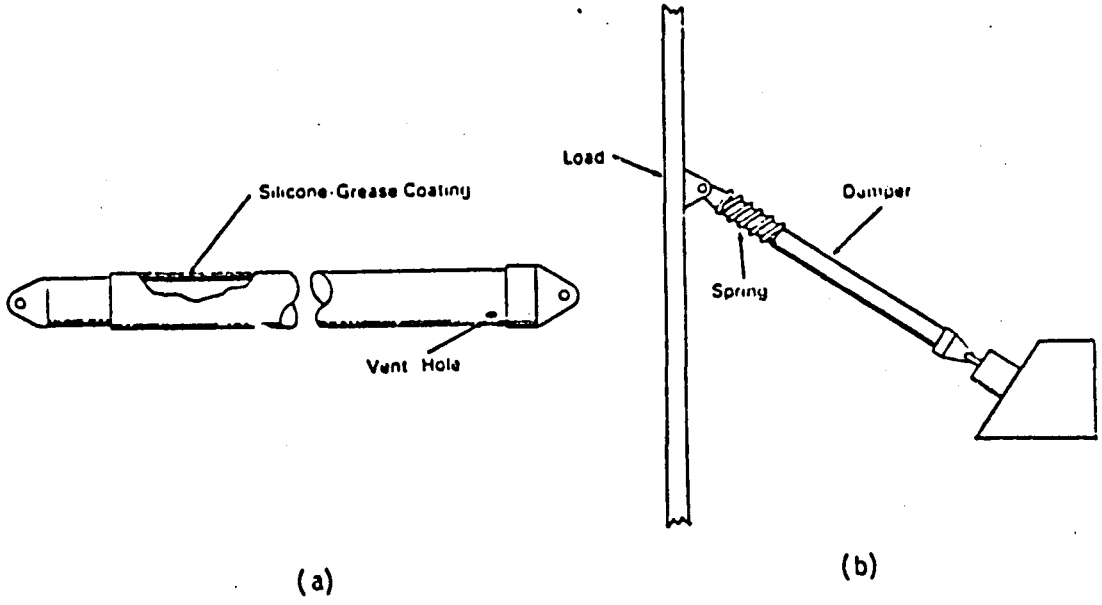

Figure 1. Lightweight Load Support Vibration Damper(Ref. 7).

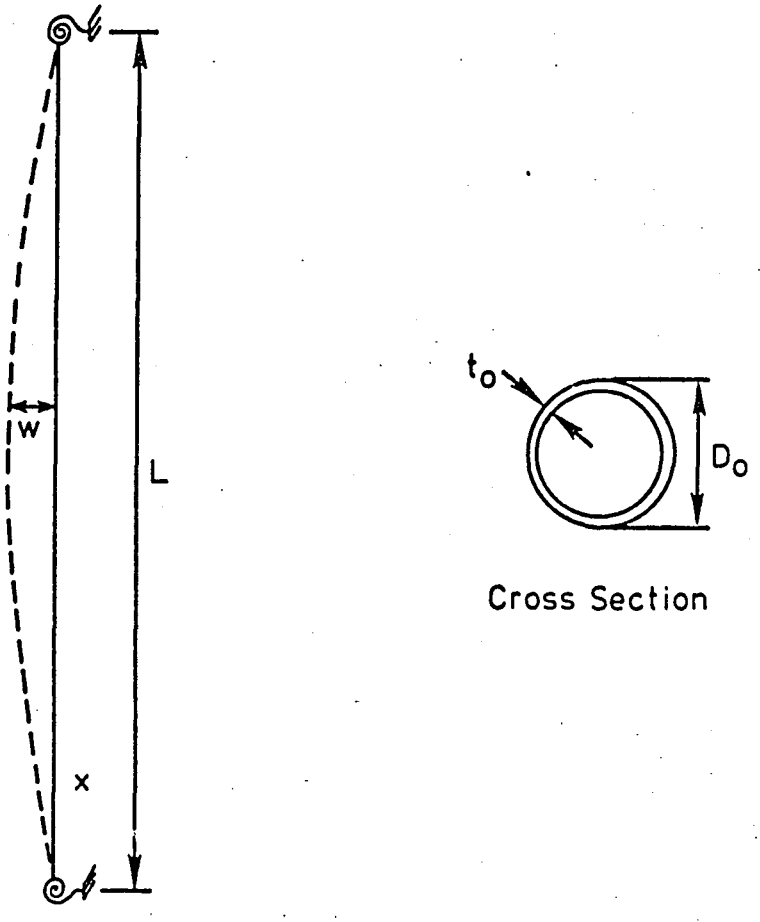

Figure 2. Partially Restrained Member.

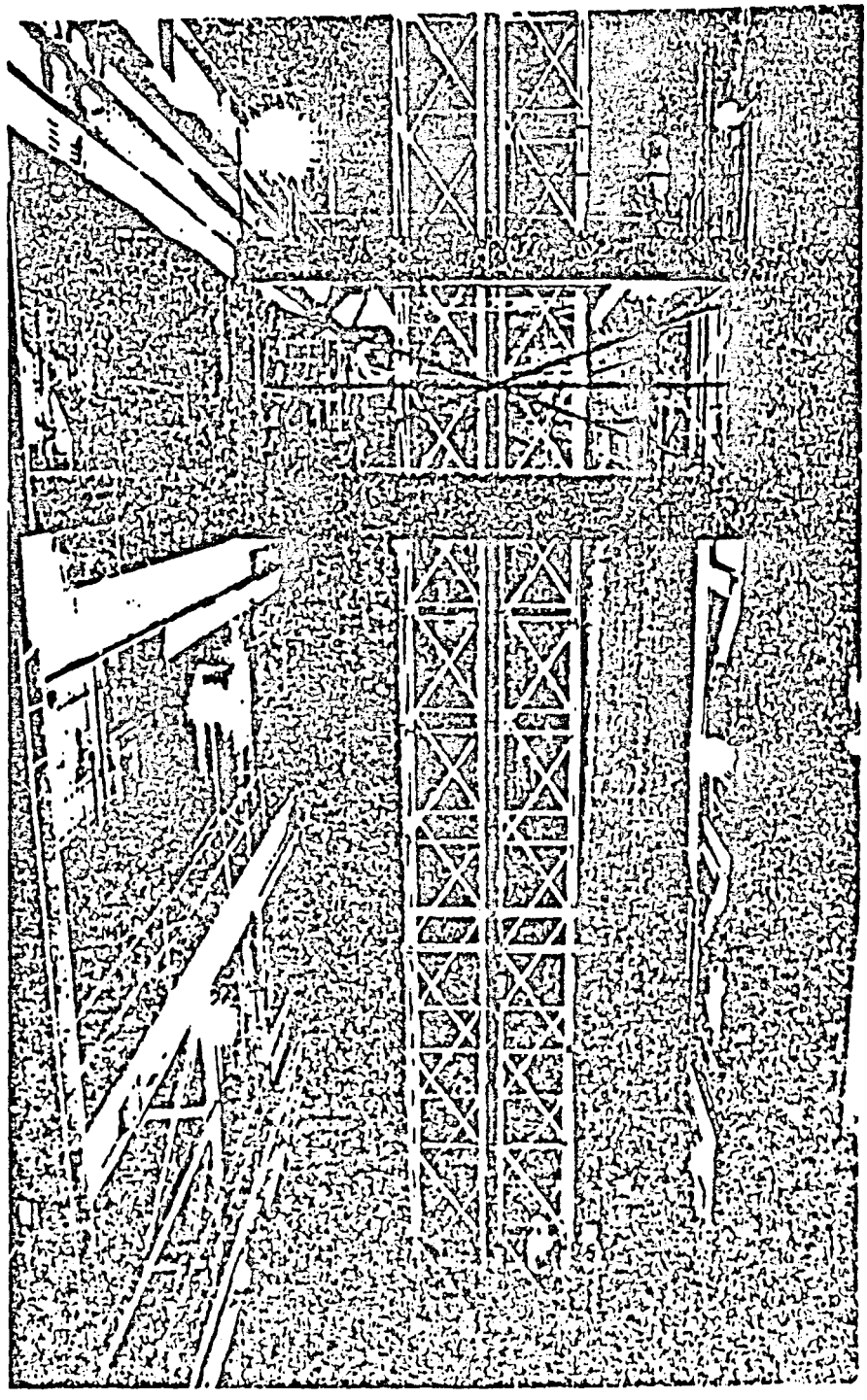

Figure 3. A 60 ft. Truss Under Vibration Testing(Ref. 2).

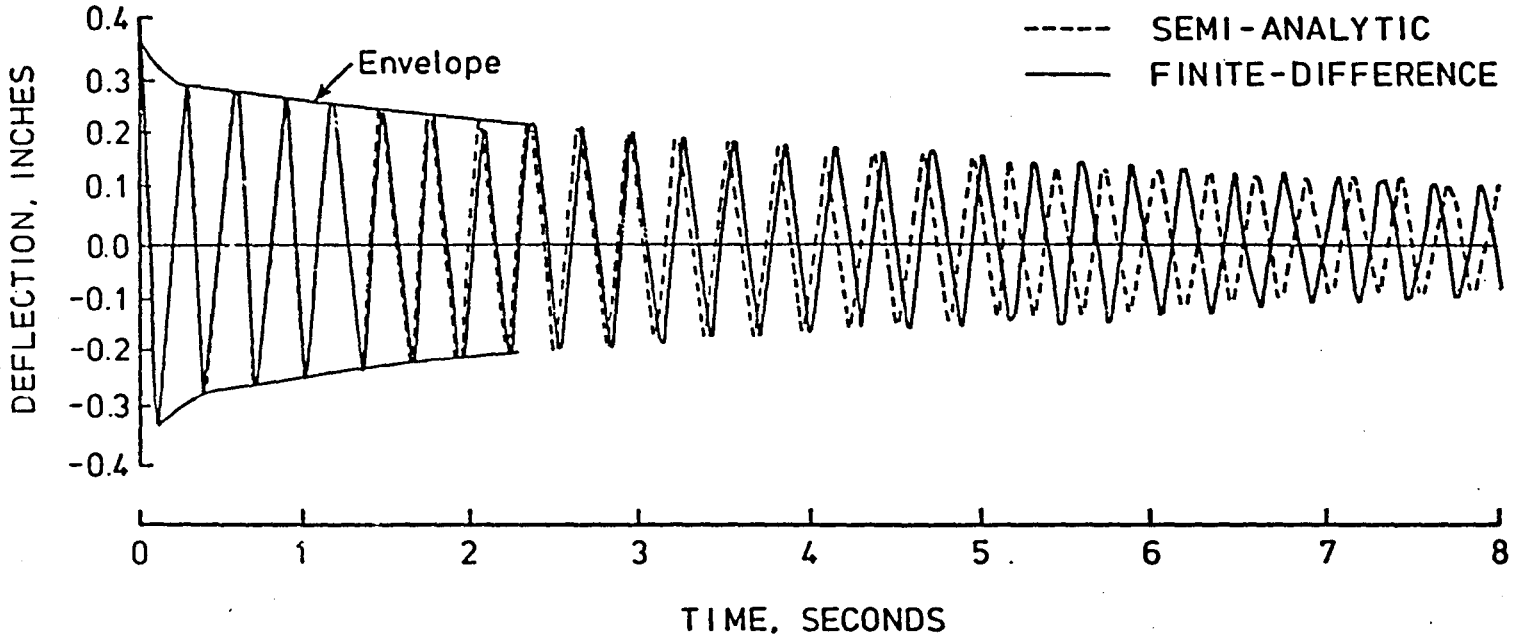

Figure 4. Comparison of Semi-Analytic and Finite-Difference Deflection-time plots for $\zeta = 0.0060$.

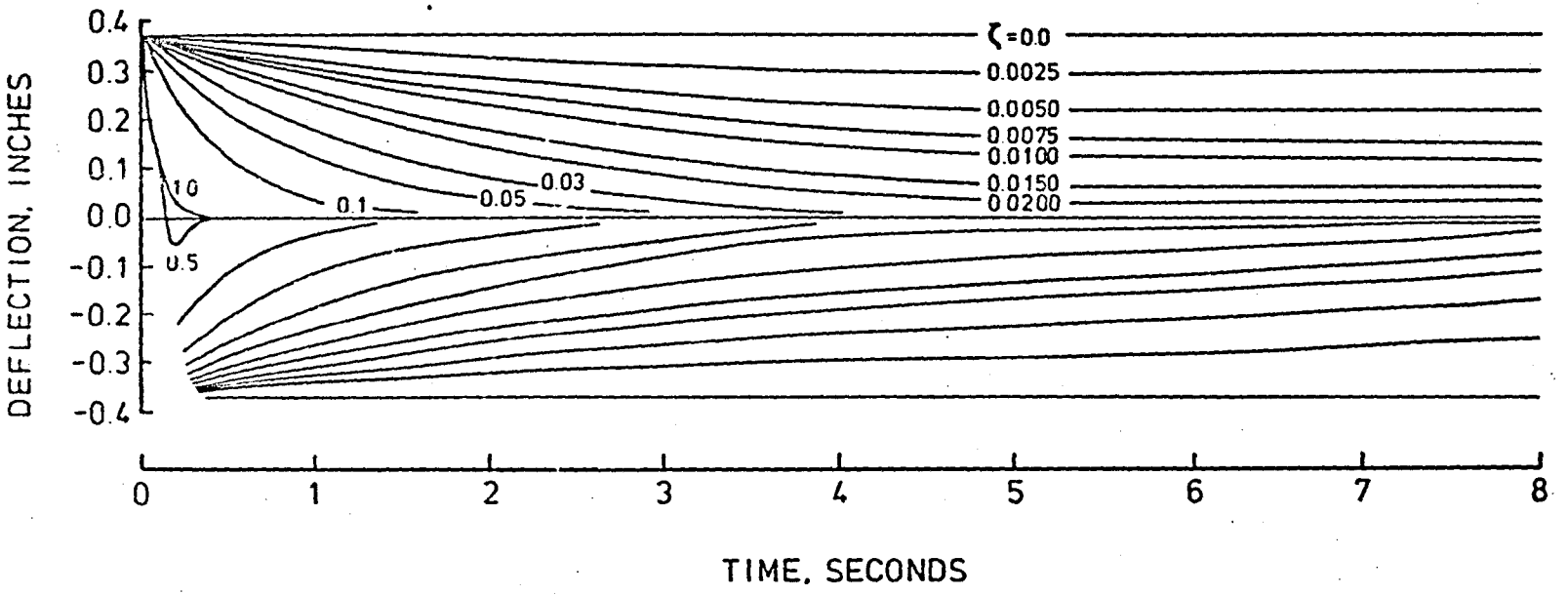

Figure 5. Deflection-time Envelopes based on Finite-Difference Solution for ζ = 0.0 to 1.0.

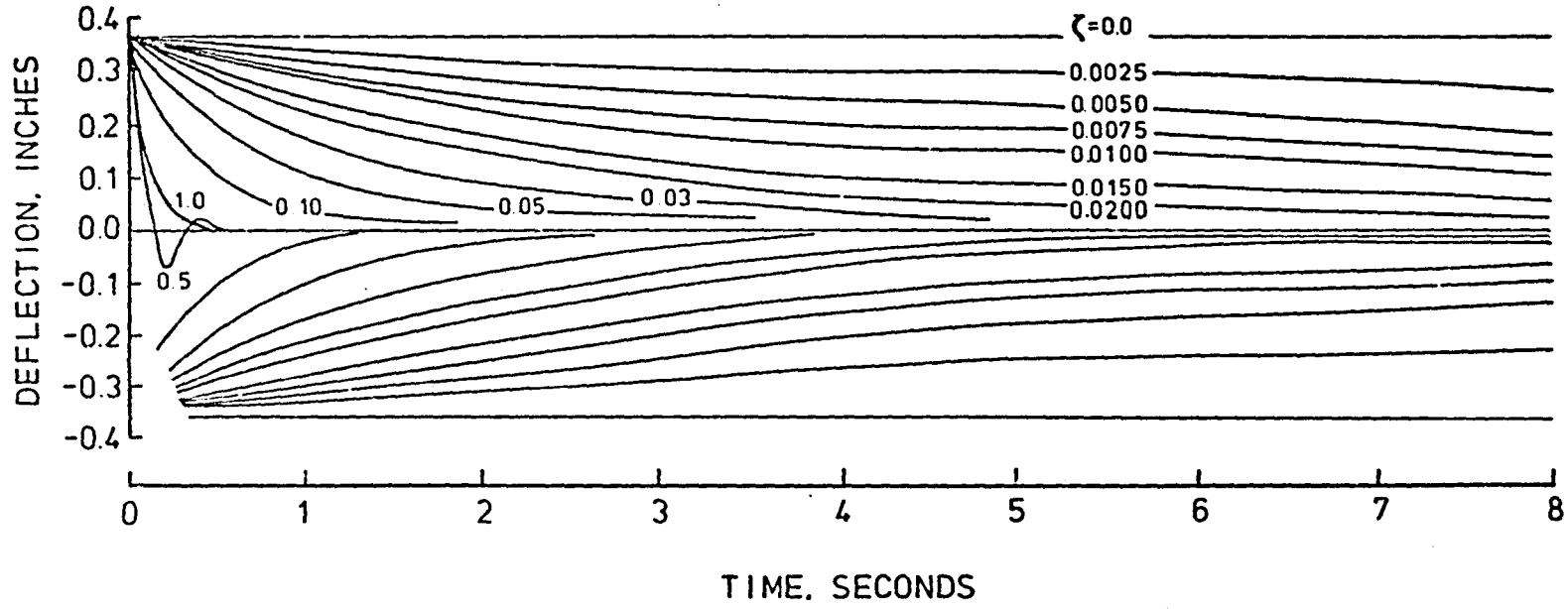

Figure 6. Deflection-time Envelopes based on Semi-Analytic Solution for ζ = 0.0 to 1.0.

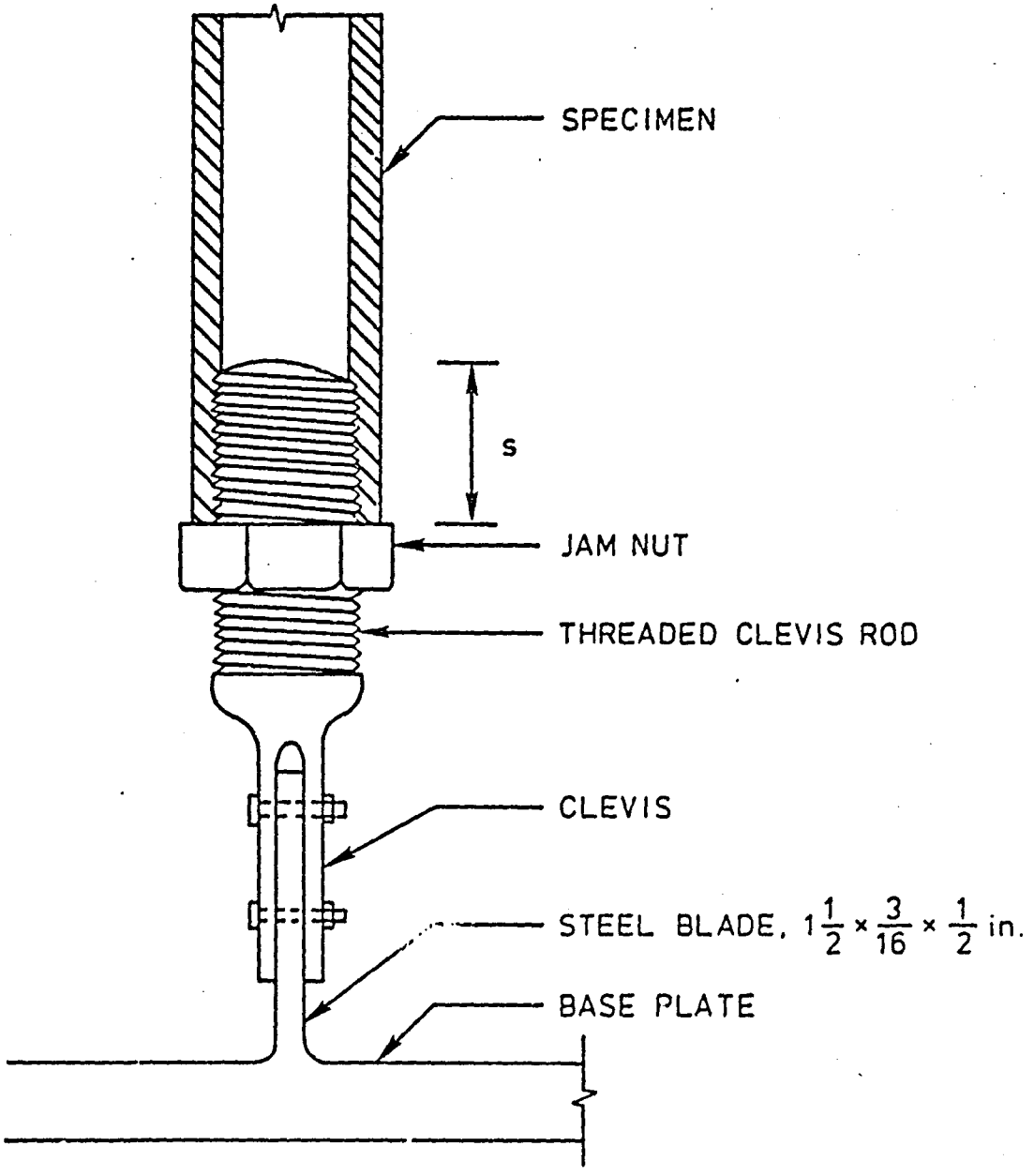

Figure 7. End Connection Details.

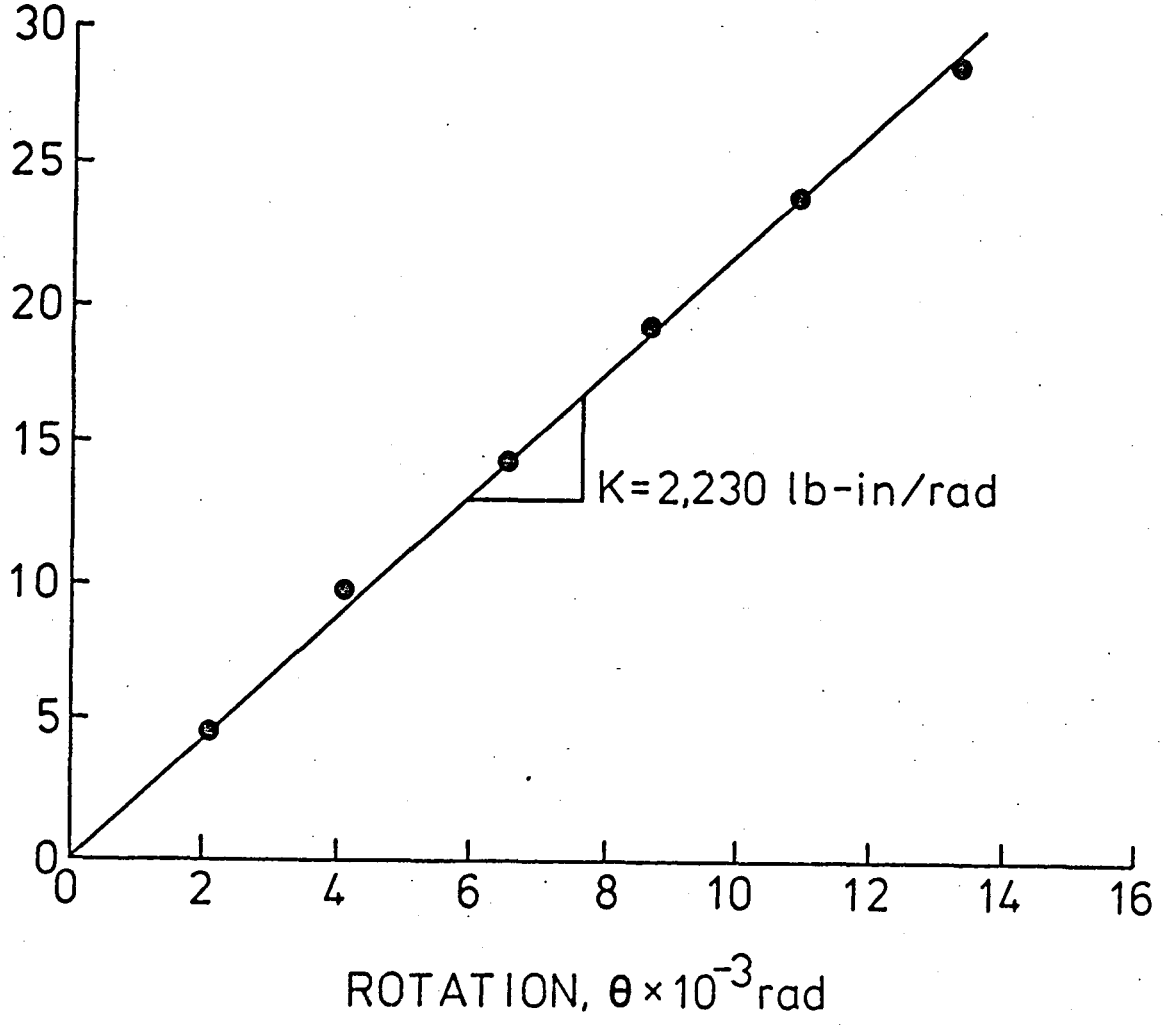

Figure 8. Minor Axis Moment-Rotation Relationship for Bottom End Connection.

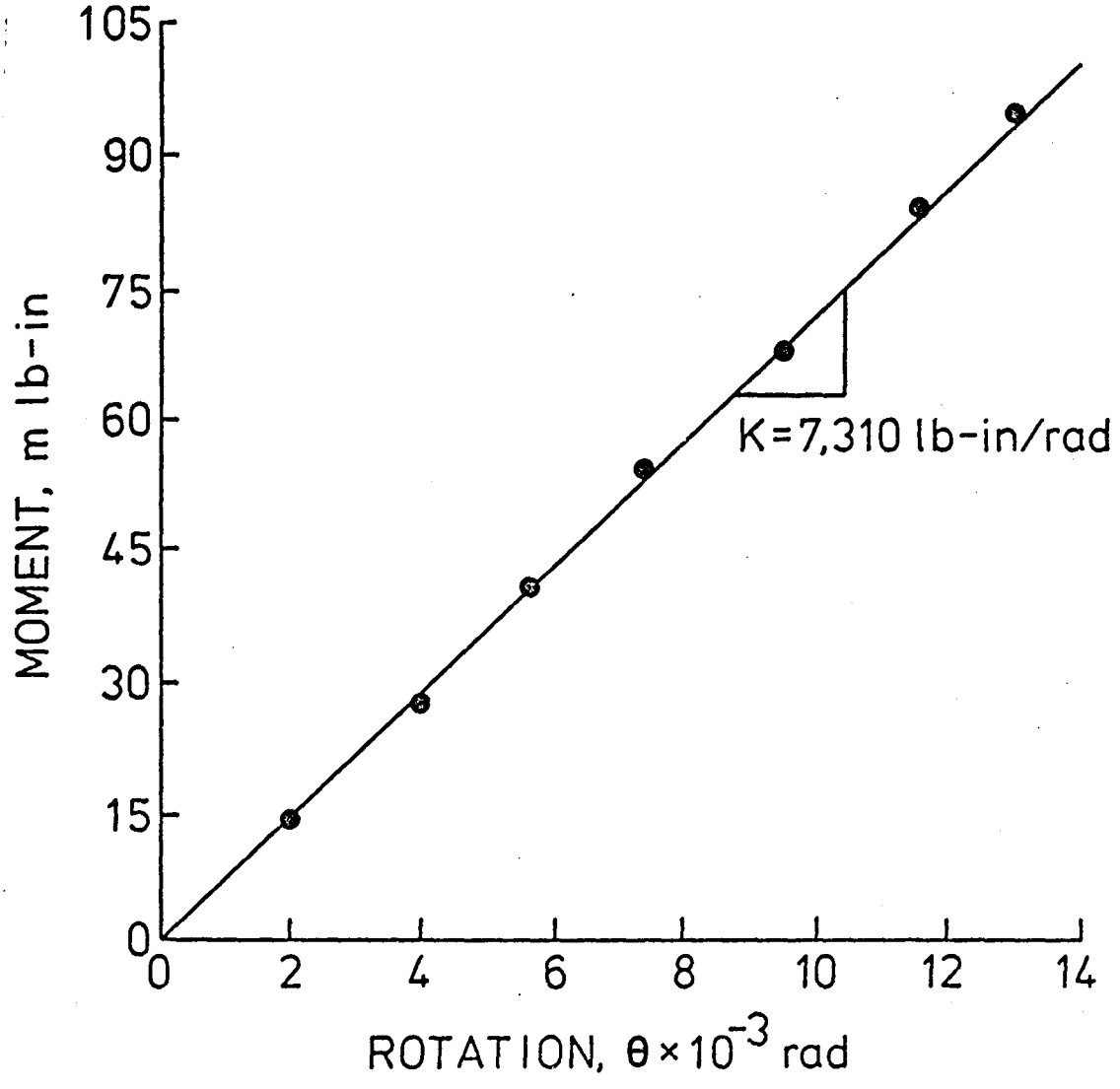

Figure 9. Major Axis Moment-Rotation Relationship for Bottom End Connection.

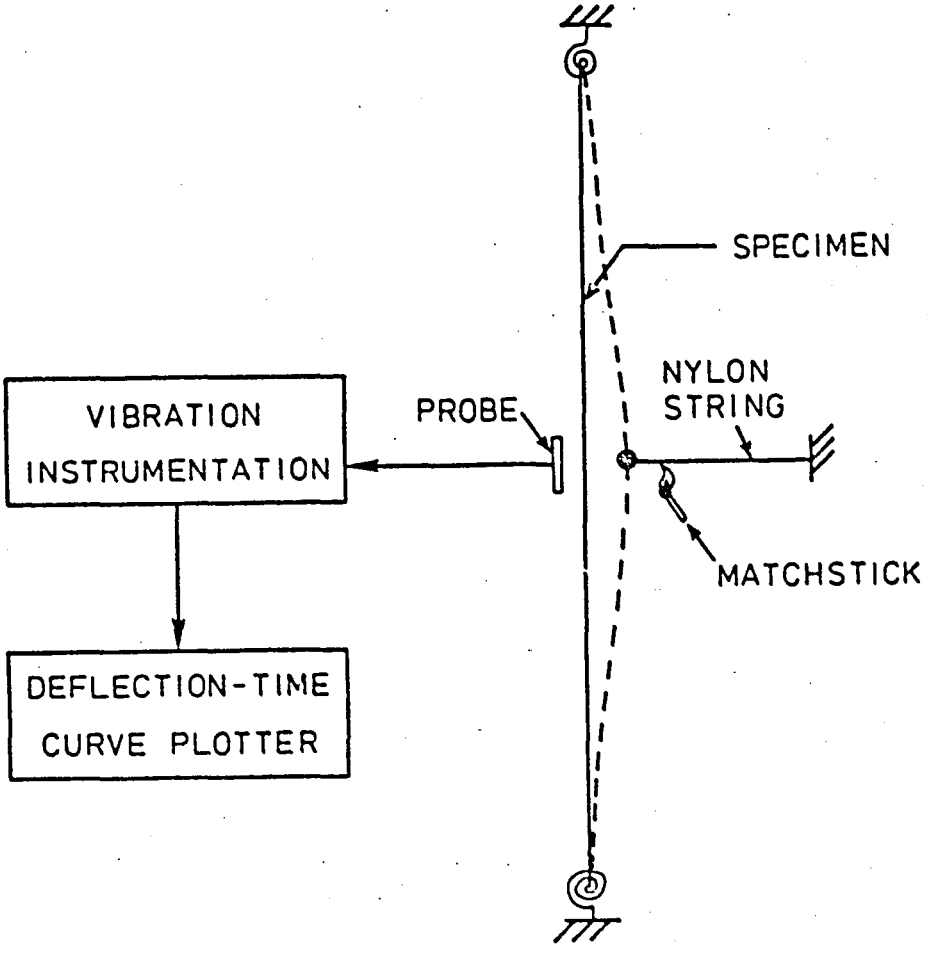

Figure 10. Schematic of Test Setup and Instrumentation.

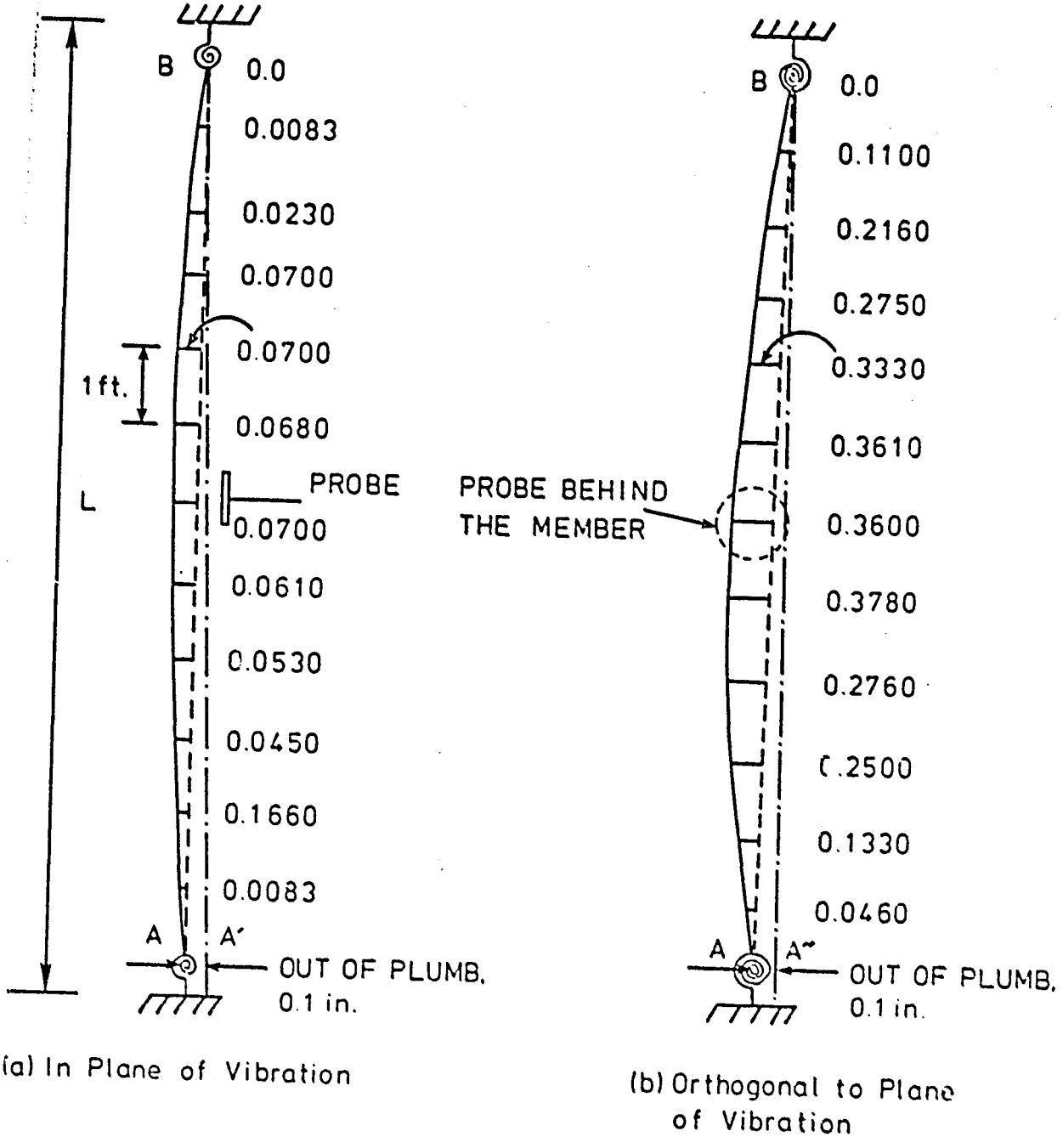

Figure 11. Spatial Initial Imperfection.

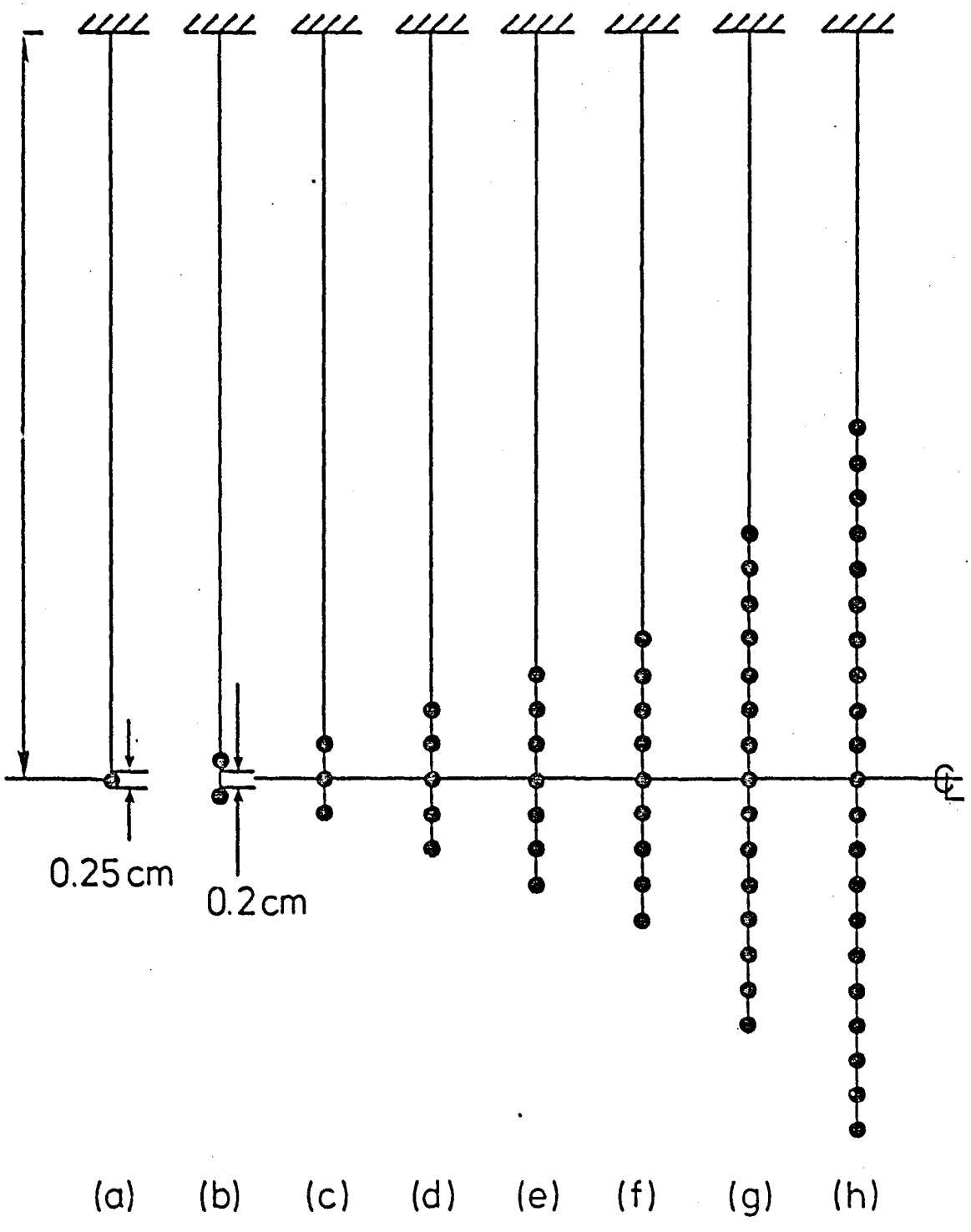

Figure 12. String-Mass Configuratiens with Lead Shots at Midheight.

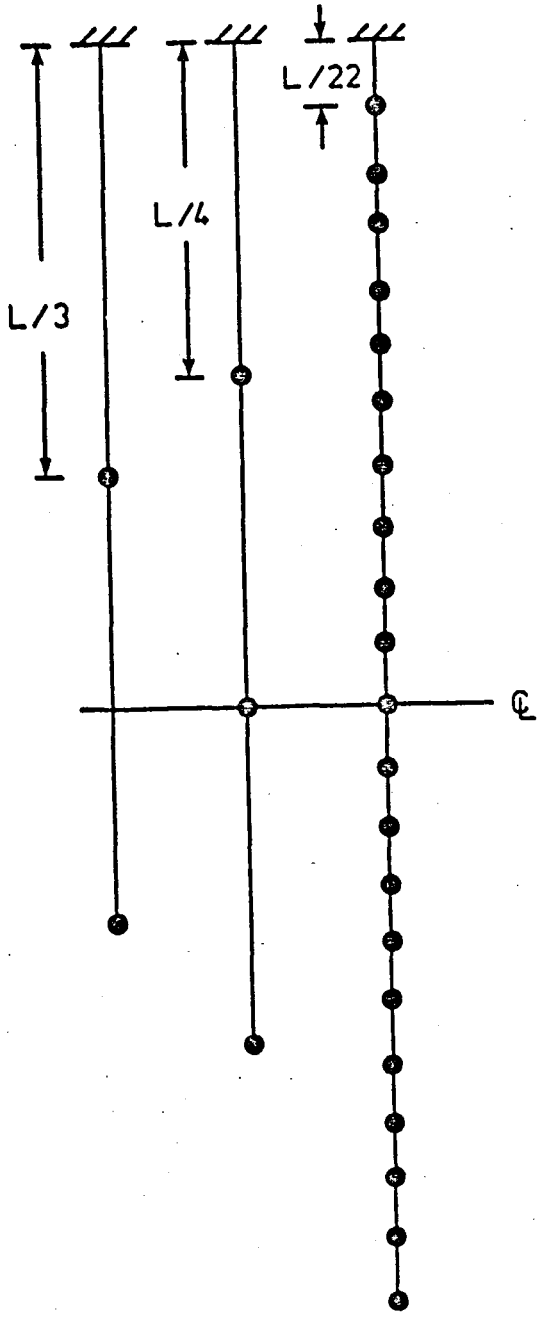

Figure 13. String-Mass Configurations with Equidistant Lead Shots.

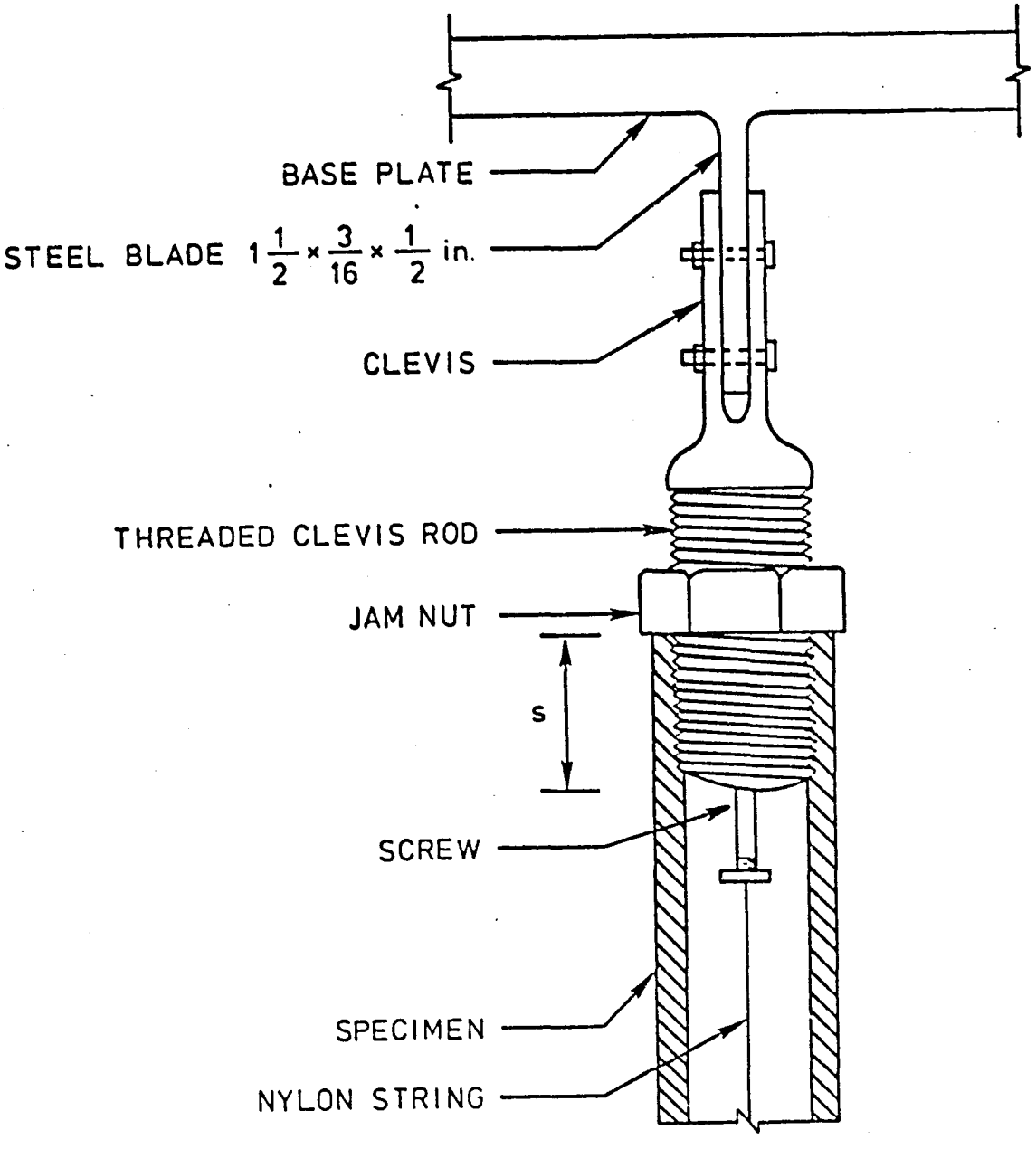

Figure 14. Suspension of Nylon String to the Top Clevis Rod.

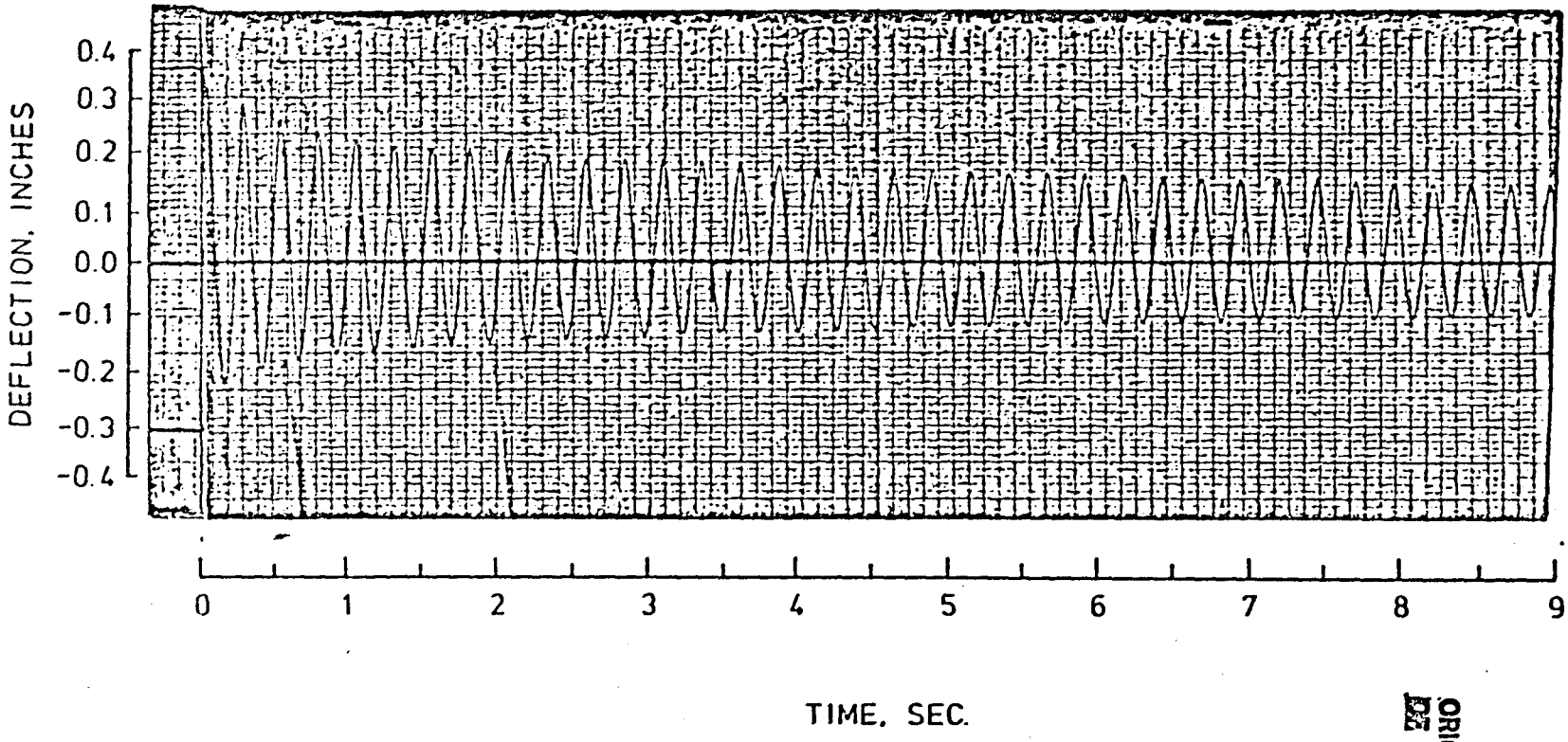

Figure 15. Δ-t plot for Test 1, Table 3, String-Mass Concept without Jam Nuts.

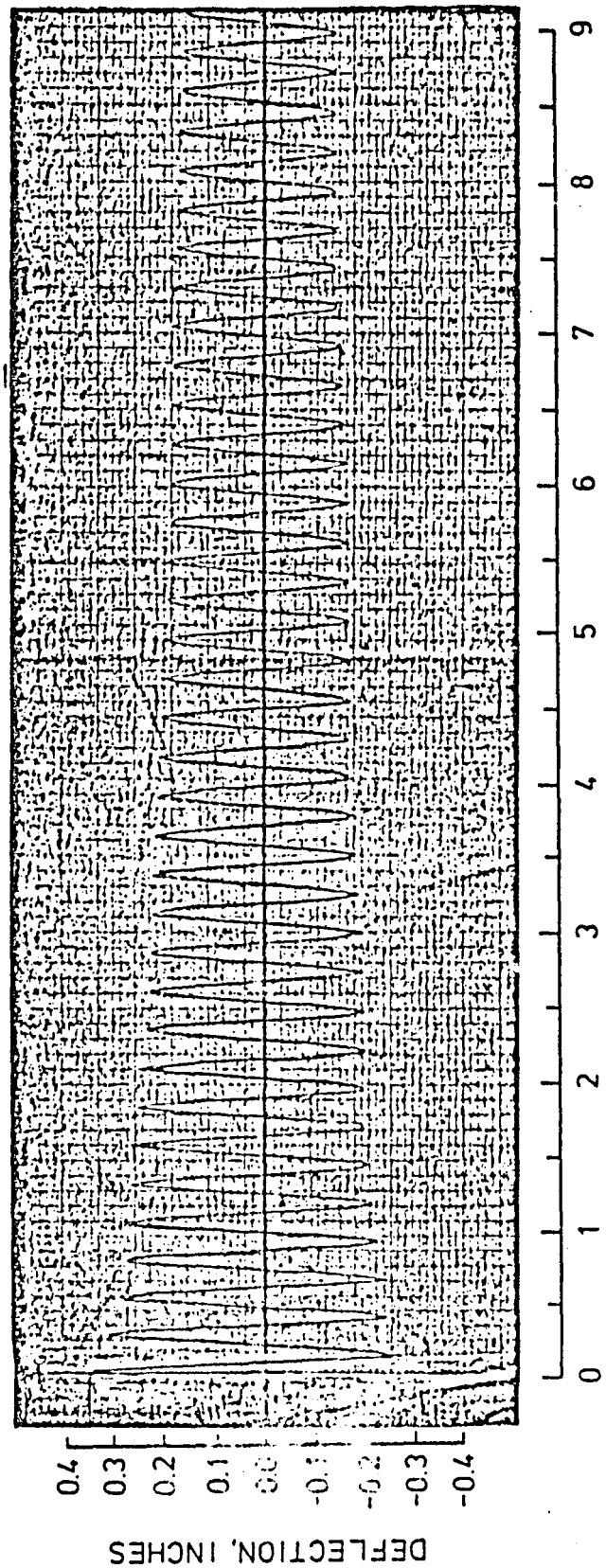

Figure 16. Δ-t plot for Test 4, Table 3, String-Mass Concept without Jam Nuts.

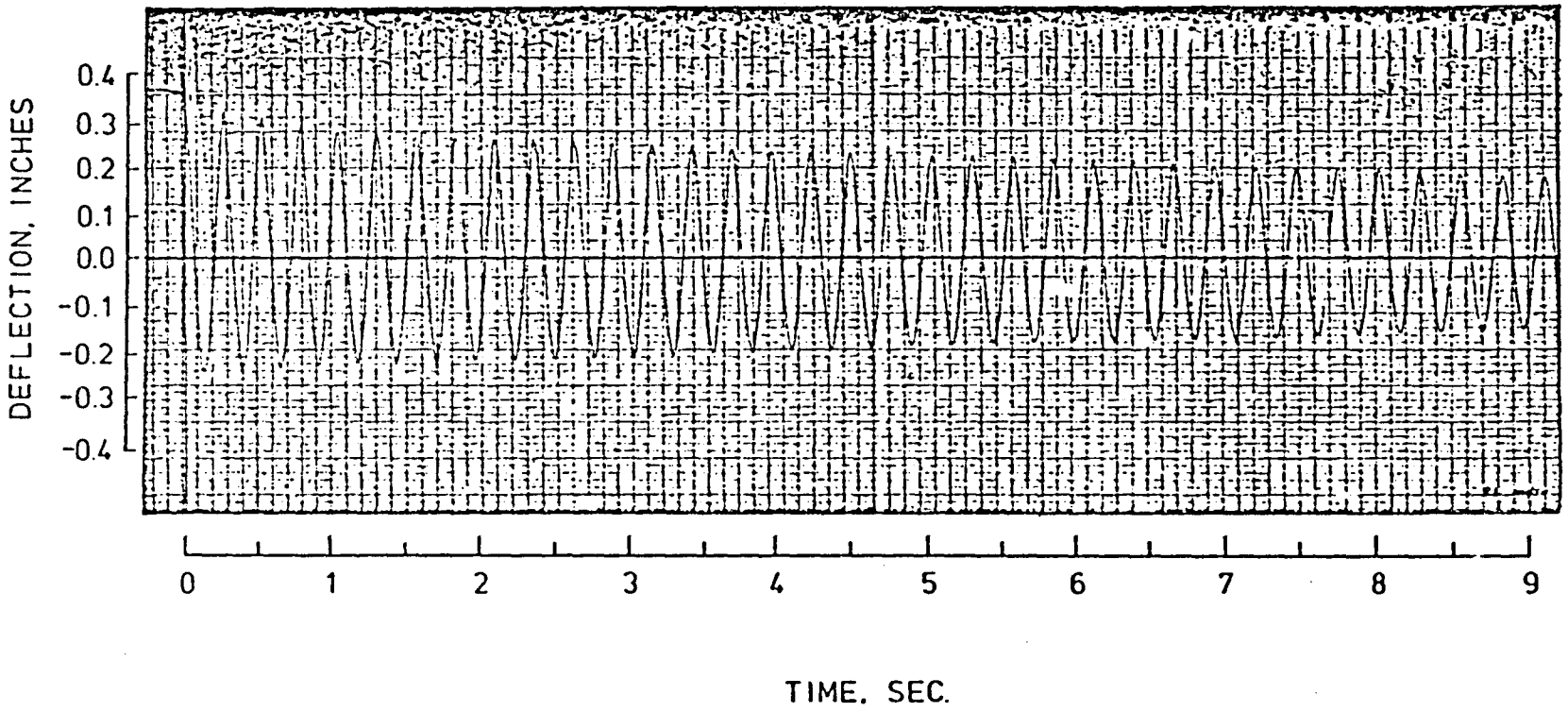

Figure 17. Δ-t plot for Test 7, Table 3, String-Mass Concept without Jam Nuts.

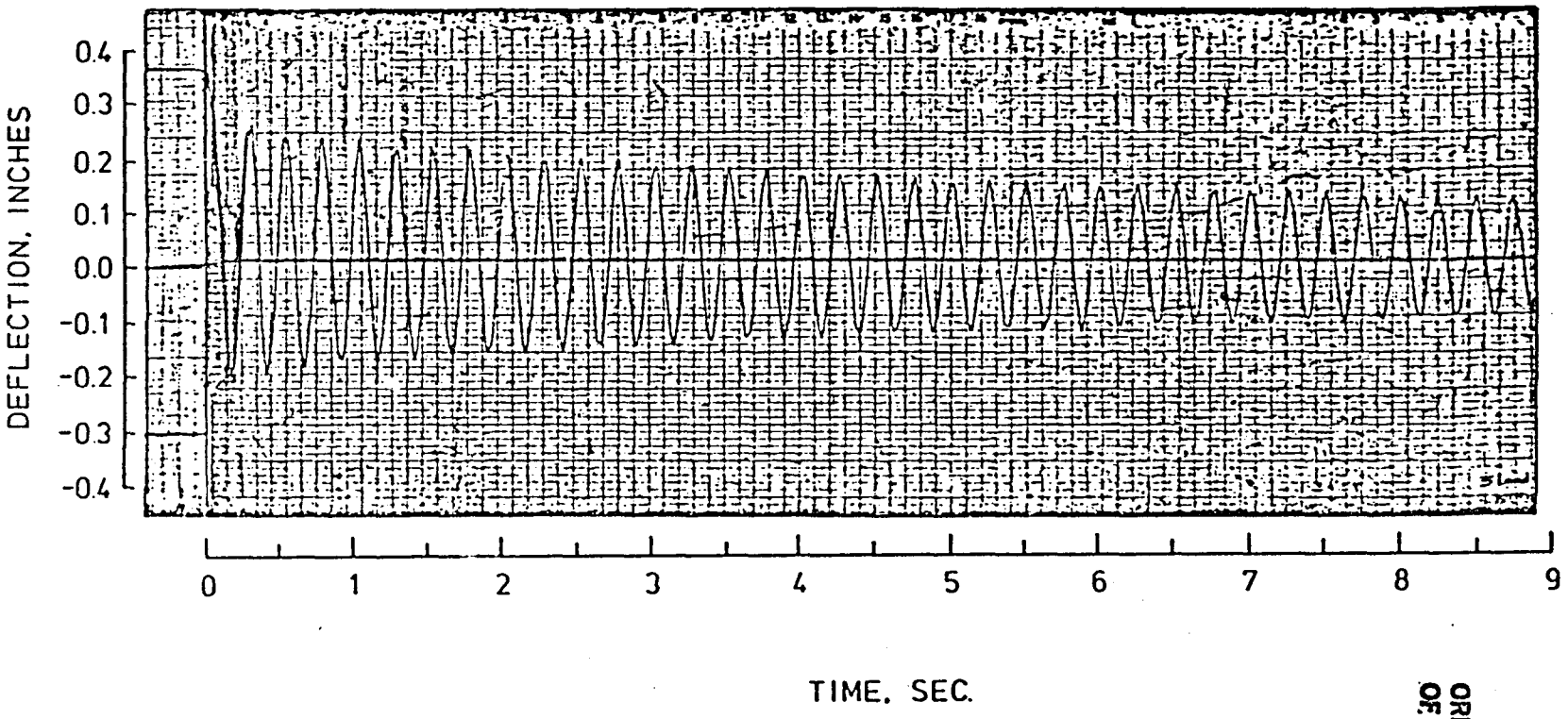

Figure 18. Δ-t plot for Test 10, Table 3, String-Mass Concept without Jam Nuts.

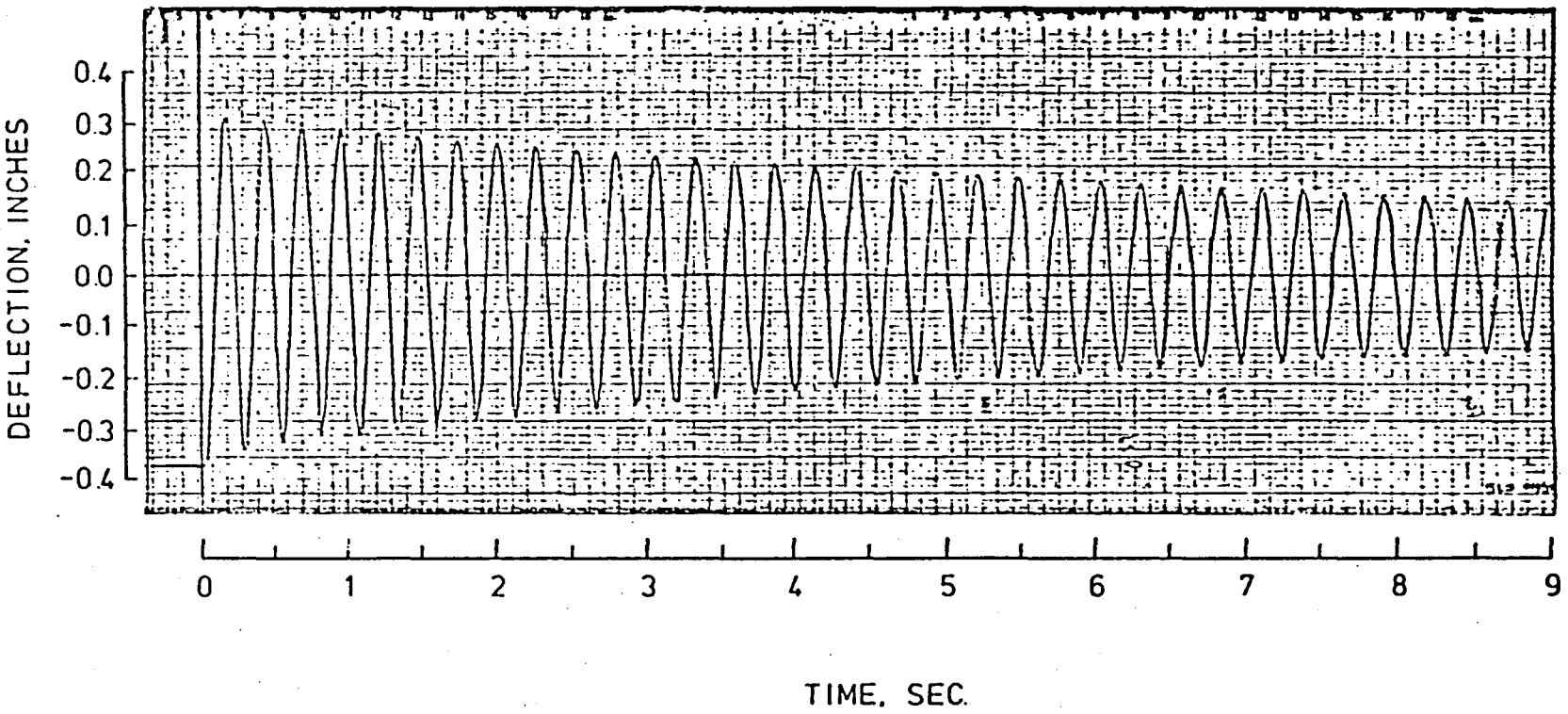

Figure 19. Δ-t plot for Test 13, Table 3, String - Mass Concept without Jam Nuts.

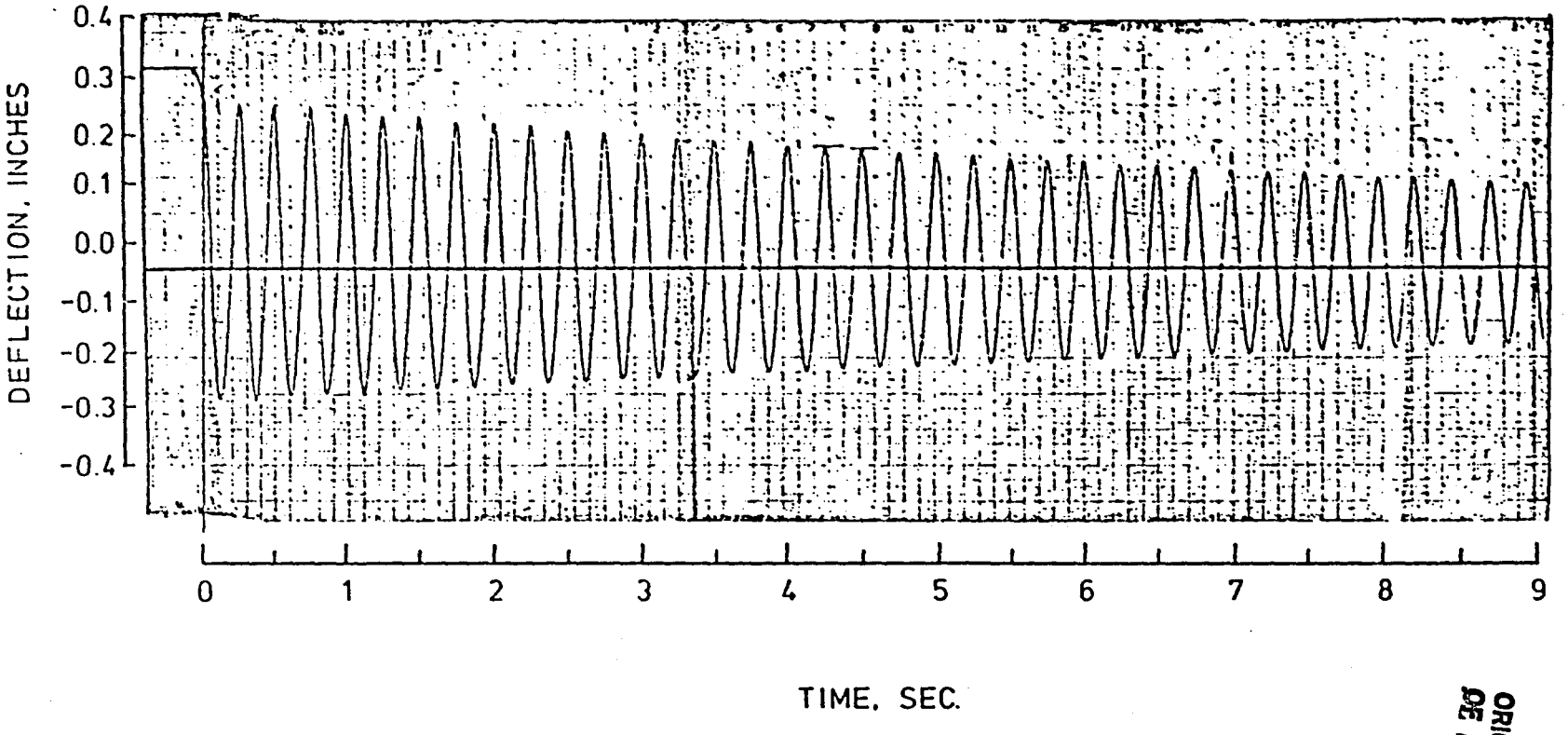

Figure 20. Δ-t plot for Test 16, Table 3, String-Mass Concept without Jam Nuts.

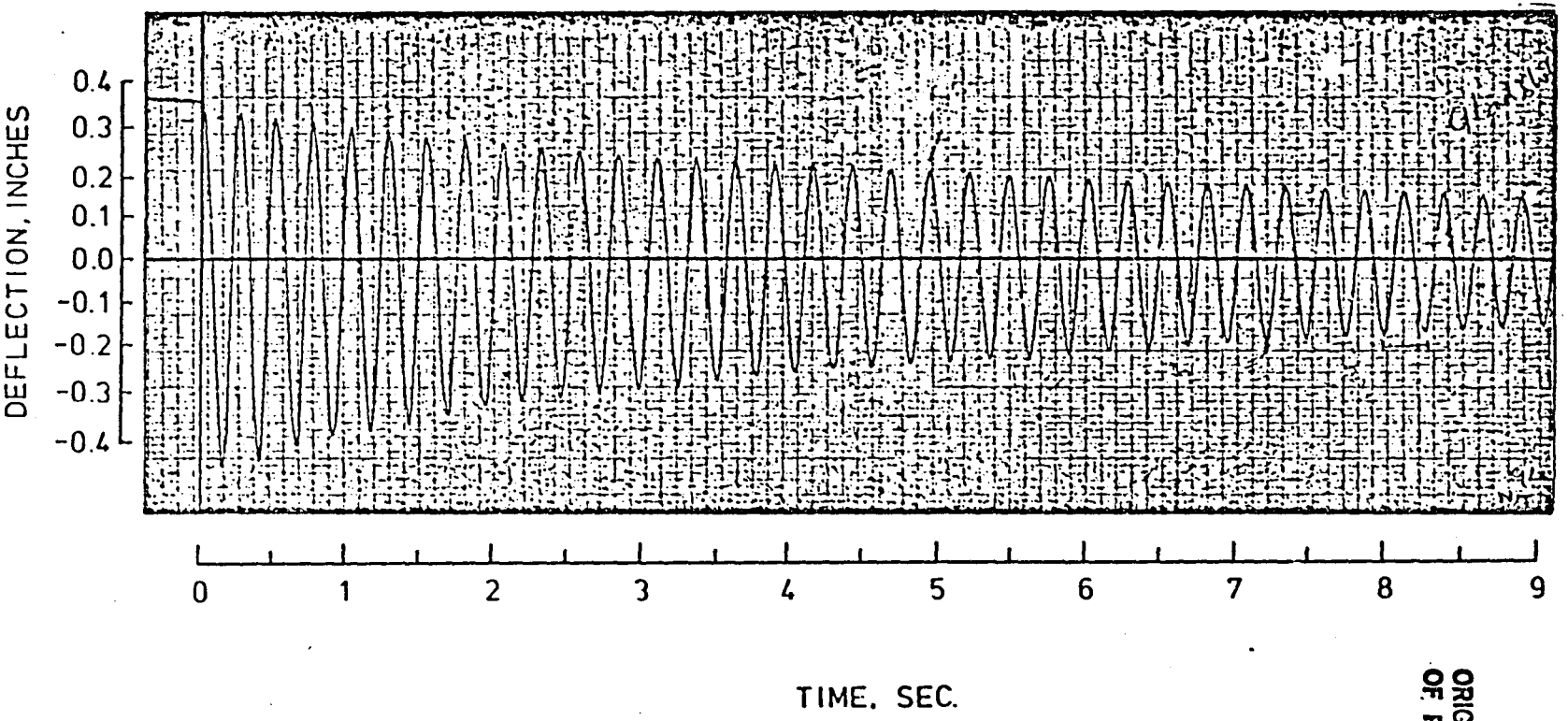

Figure 21. Δ-t plot for Test 19, Table 3, String-Mass Concept without Jam Nuts.

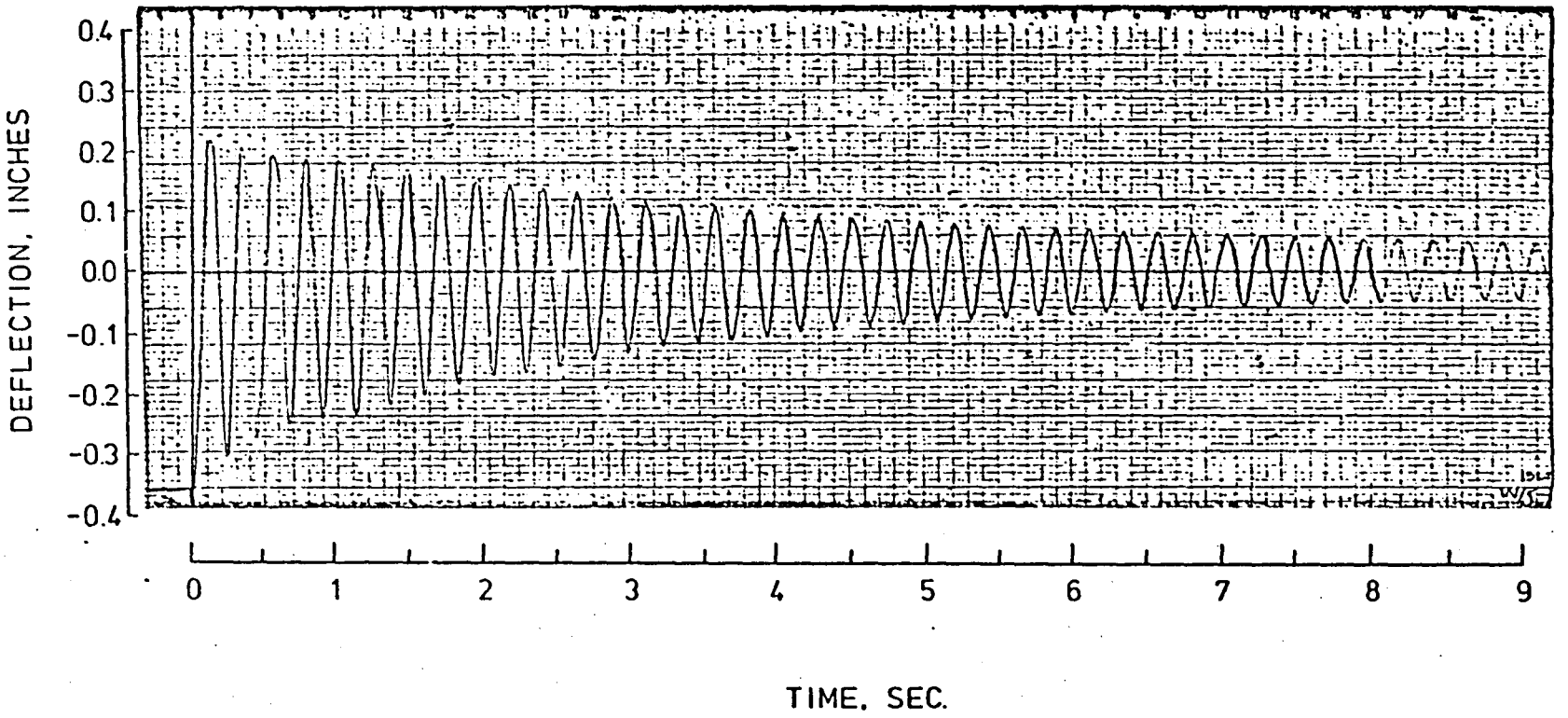

Figure 22. Δ-t plot for Test 22, Table 3, String-Mass Concept without Jam Nuts.

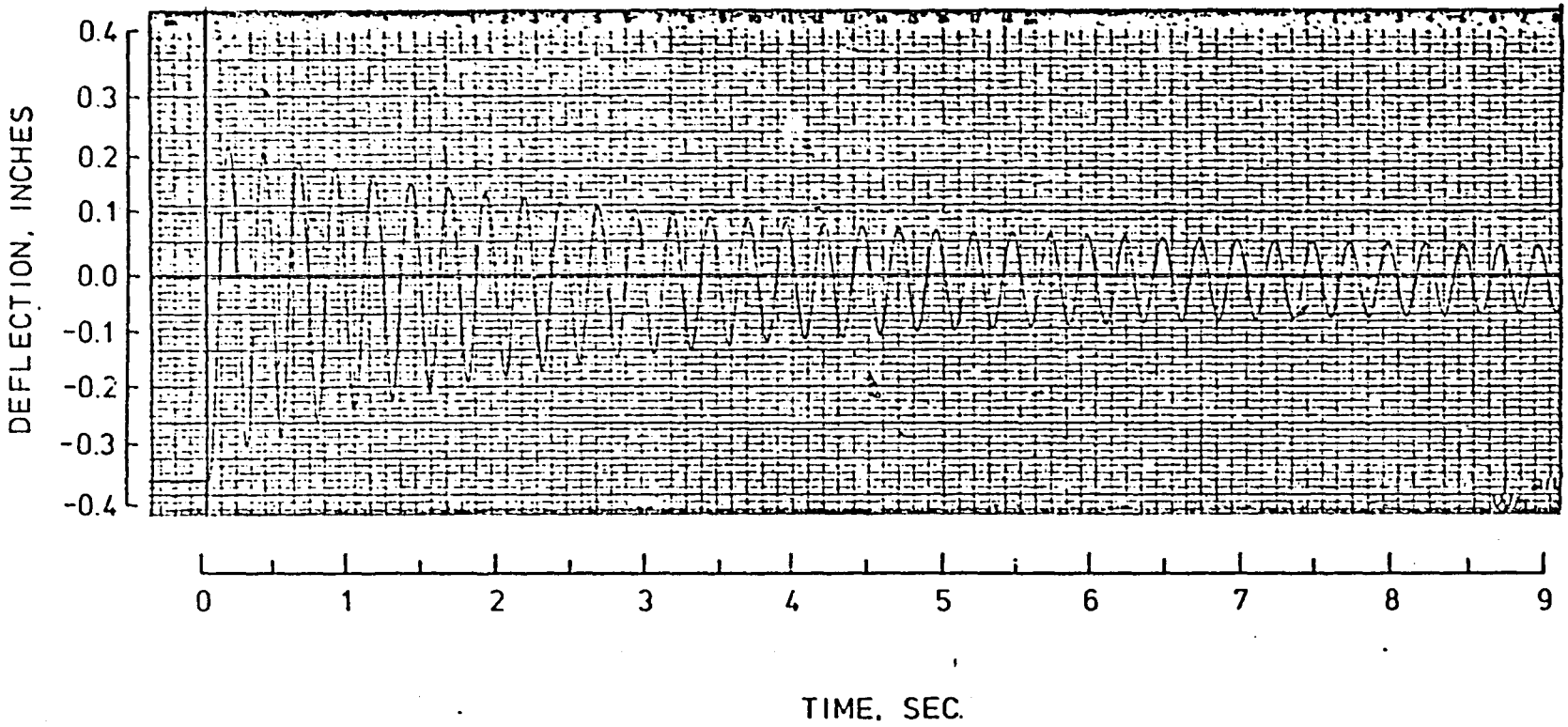

Figure 23. Δ-t plot for Test 25, Table 3, String-Mass Concept without Jam Nuts.

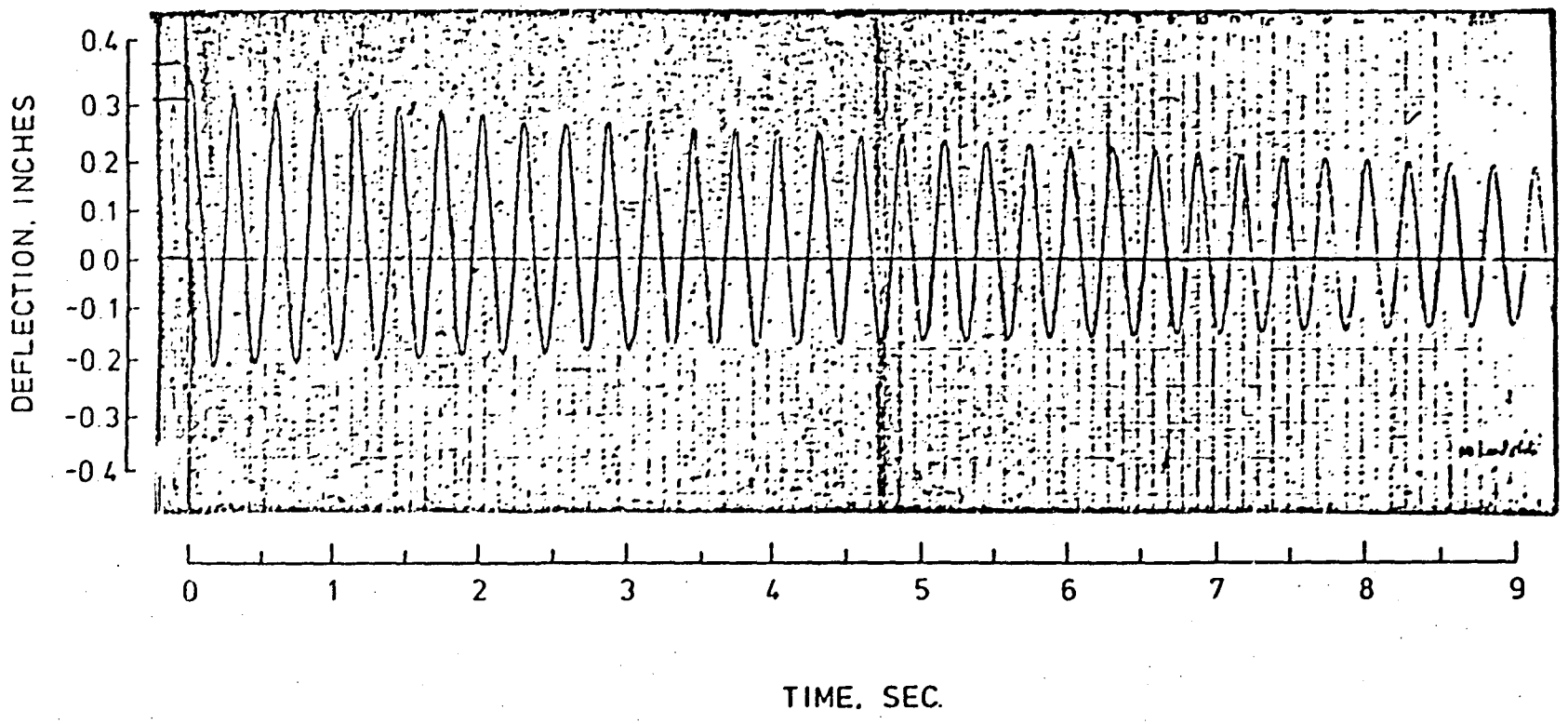

Figure 24. Δ-t plot for Test 28, Table 4, String-Mass Concept with Jam Nuts.

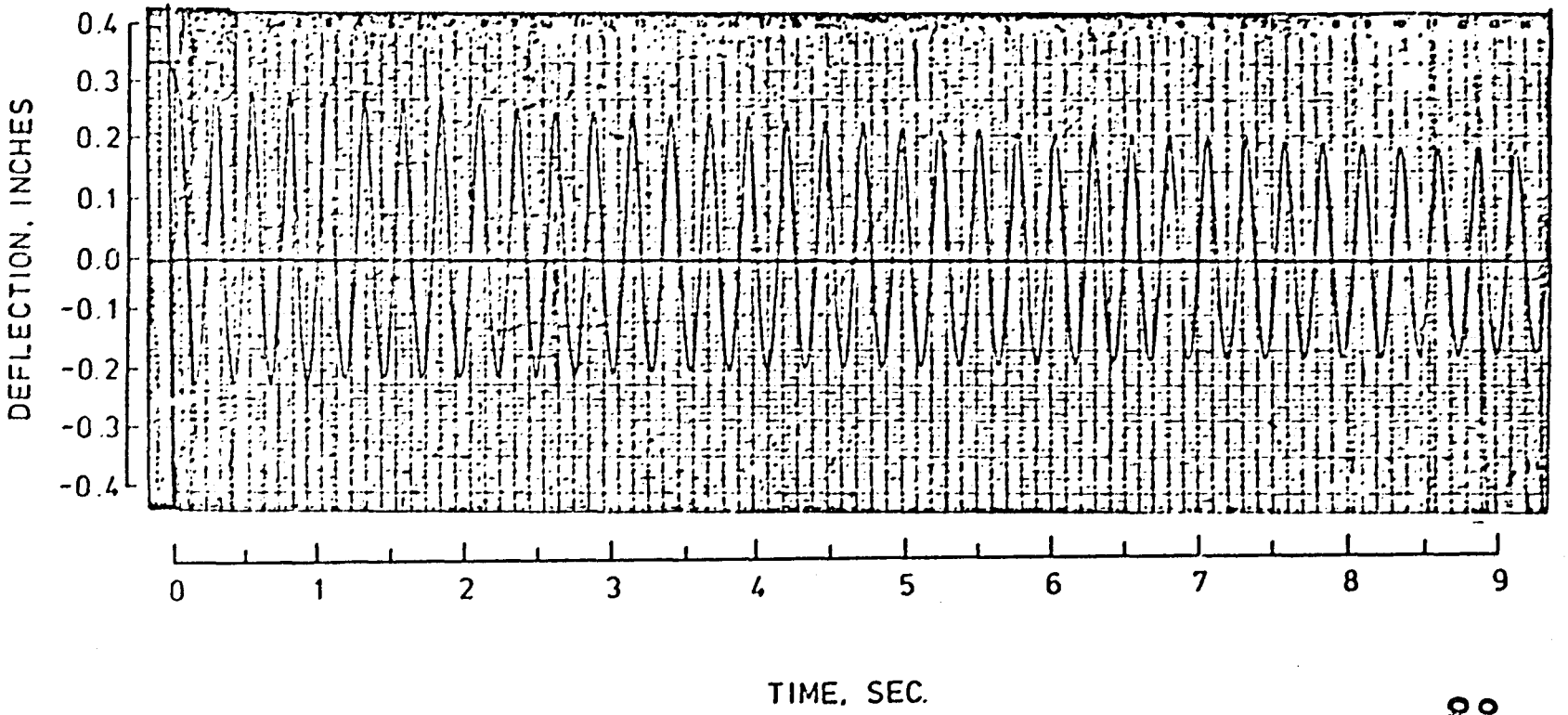

Figure 25. Δ-t plot for Test 31, Table 4, String-Mass Concept with Jam Nuts.

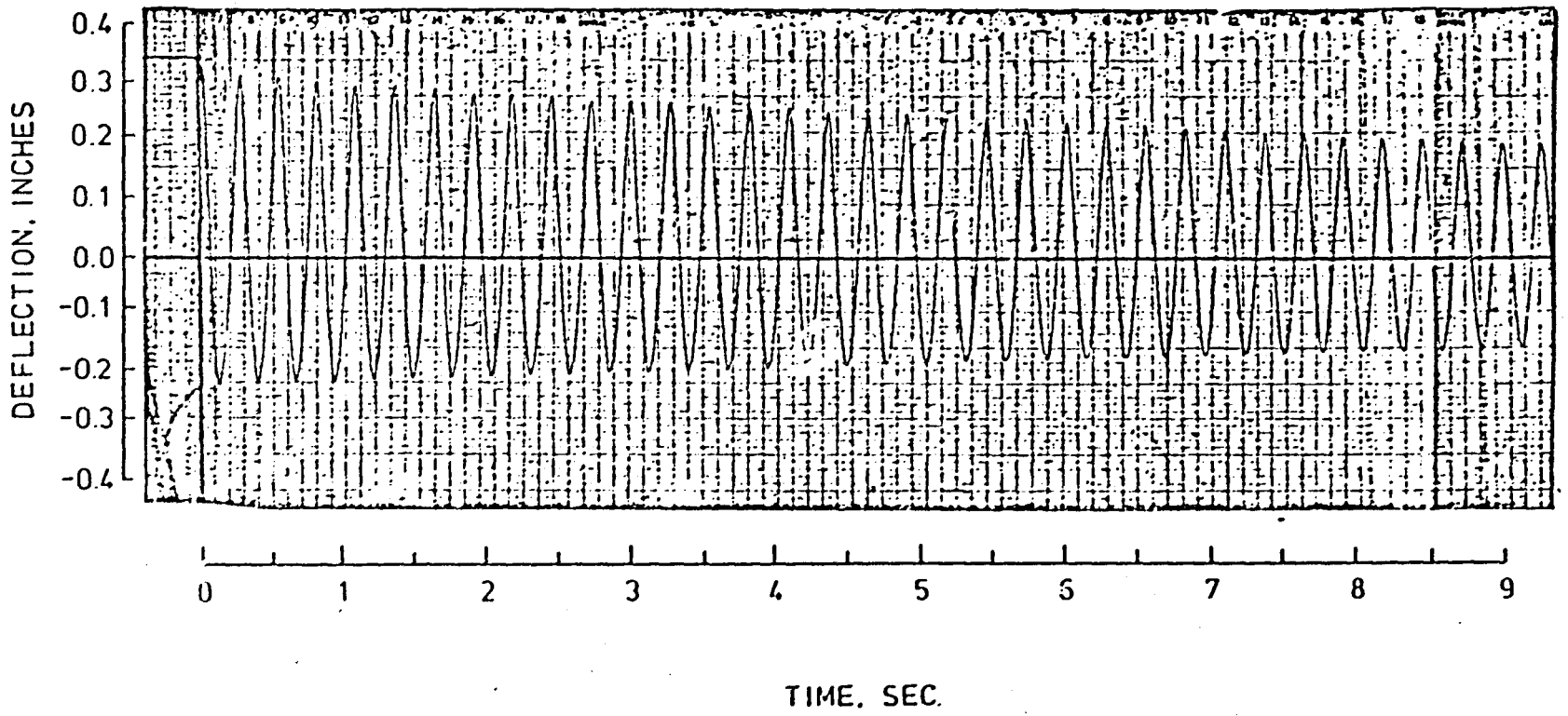

Figure 26. Δ-t plot for Test 34, Table 4, String-Mass Concept with Jam Nuts.

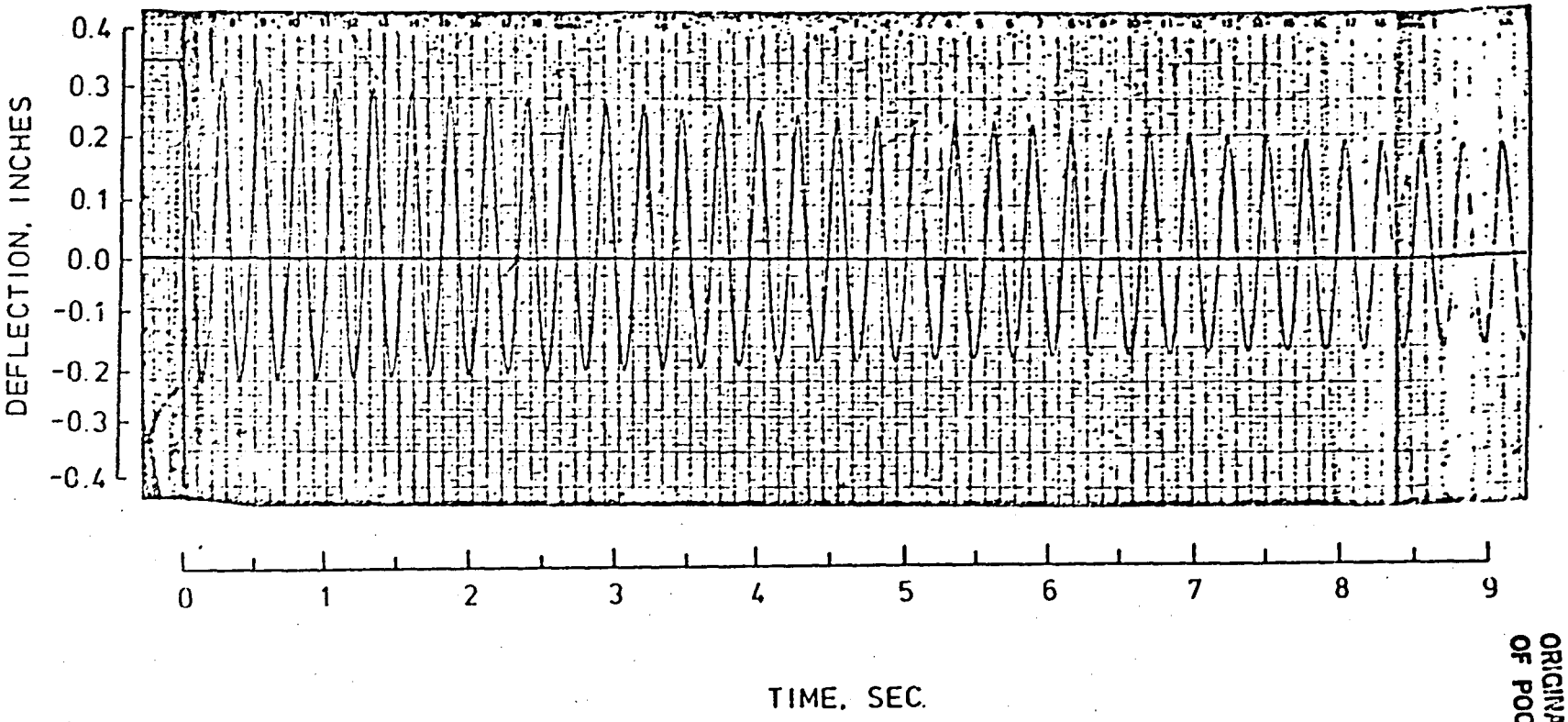

Figure 27. Δ-t plot for Test 37, Table 4, String-Mass Concept with Jam Nuts.

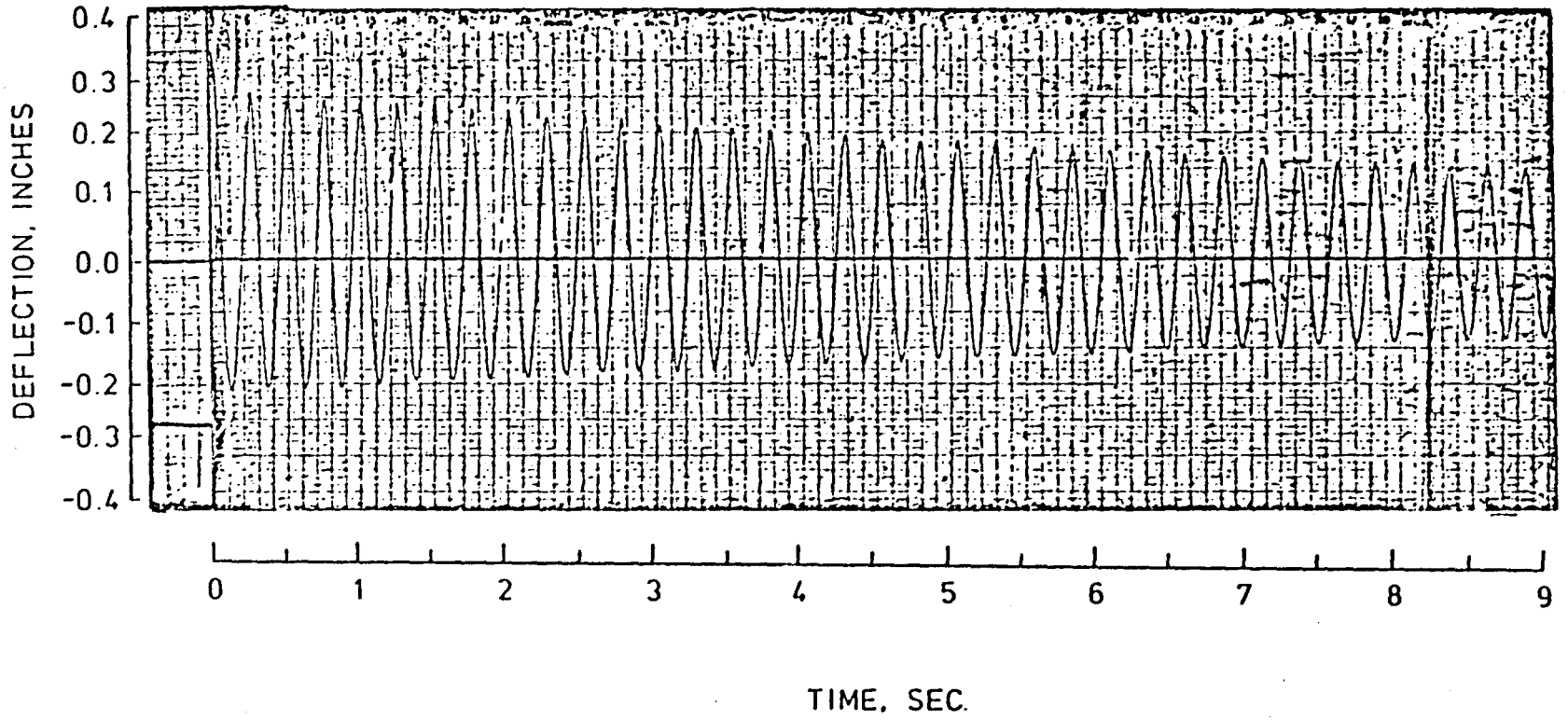

Figure 28. Δ-t plot for Test 40, Table 4, String-Mass Concept with Jam Nuts.

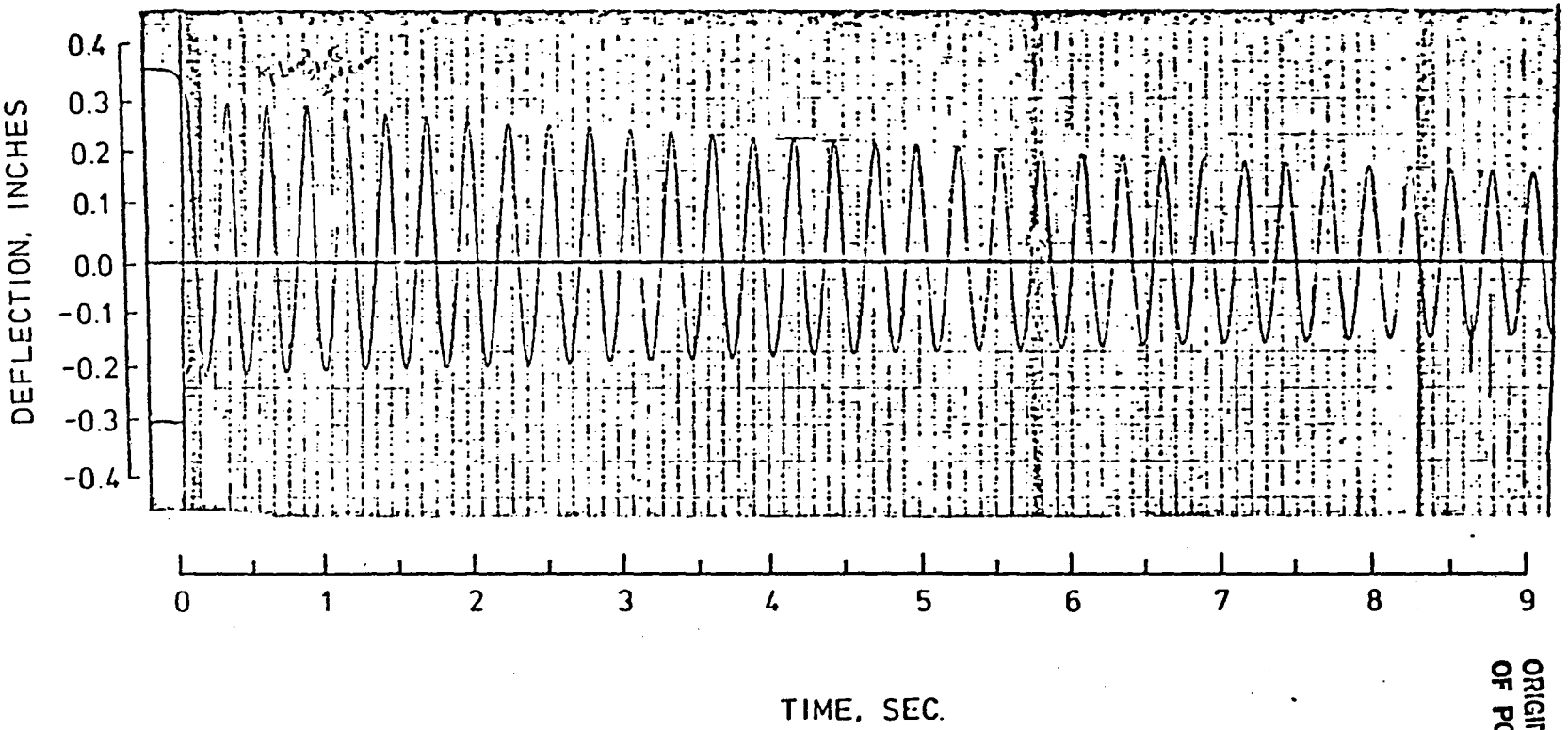

Figure 29. Δ-t plot for Test 43, Table 4, String-Mass Concept with Jam Nuts.

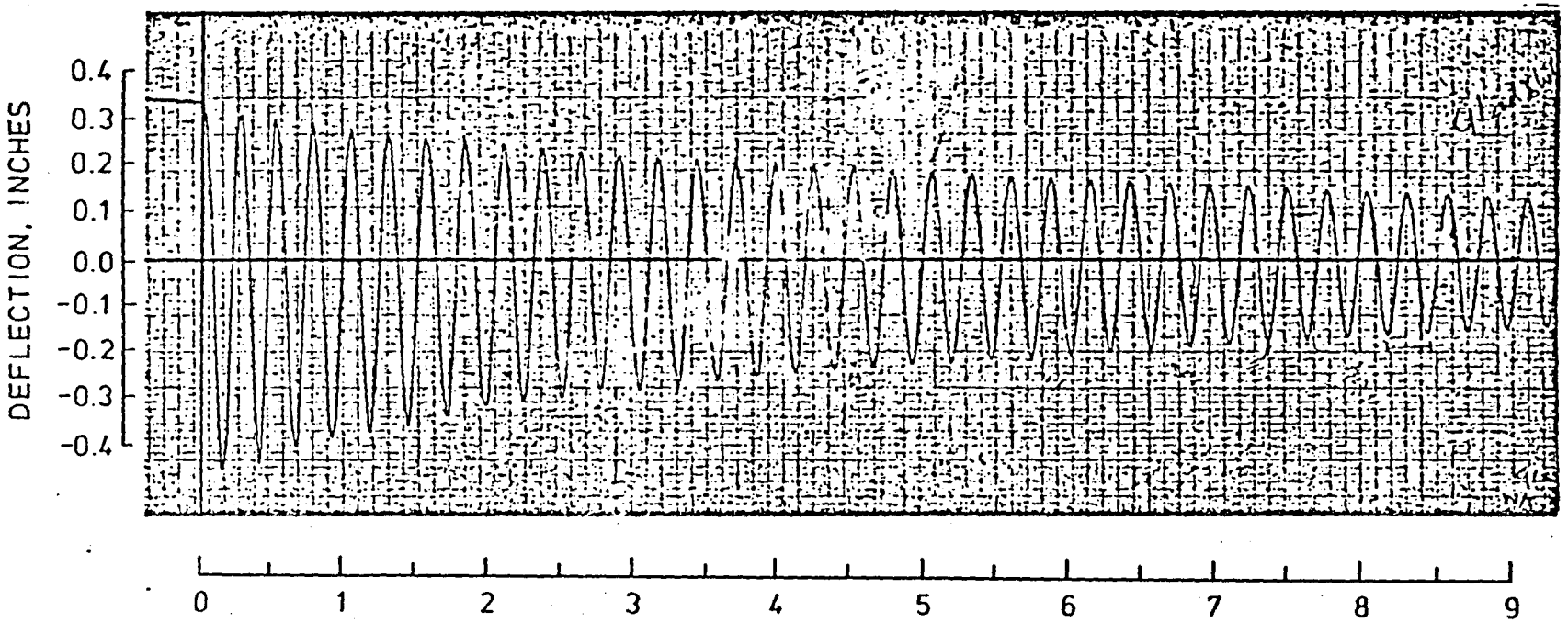

Figure 30. Δ-t plot for Test 46, Table 4, String-Mass Concept with Jam Nuts.

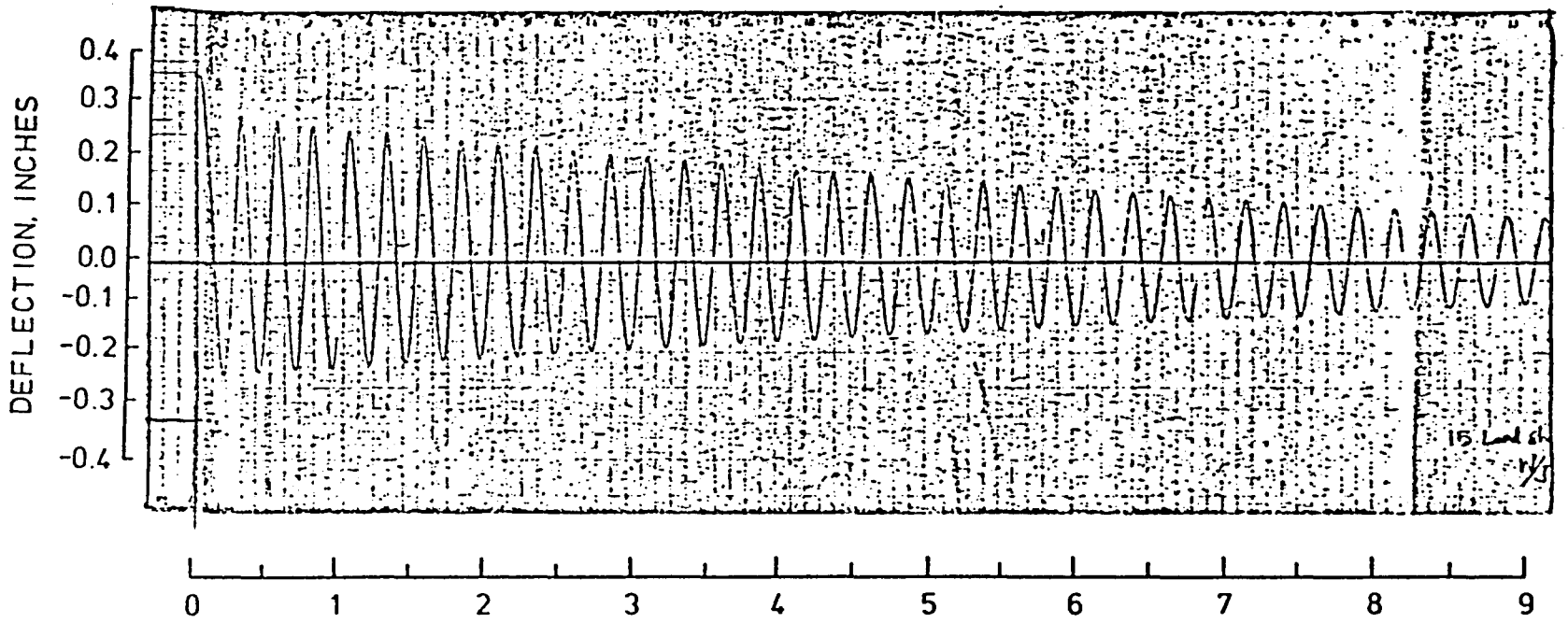

Figure 31. Δ-t plot for Test 49, Table 4, String-Mass Concept with Jam Nuts.

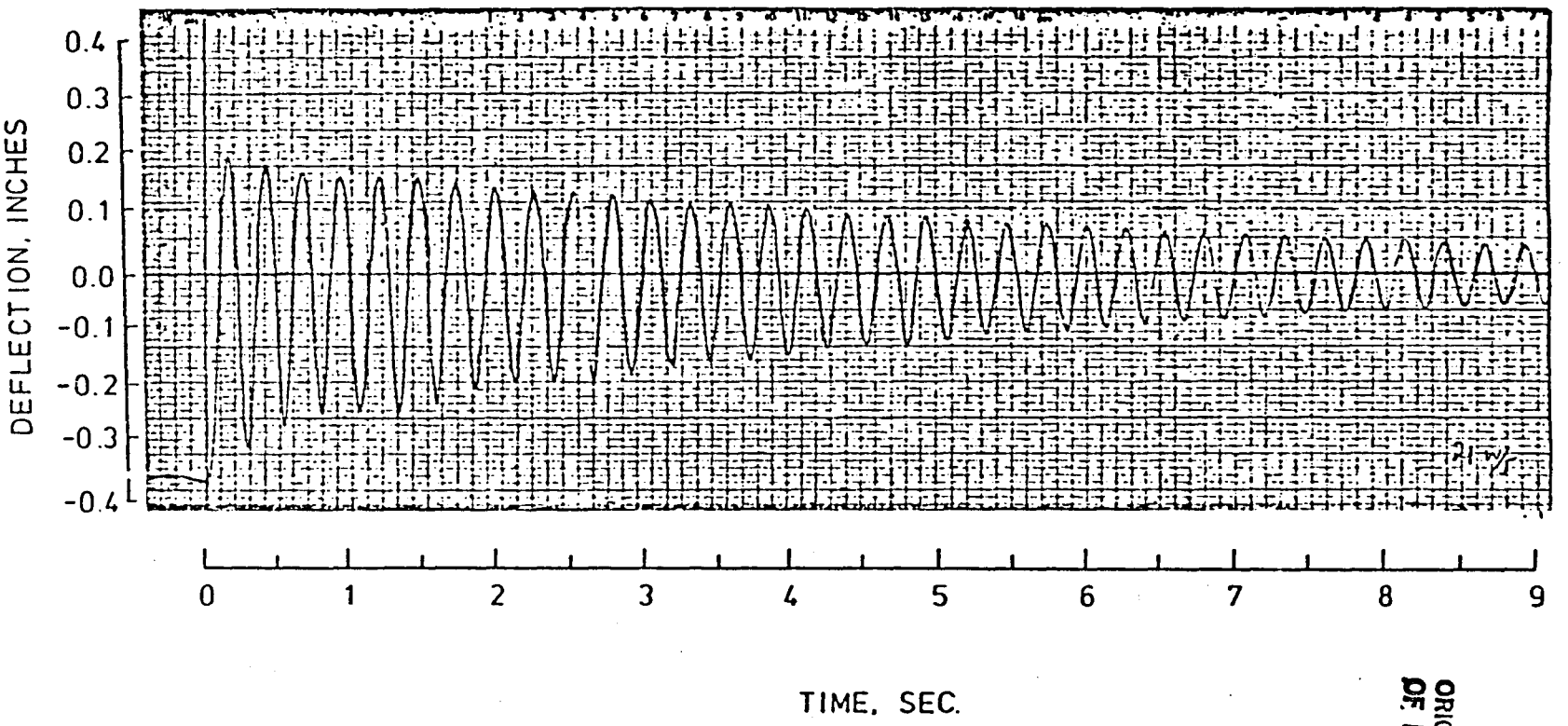

Figure 32. Δ-t plot for Test 52, Table 4, String-Mass Concept with Jam Nuts.

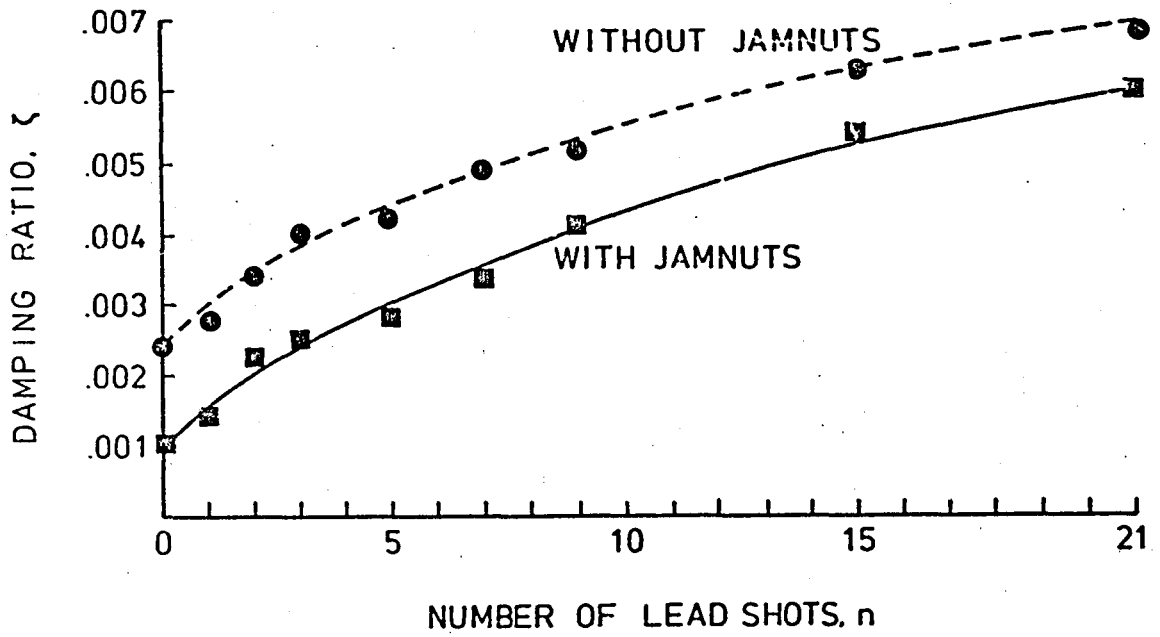

Figure 33. Effect of Connection Friction on ζ-n Relationship with Lead Shots at Midheight.

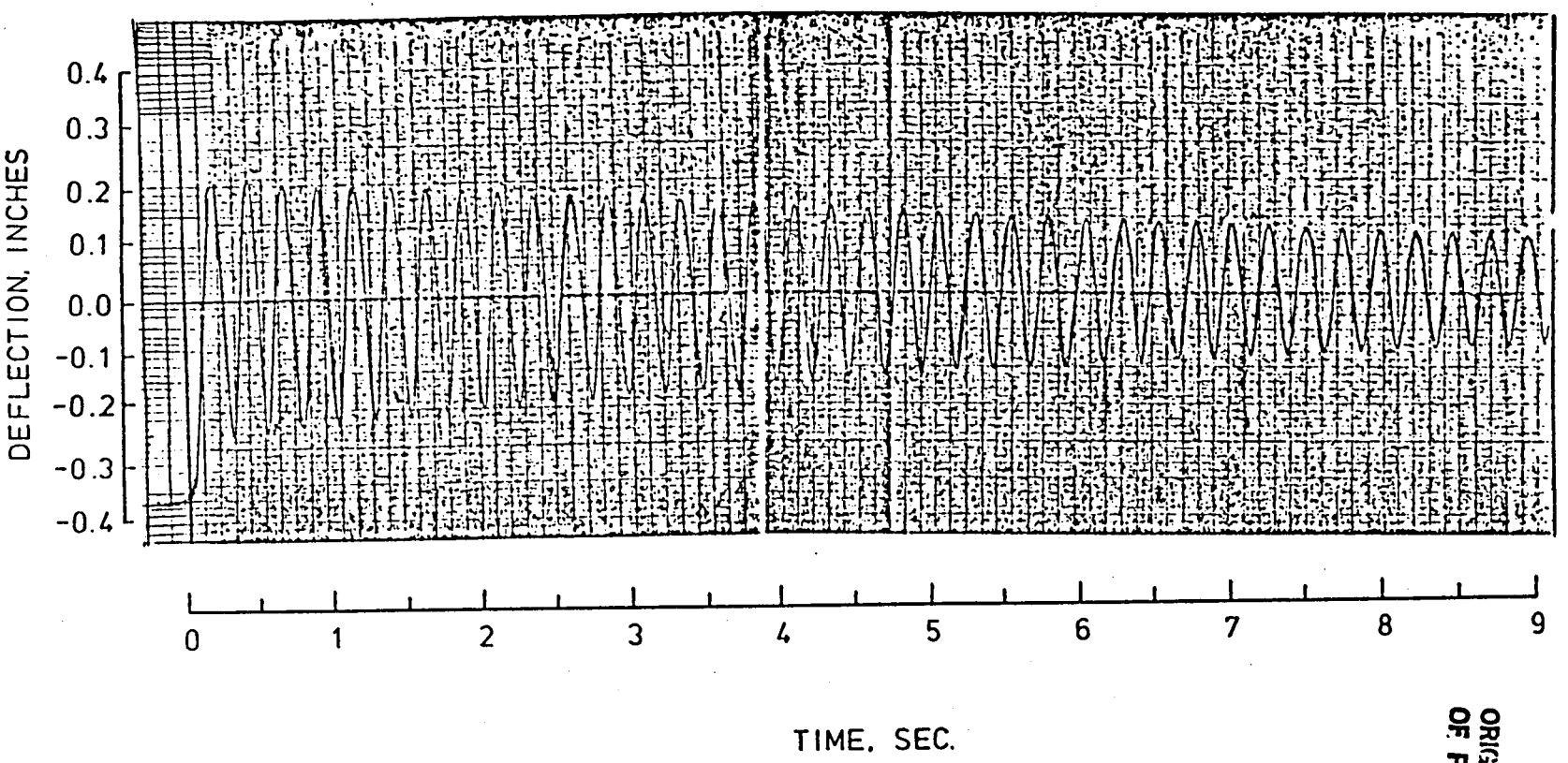

Figure 34. Δ-t plot for Test 55, Table 5, String-Mass Concept, Equidistant Lead Shots.

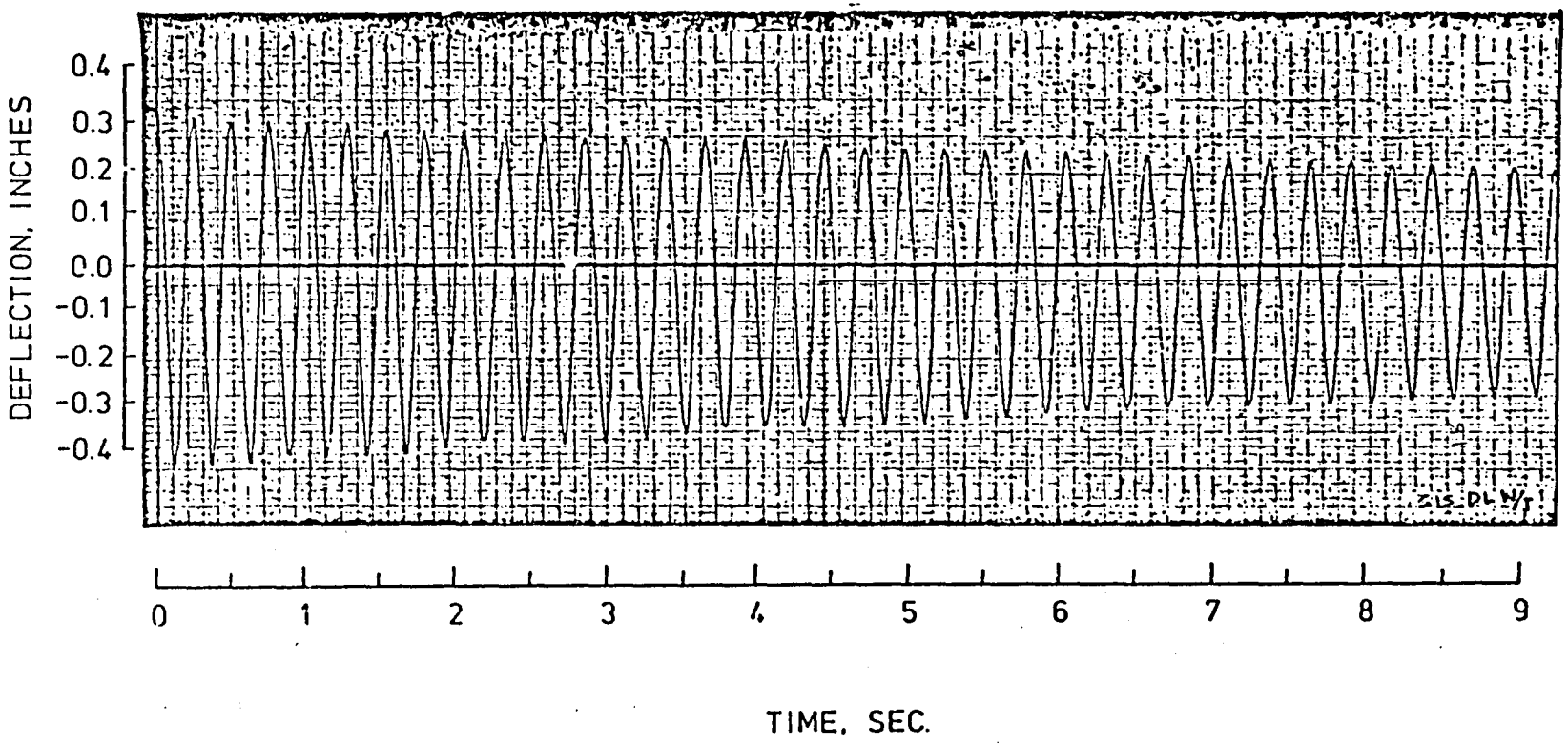

Figure 35. Δ-t plot for Test 58, Table 5, String-Mass Concept, Equidistant Lead Shots.

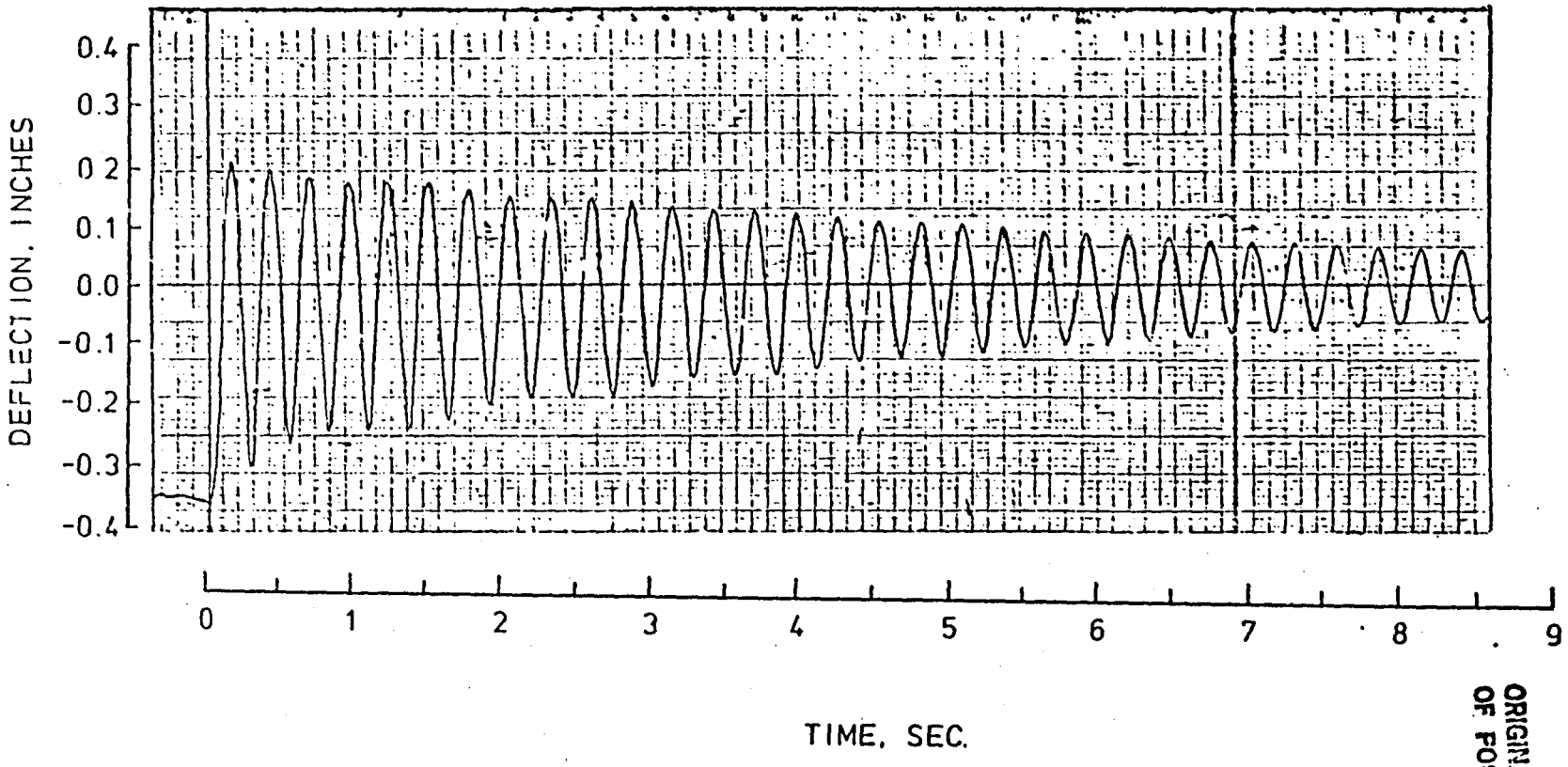

Figure 36. Δ-t plot for Test 61, Table 5, String-Mass Concept, Equidistant Lead Shots.

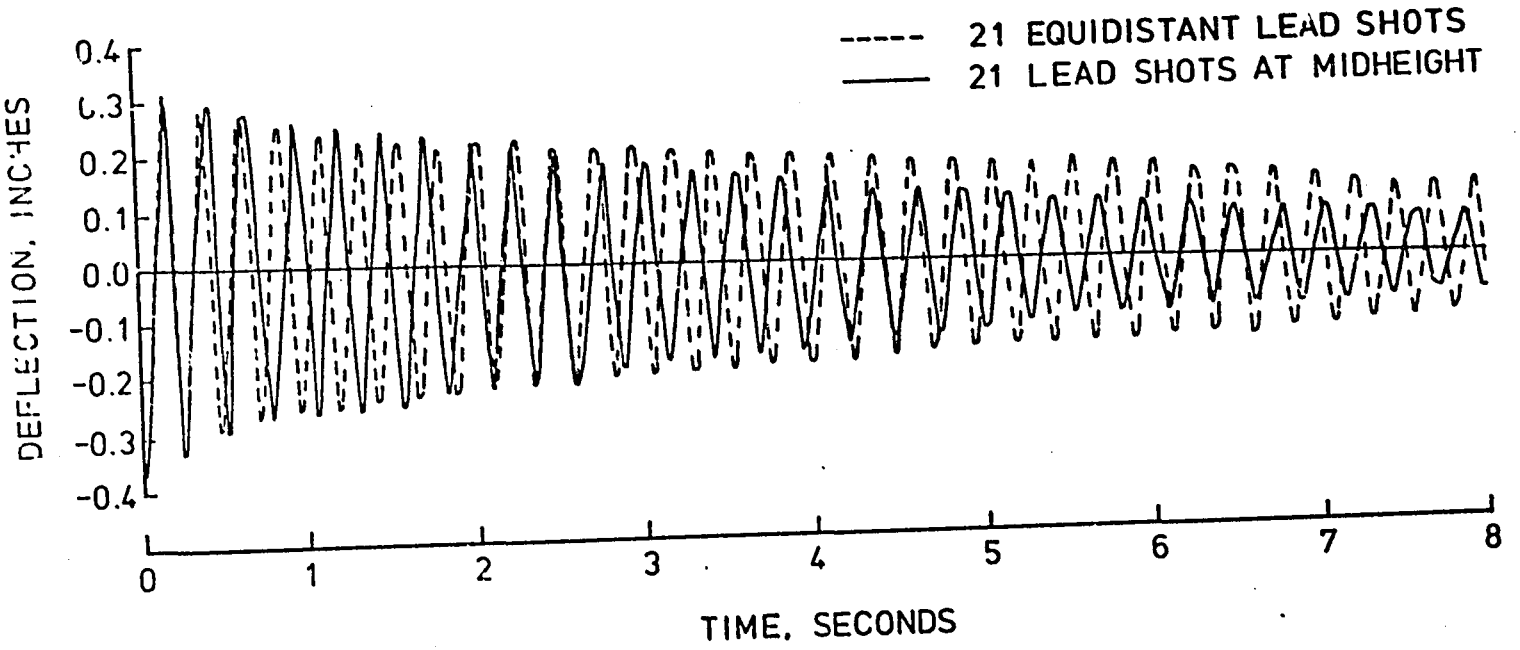

Figure 37. Comparison of Experimental Δ-t Plots for 21 Lead Shots at Center and at L/22.

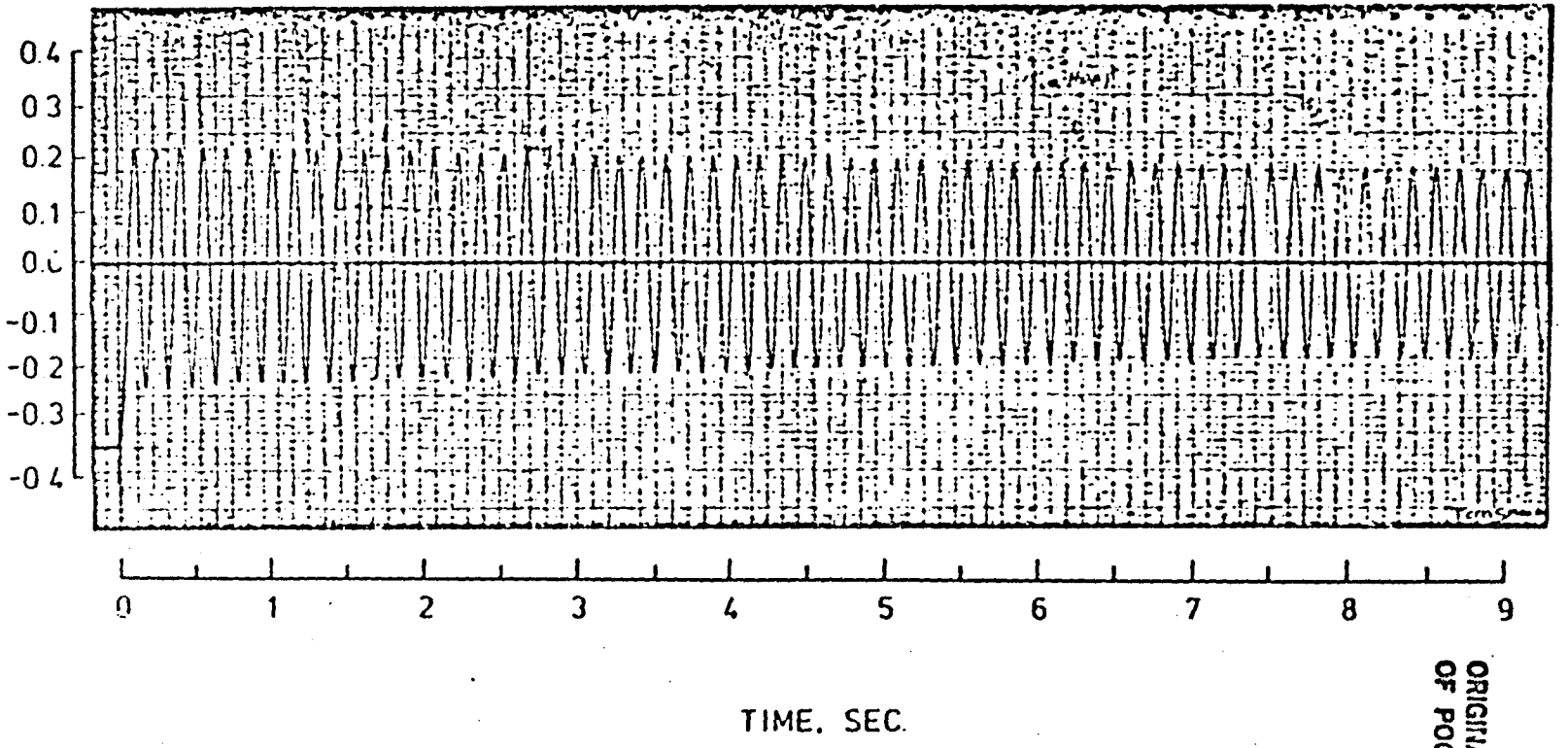

Figure 38. Δ-t plot for Test 64, Table 6, Effect of Axial Force (P = -155.0 lb)

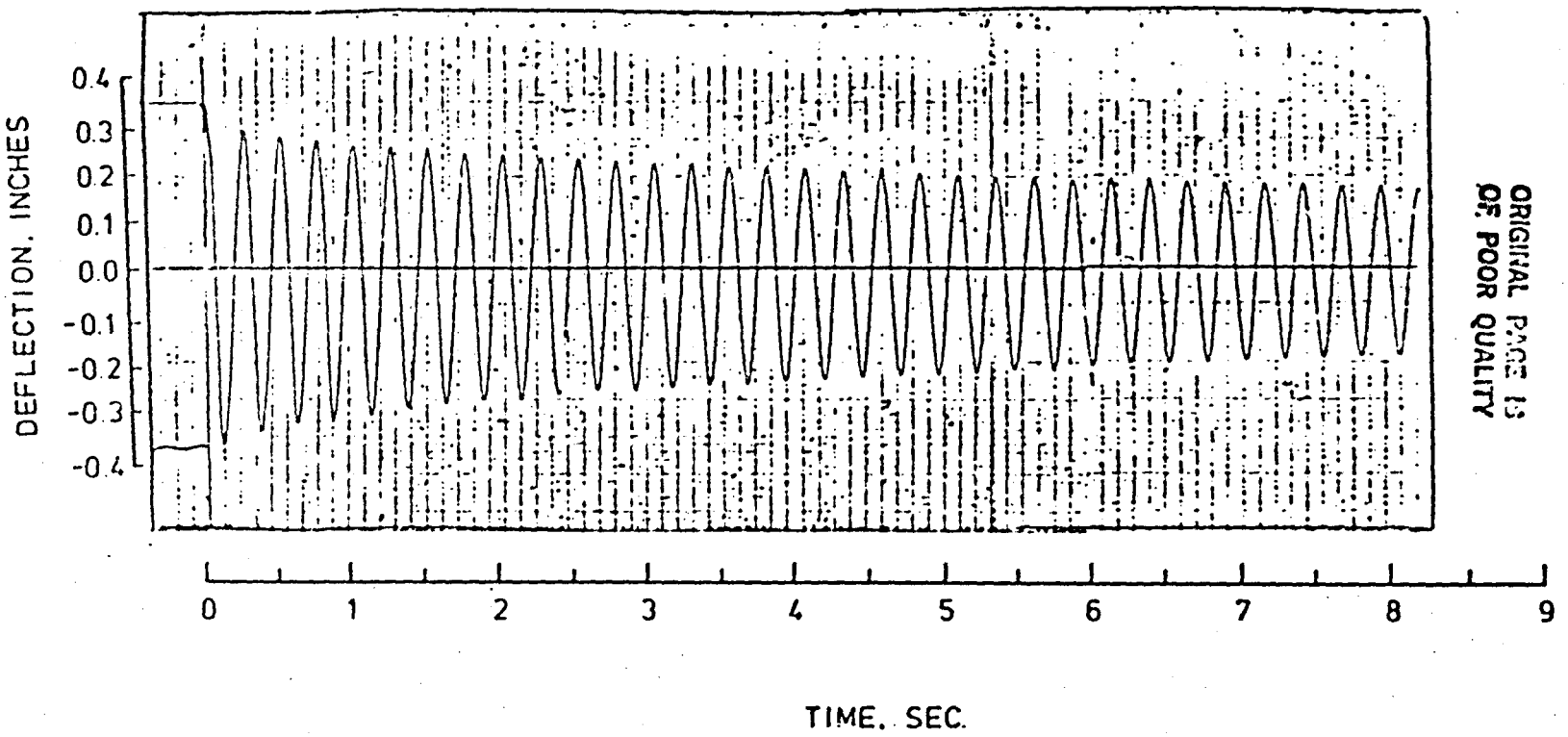

Figure 39. Δ-t plot for Test 67, Table 6, Effect of Axial Force (P = -19.0 lb)

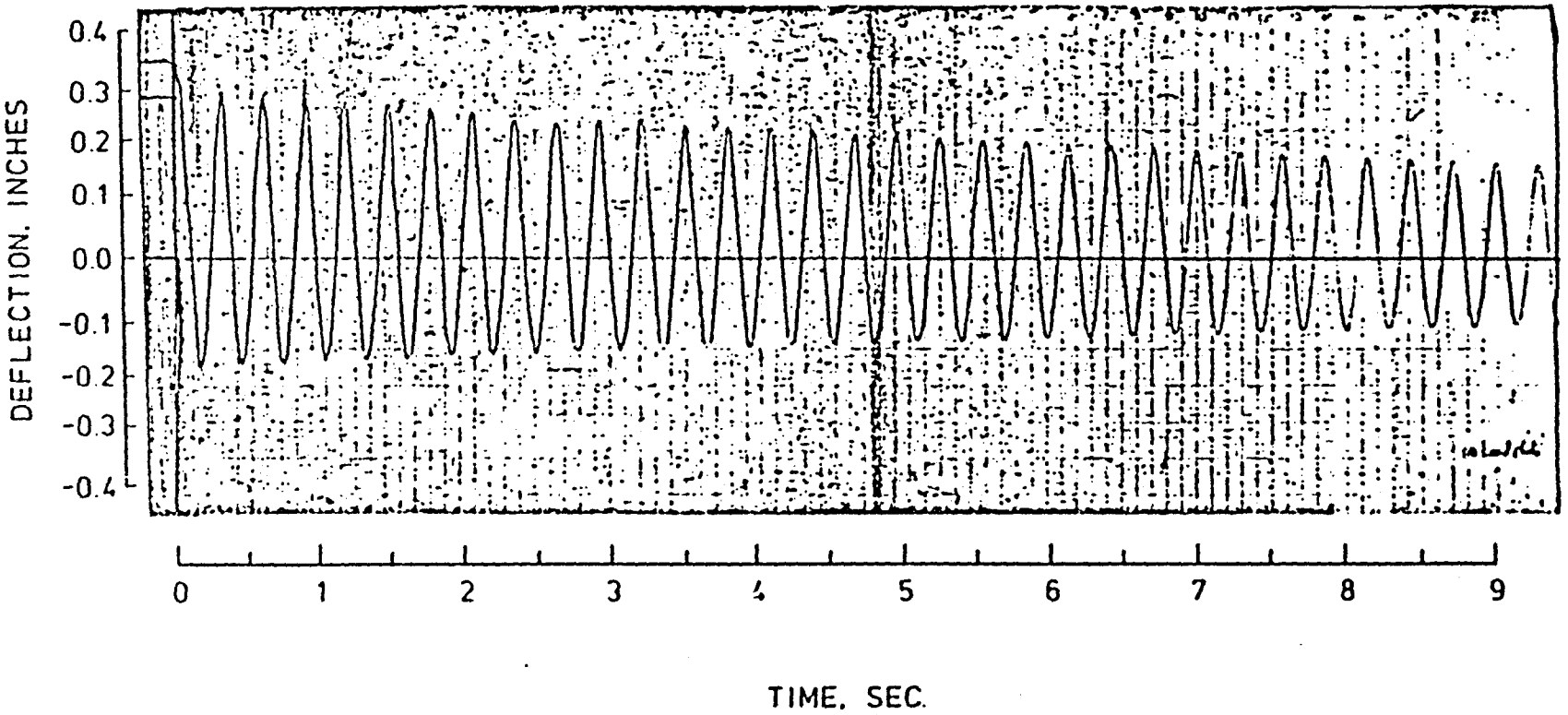

Figure 40. Δ-t plot for Test 70, Table 6, Effect of Axial Force (P = -4.5 lb)

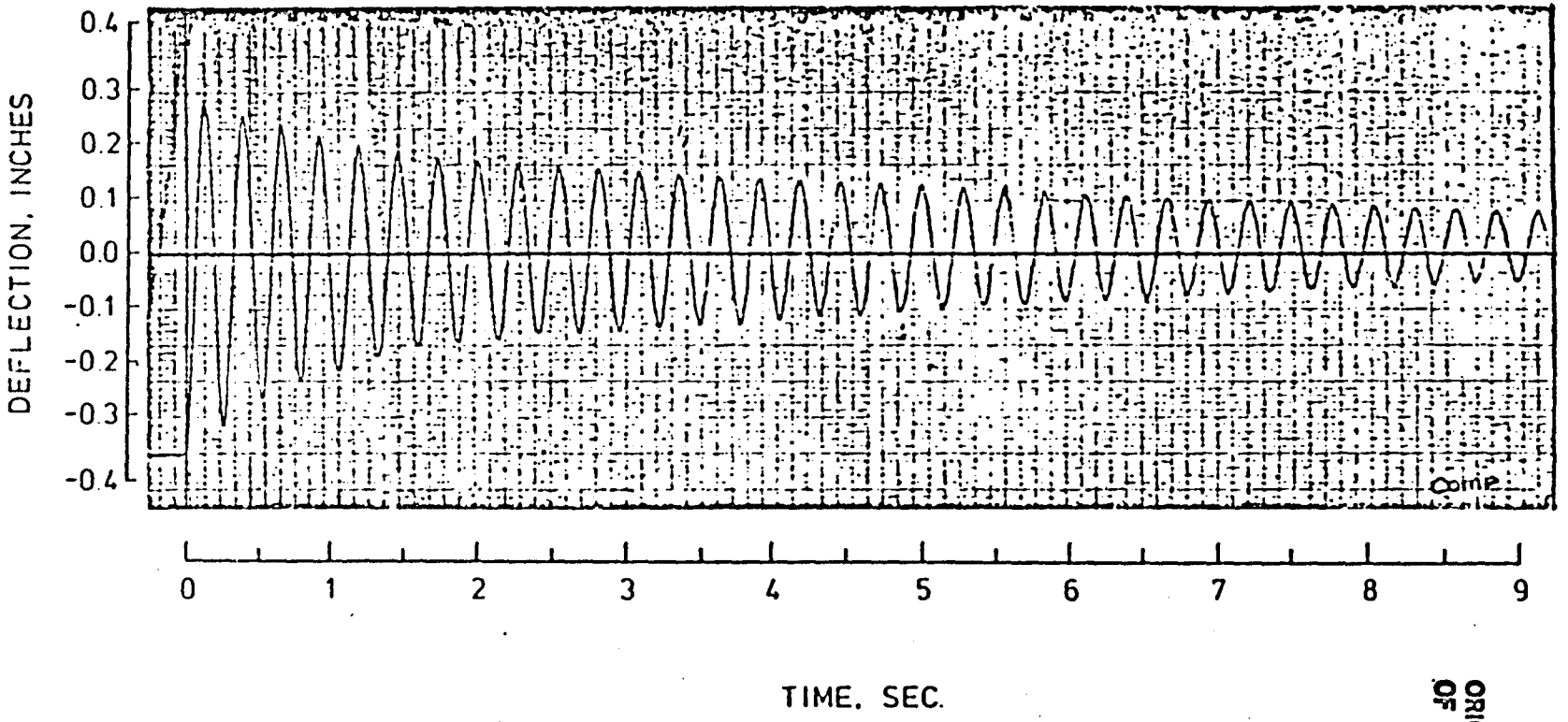

Figure 41. Δ-t plot for Test 73, Table 6, Effect of Axial Force (P = +10.0 lb)

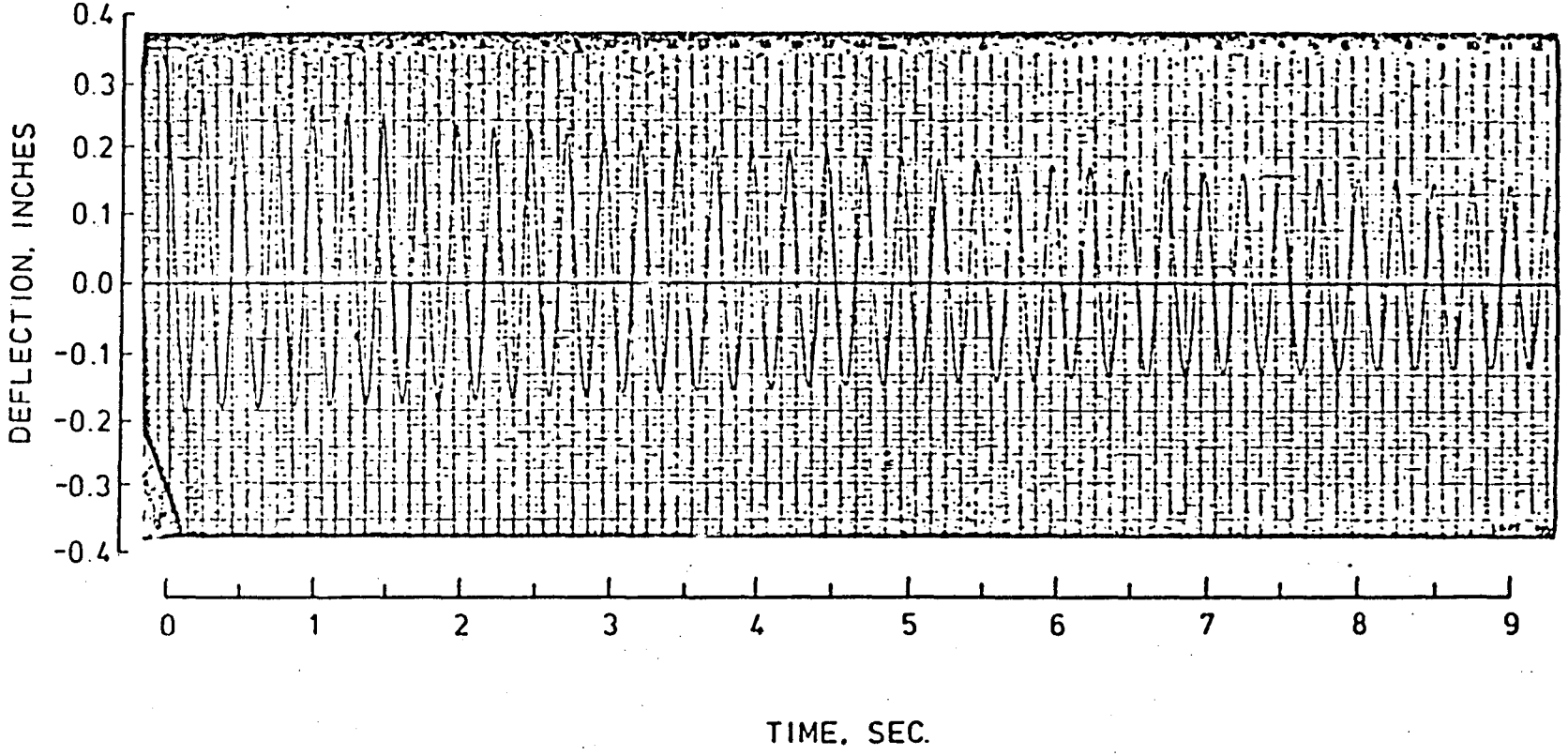

Figure 42. Δ-t plot for Test 76, Table 7, Polyethylene Tubing Concept (a).

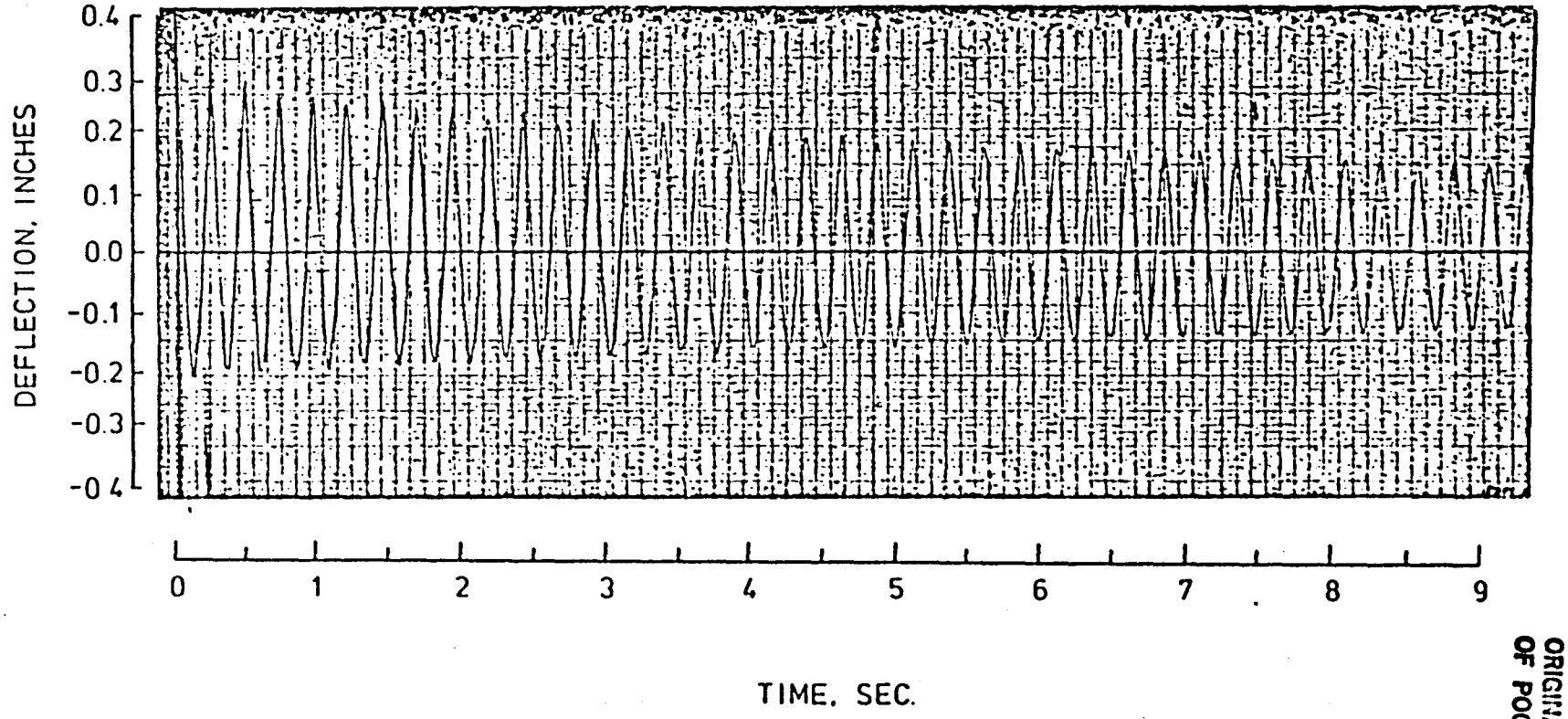

Figure 43. Δ-t plot for Test 79, Table 7, Polyethylene Tubing Concept (b).

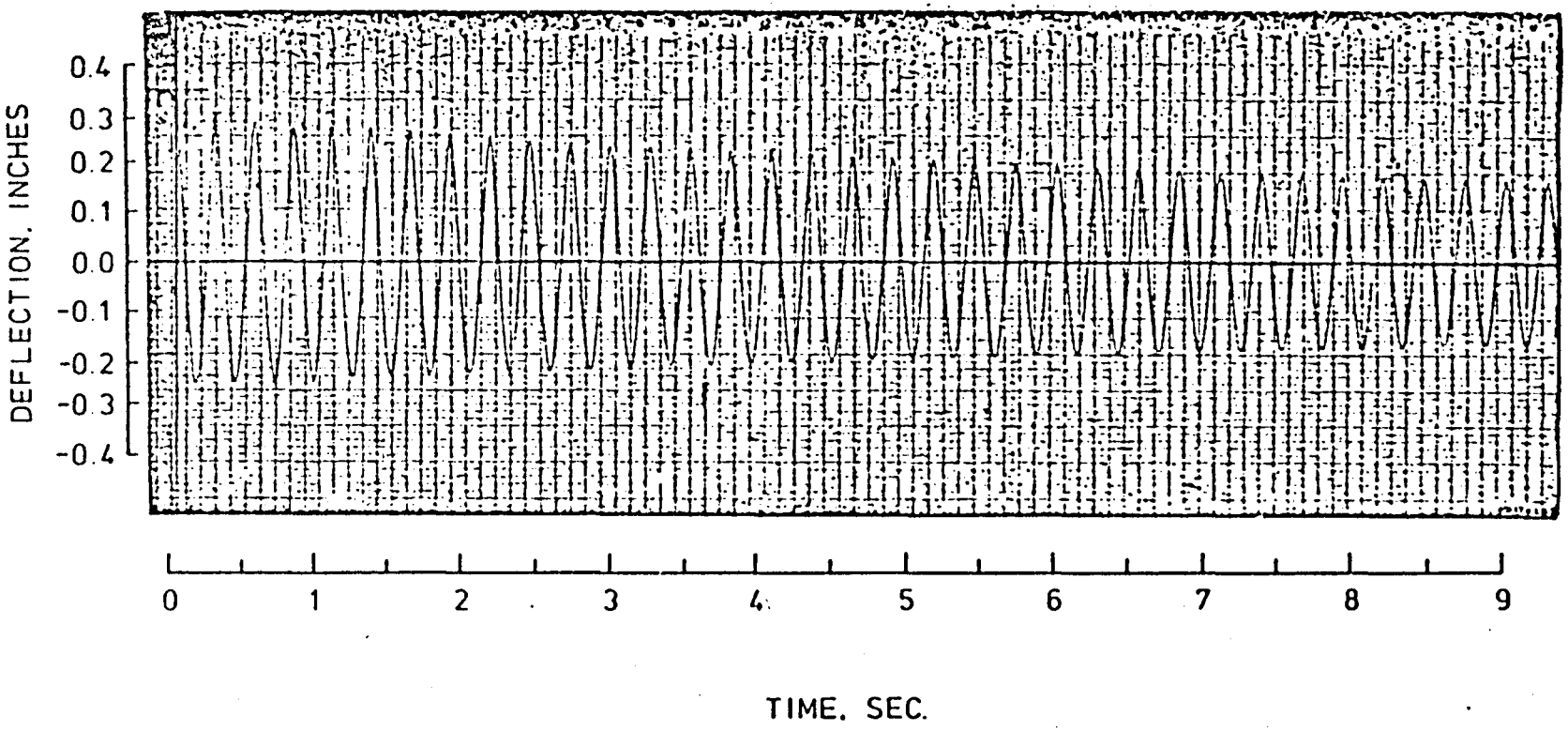

Figure 44. Δ-t plot for Test 82, Table 7, Polyethylene Tubing Concept (c).

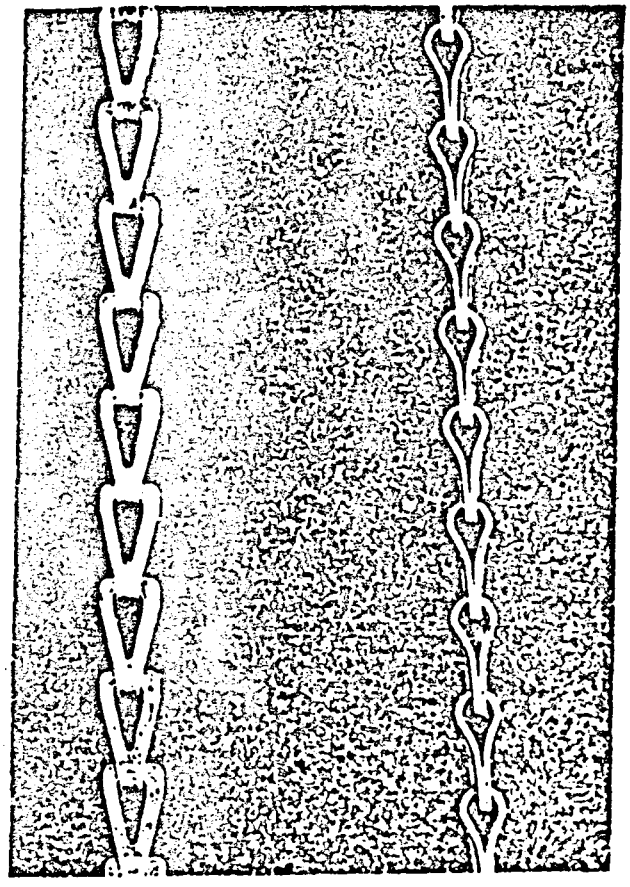

Figure 45. Details of Chain Links.

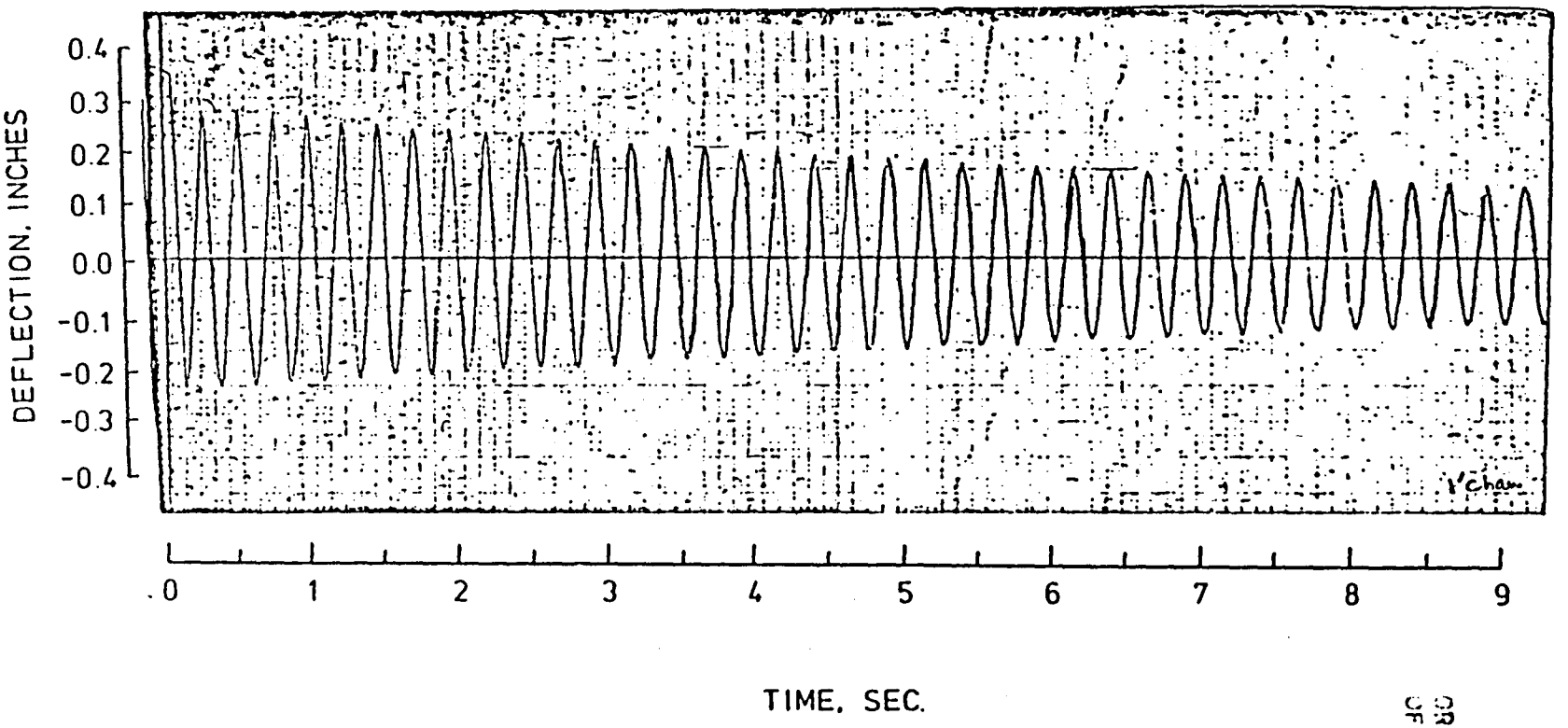

Figure 46. Δ-t plot for Test 85, Table 8, Chain Damping Concept (1 ft. Chain).

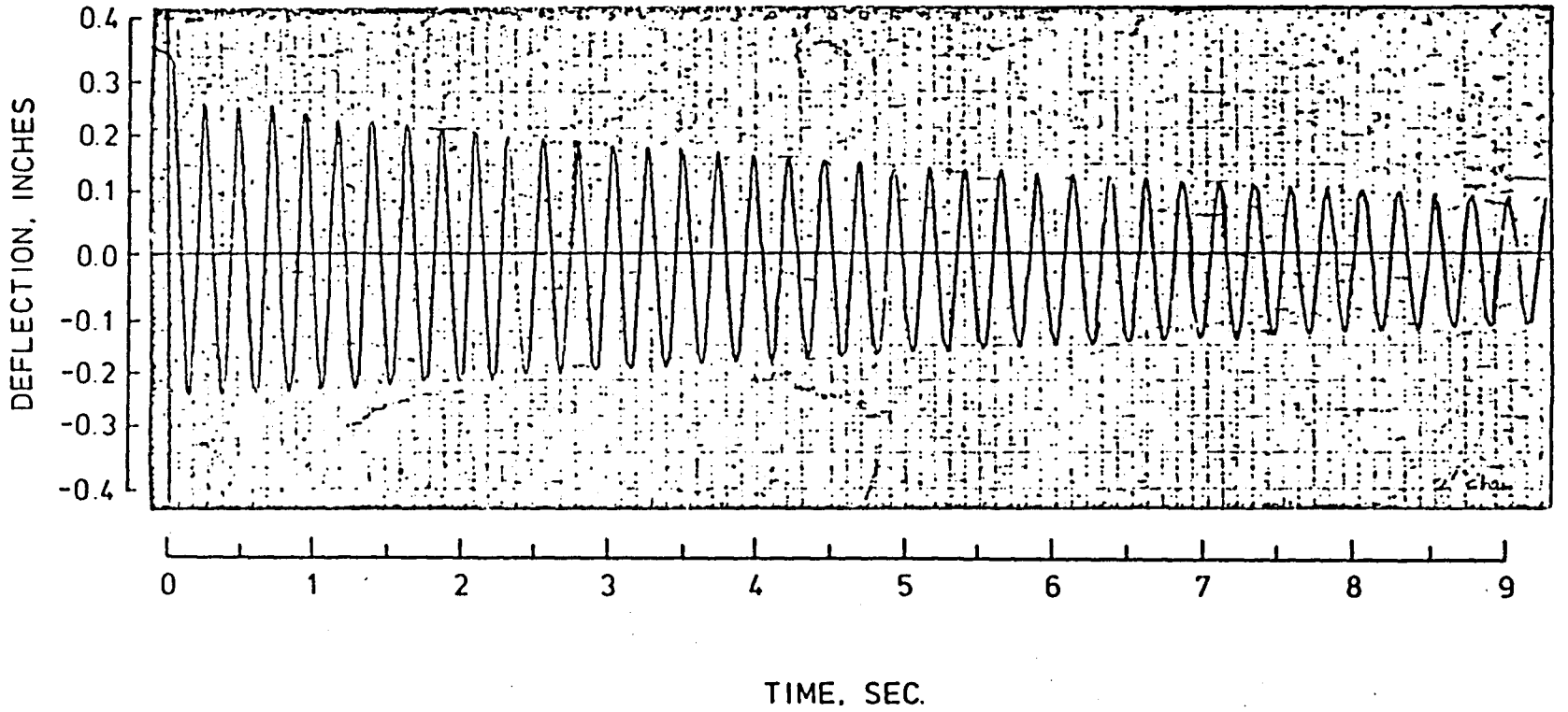

Figure 47. Δ-t plot for Test 88, Table 8, Chain Damping Concept (2 ft. Chain).

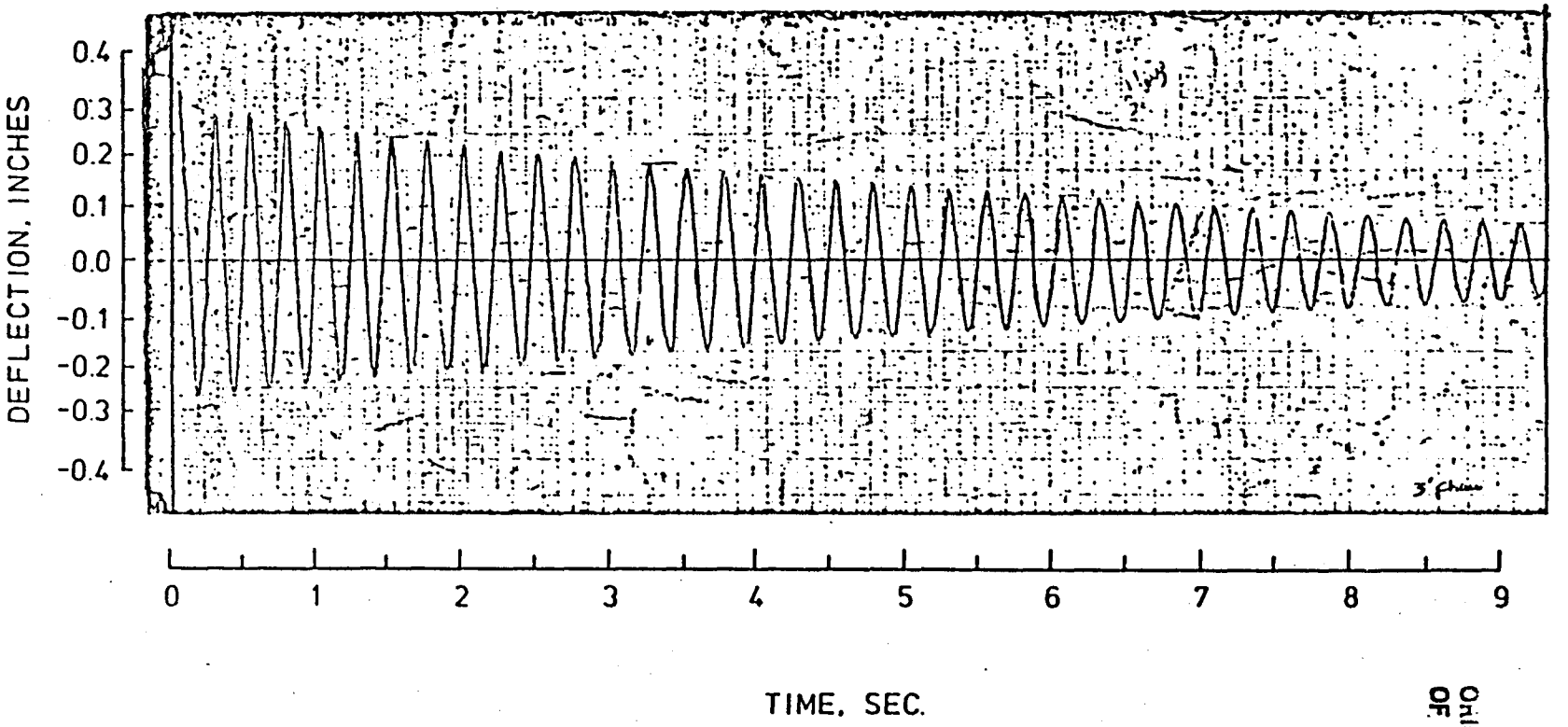

Figure 48. Δ-t plot for Test 91, Table 8, Chain Damping Concept (3 ft. Chain).

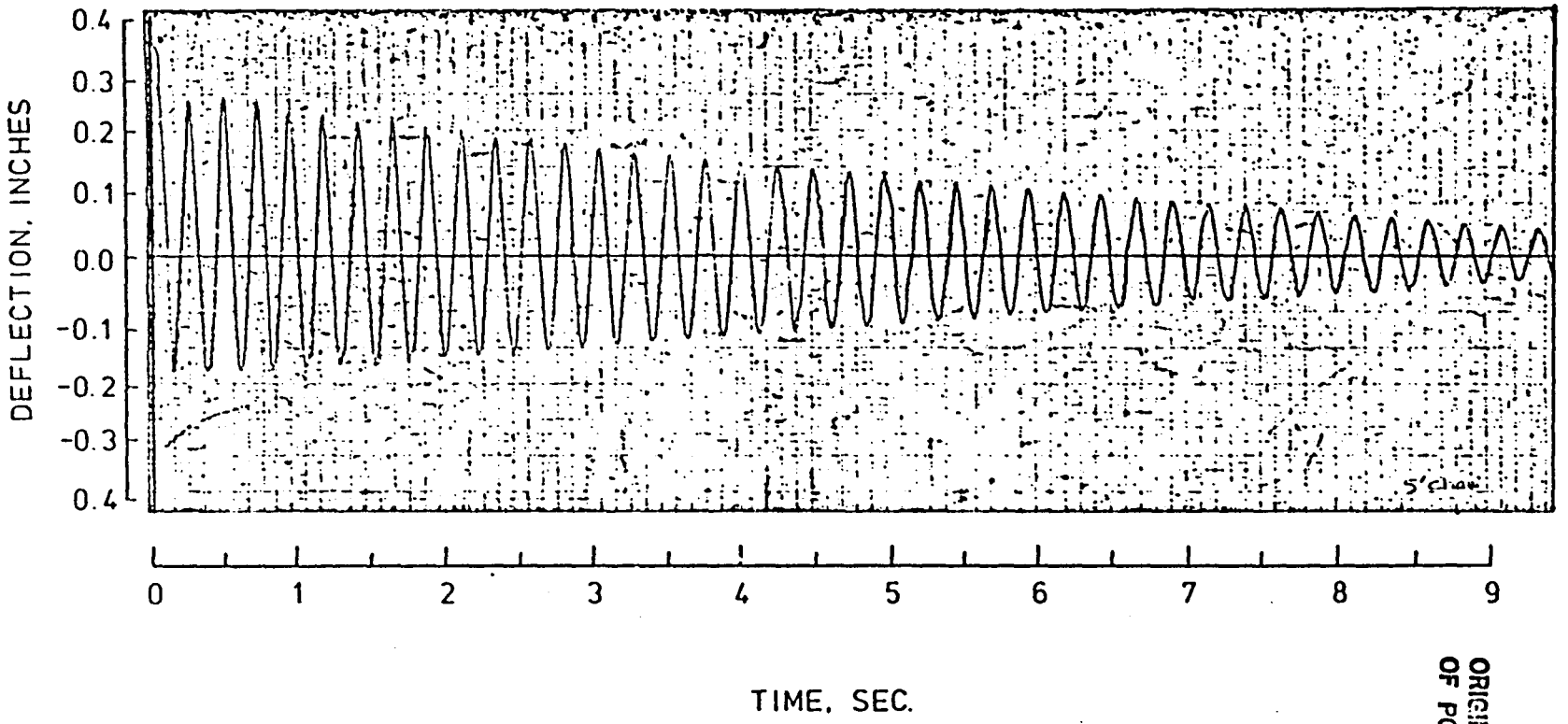

Figure 49. Δ-t plot for Test 94, Table 8, Chain Damping Concept (5 ft. Chain).

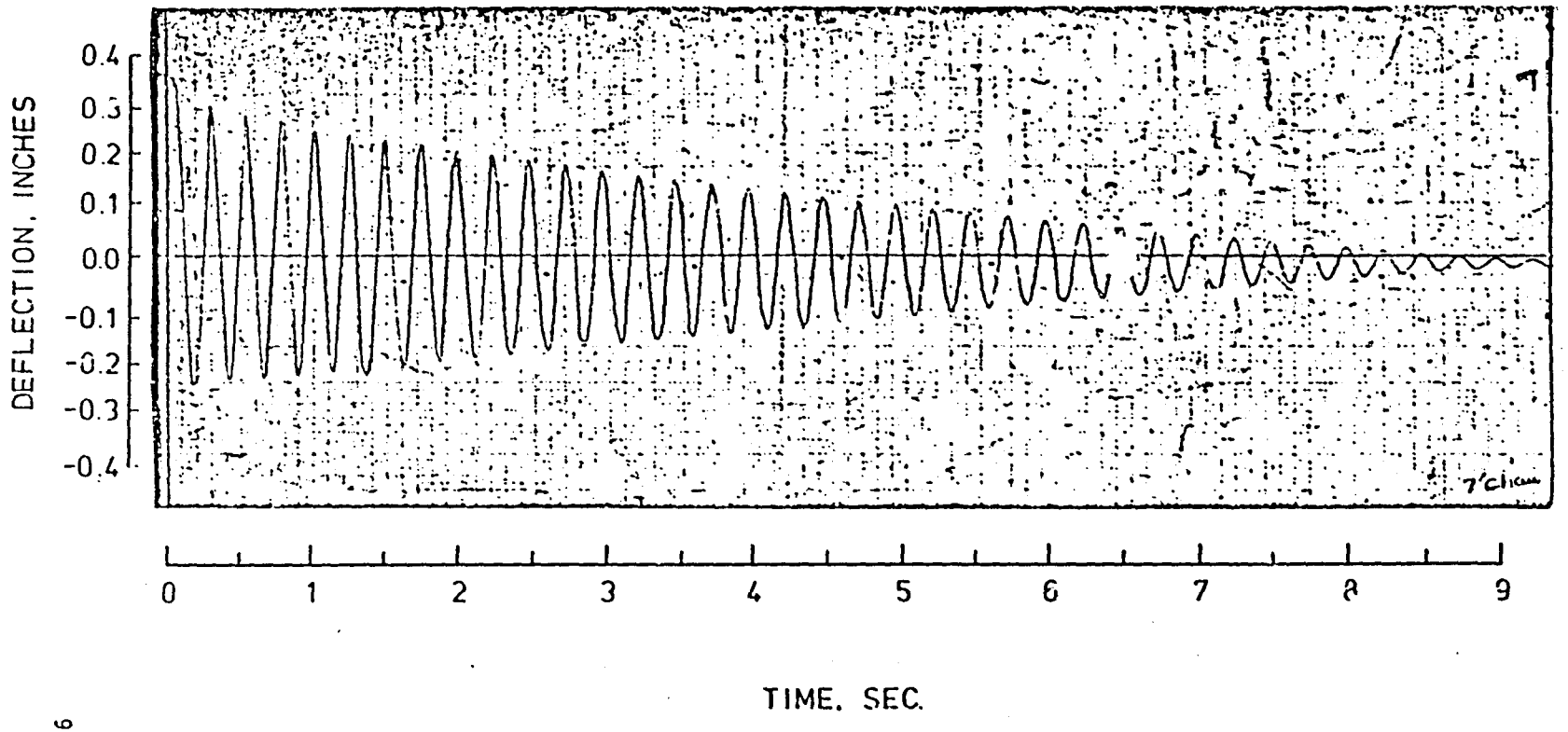

Figure 50. Δ-t plot for Test 97, Table 8, Chain Damping Concept (7 ft. Chain).

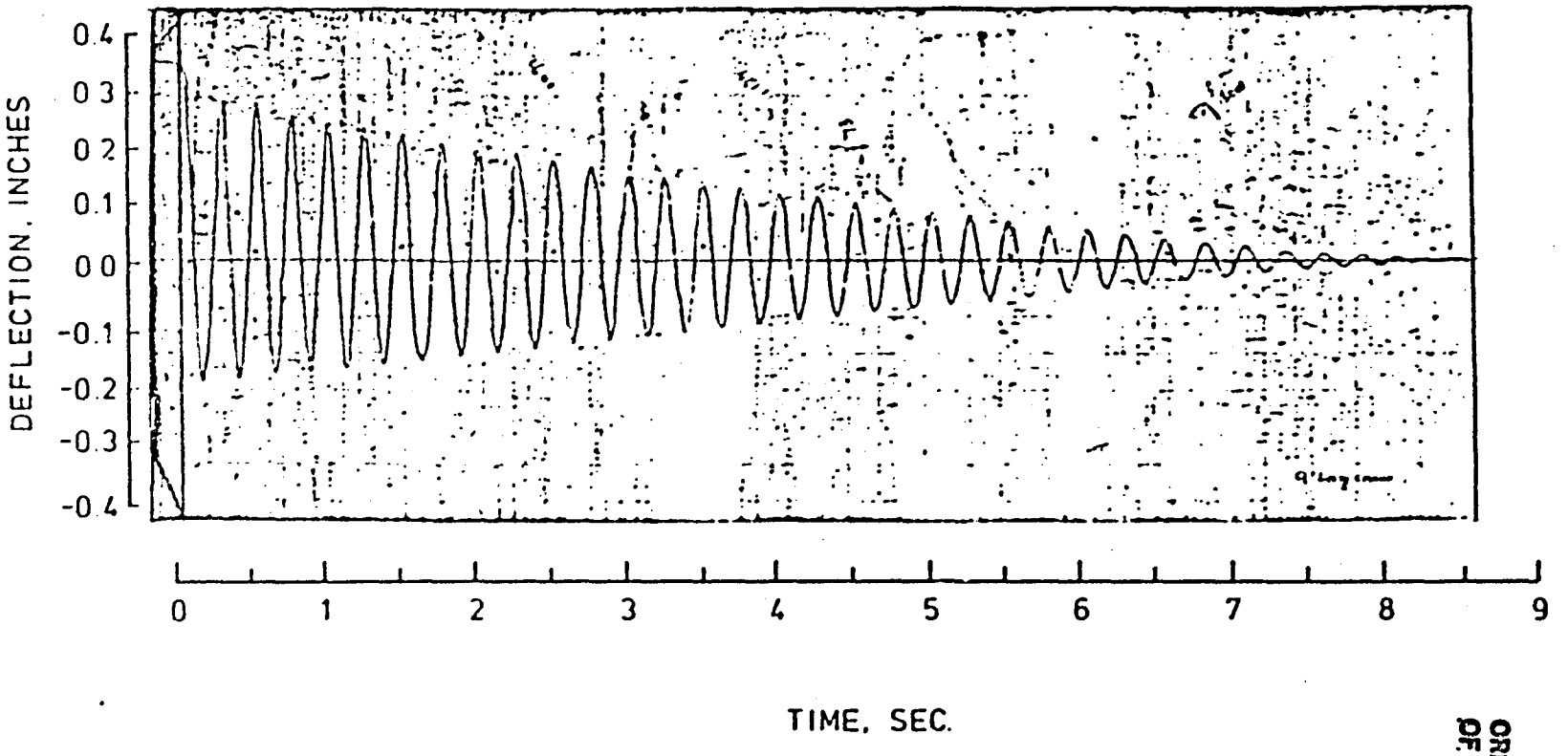

Figure 51. A-t plot for Test 100, Table 8, Chain Damping Concept (9 ft. Chain).

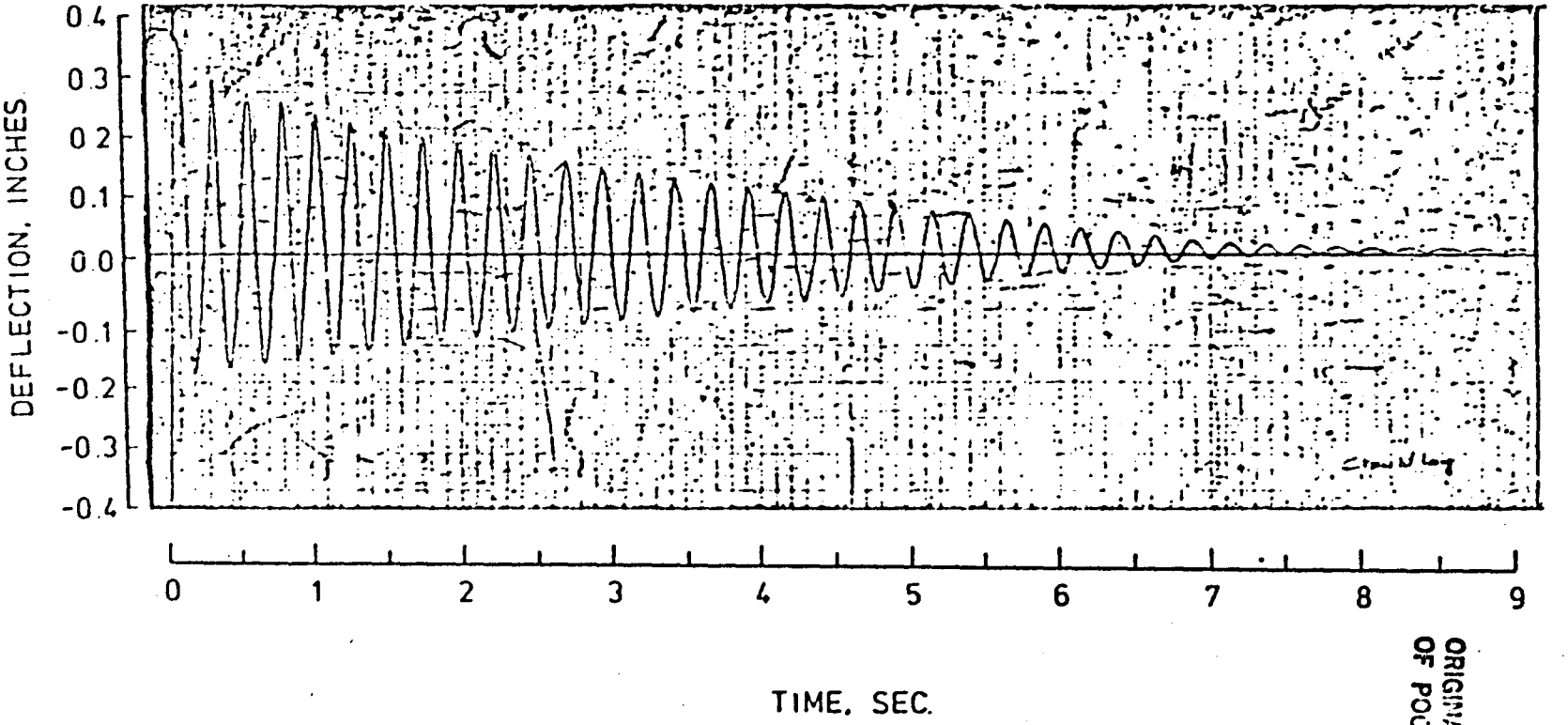

Figure 52. Δ-t plot for Test 103, Table 8, Chain Damping Concept (10 ft. Chain).

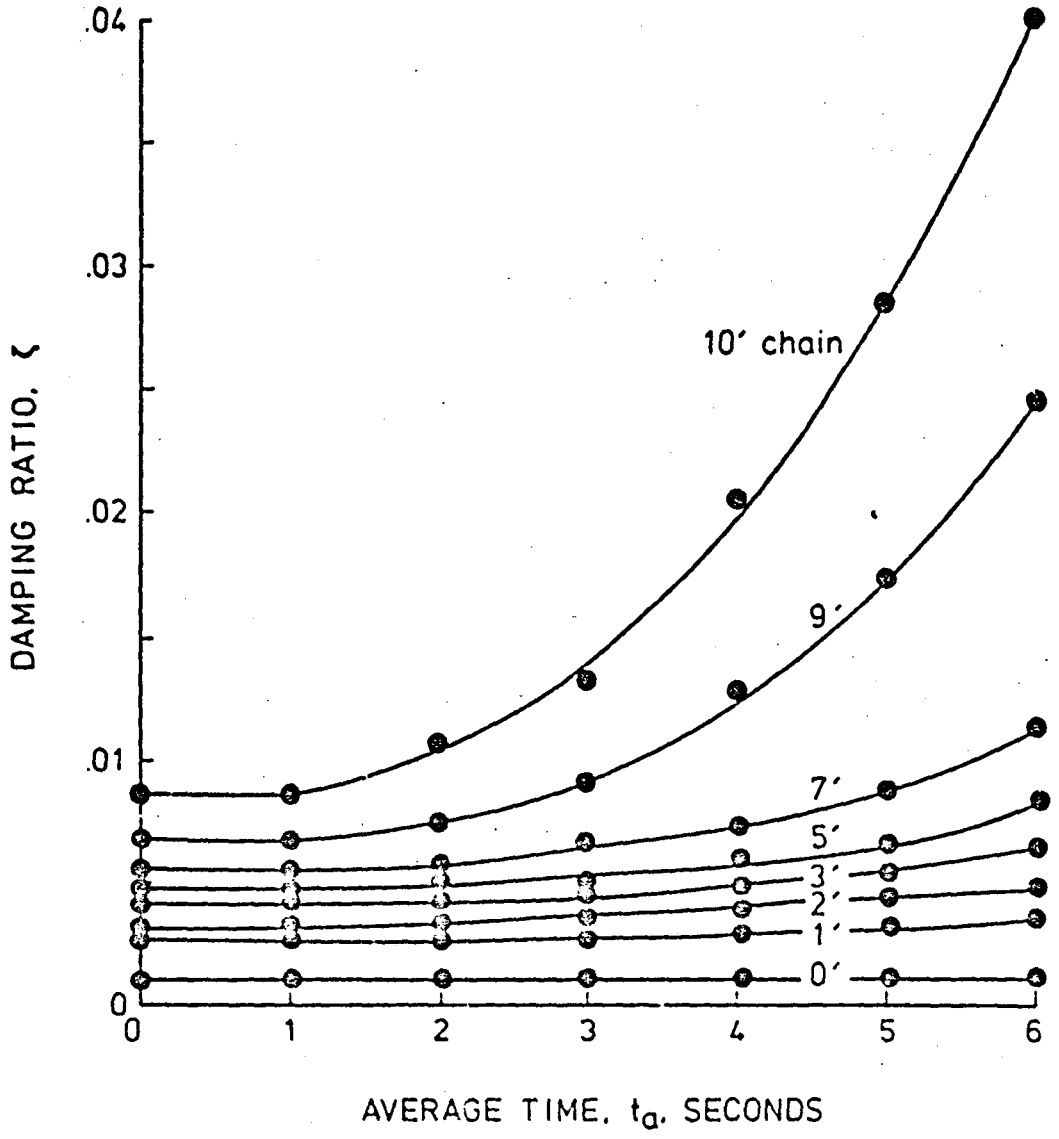

Figure 53. Effect of Chain Length on Damping Ratio for Average Time.

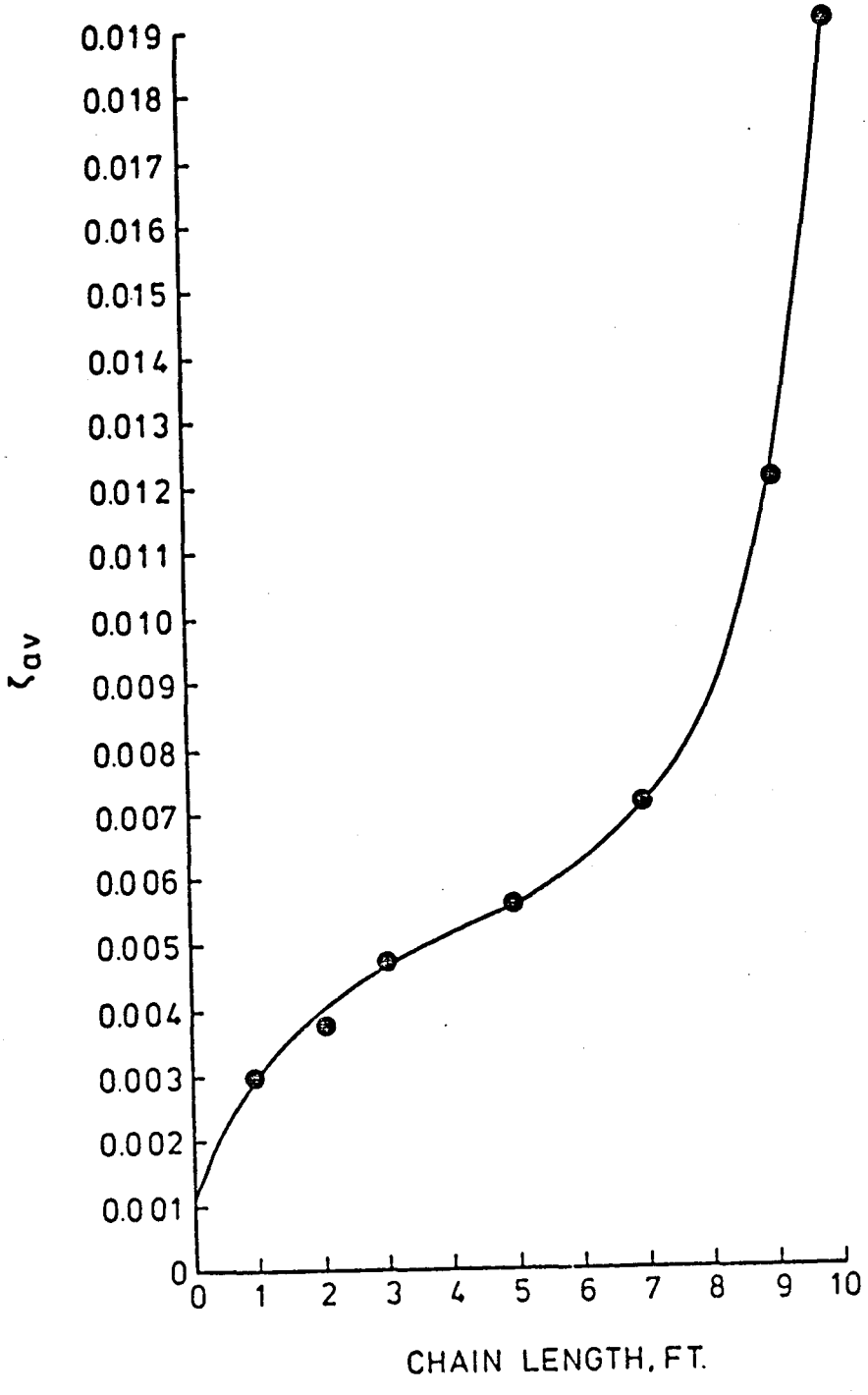

Figure 54. Effect of Chain Length on Average Damping Ratio.

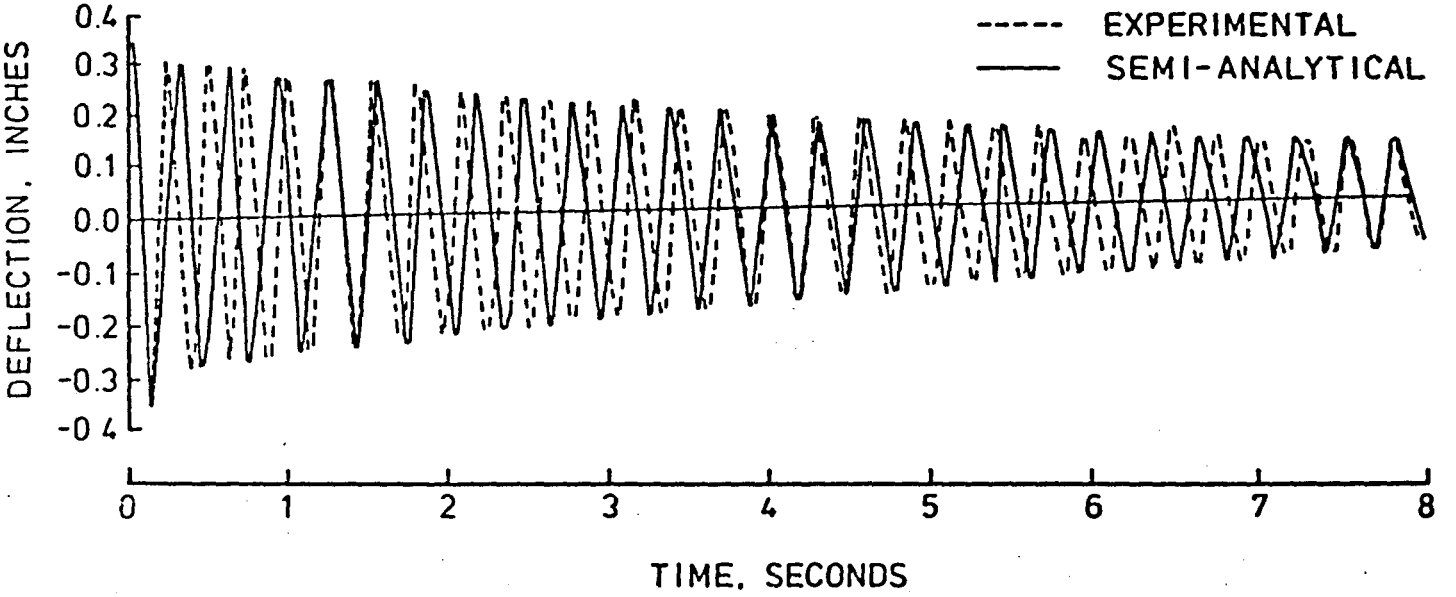

Figure 55. Comparison of Experimental and Semi-Analytic Δ-t plots for Test 52, String-Mass Concept.

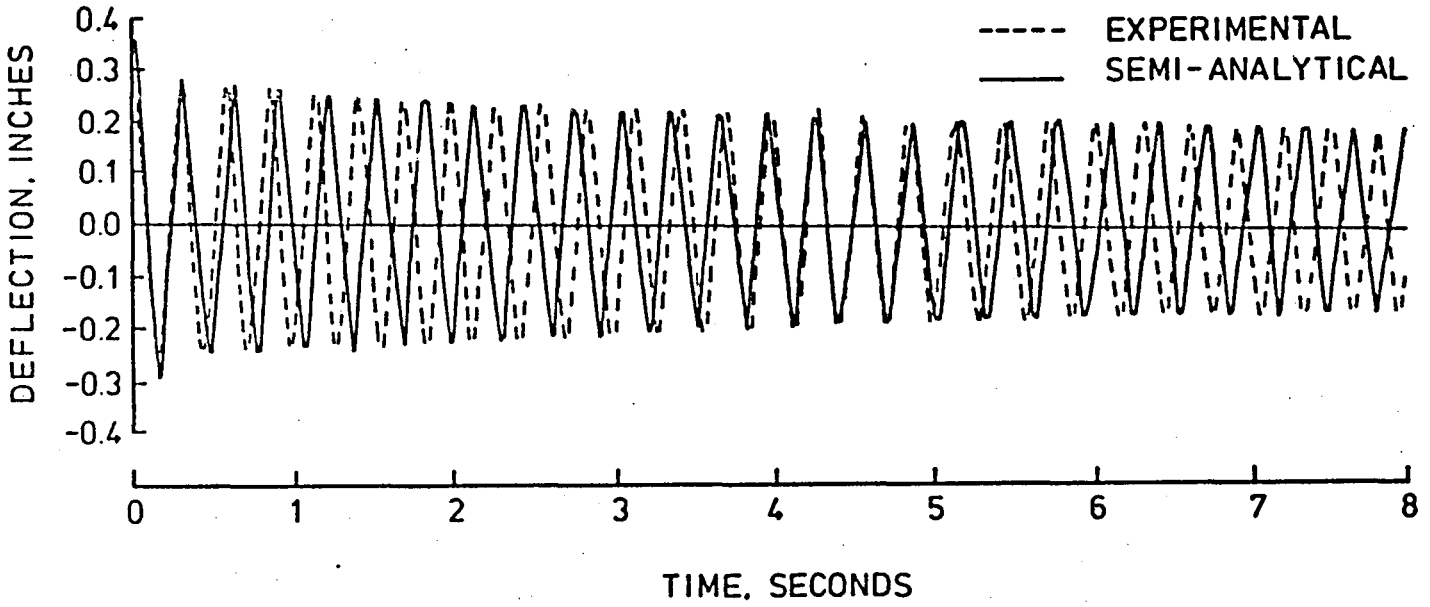

Figure 56. Comparison of Experimental and Semi-Analytic Δ-t plots for Test 76, Polyethylene Tubing Concept.

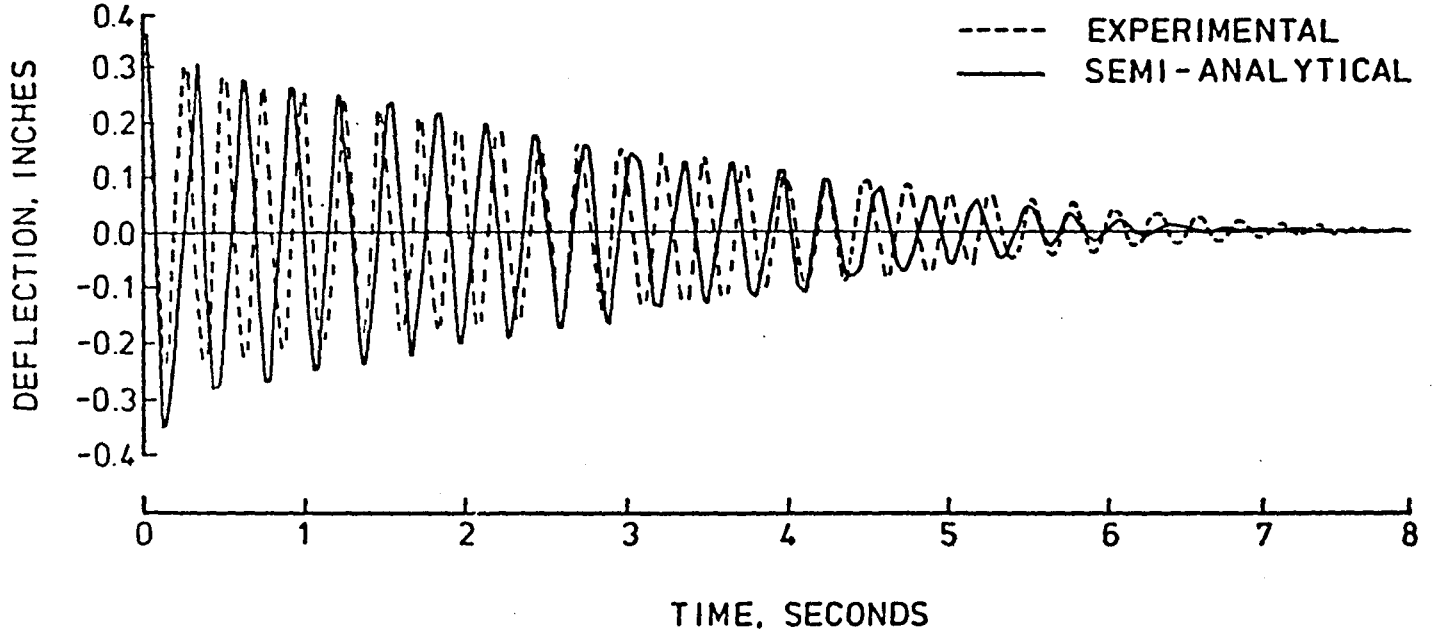

Figure 57. Comparison of Experimental and Semi-Analytic Δ-t plots for Test 103, Chain Damping Concept.

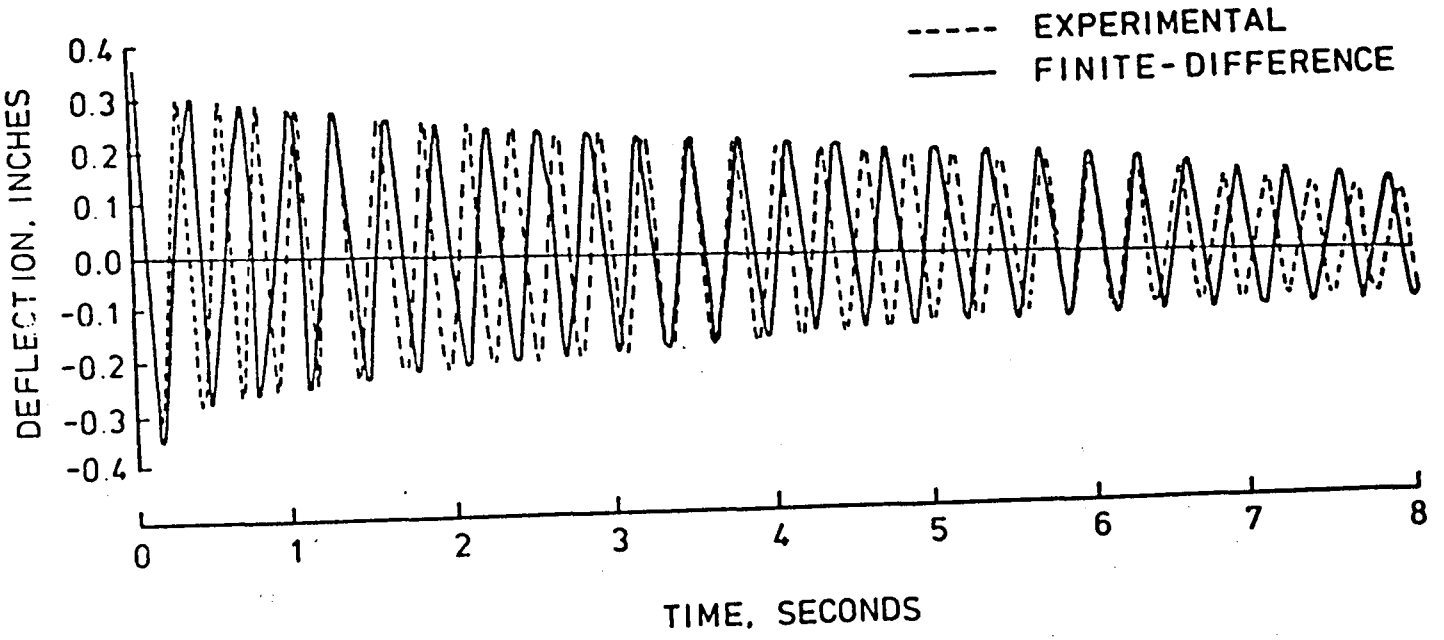

Figure 58. Comparison of Experimental and Finite-Difference Δ-t plots for Test 52, String-Mass Concept.

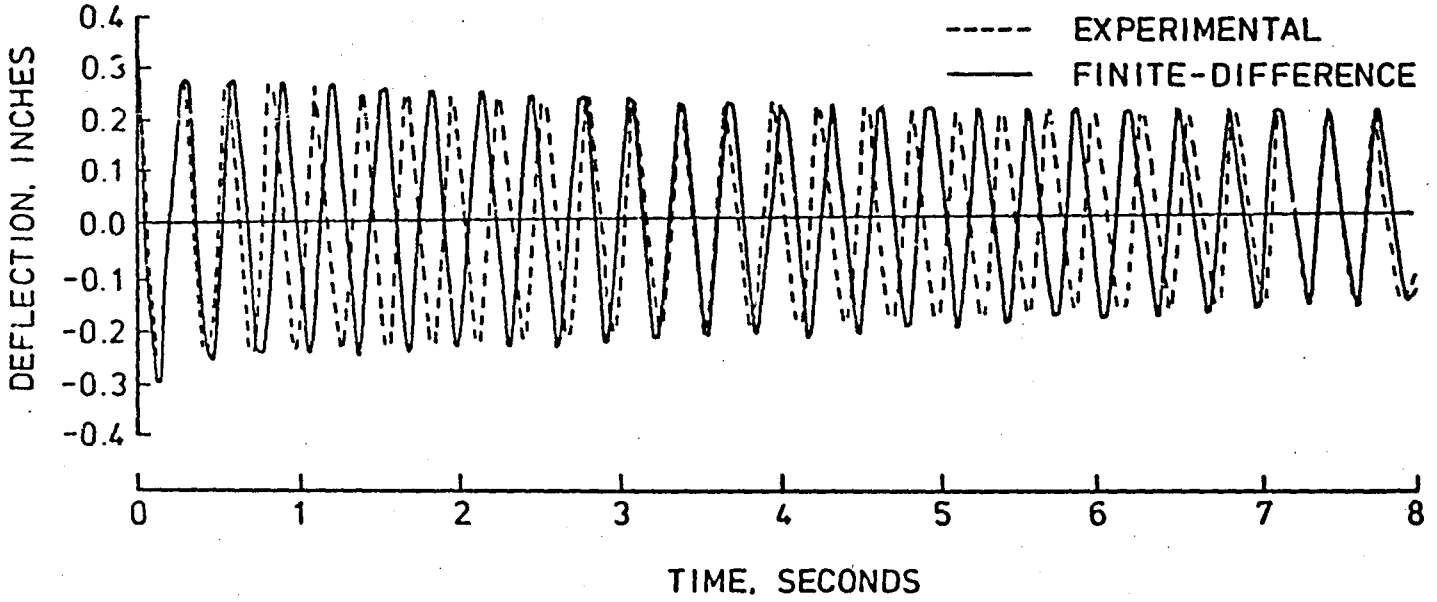

Figure 59. Comparison of Experimental and Finite-Difference Δ-t plots for Test 76, Polyethylene Tubing Concept.

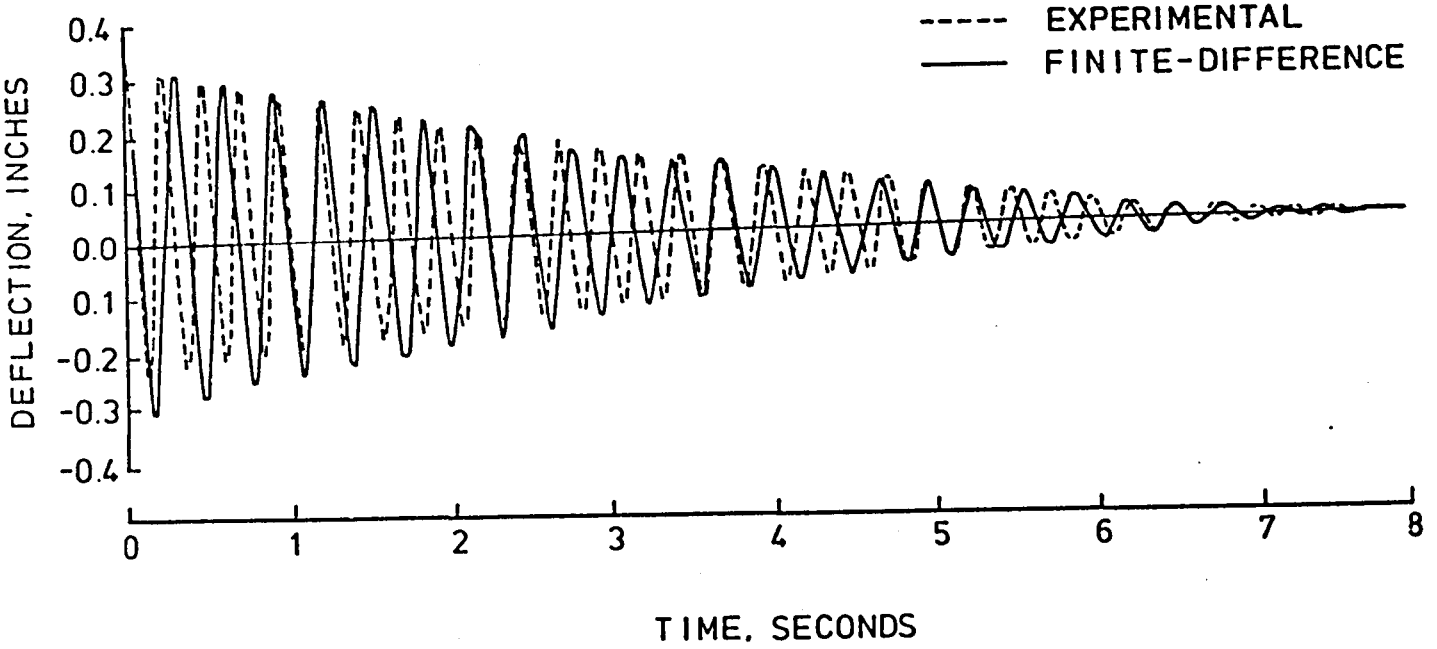

Figure 60. Comparison of Experimental and Finite-Difference Δ-t plots for Test 103, Chain Damping Concept.

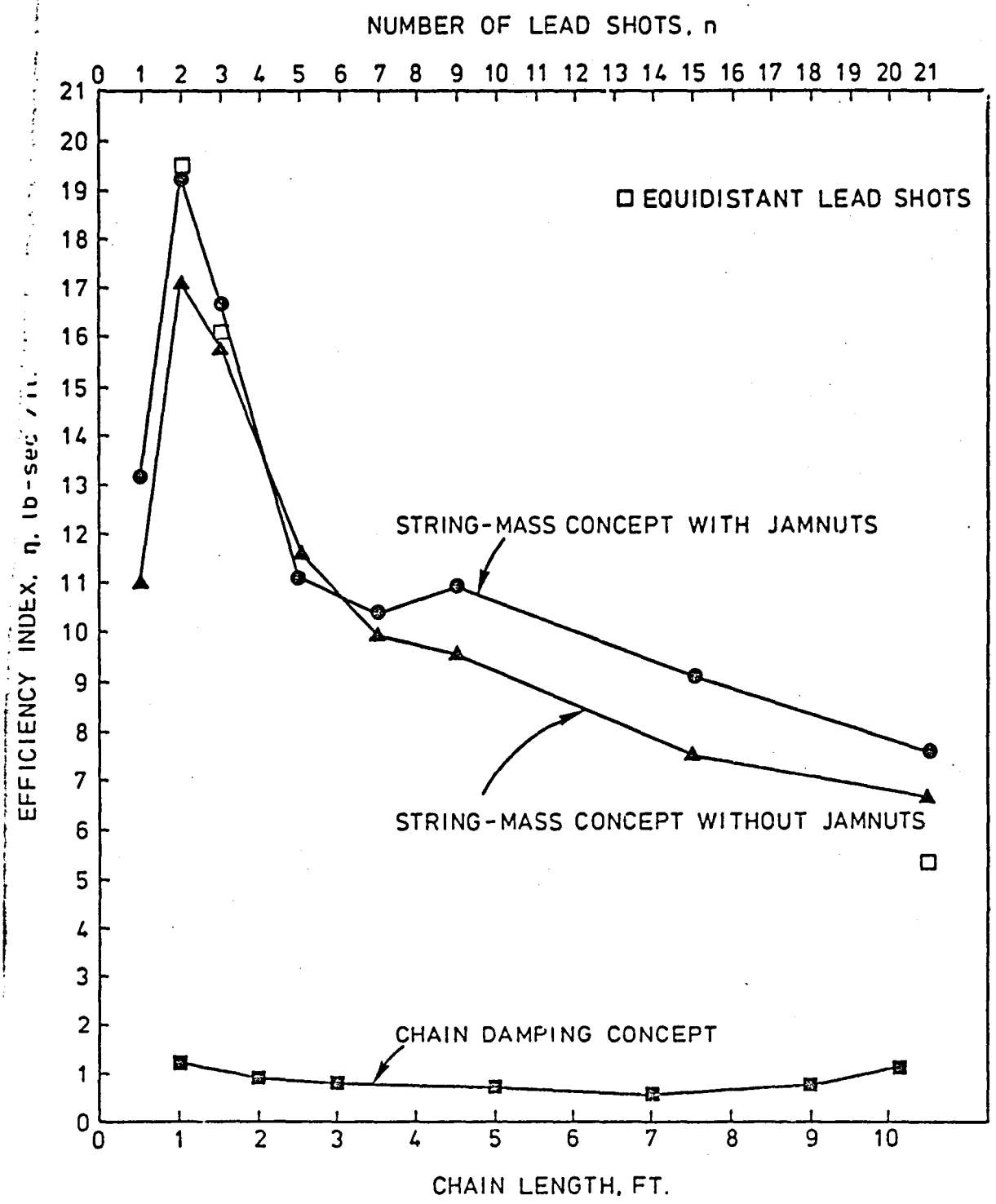

Figure 61. Efficiency Index Relationships.

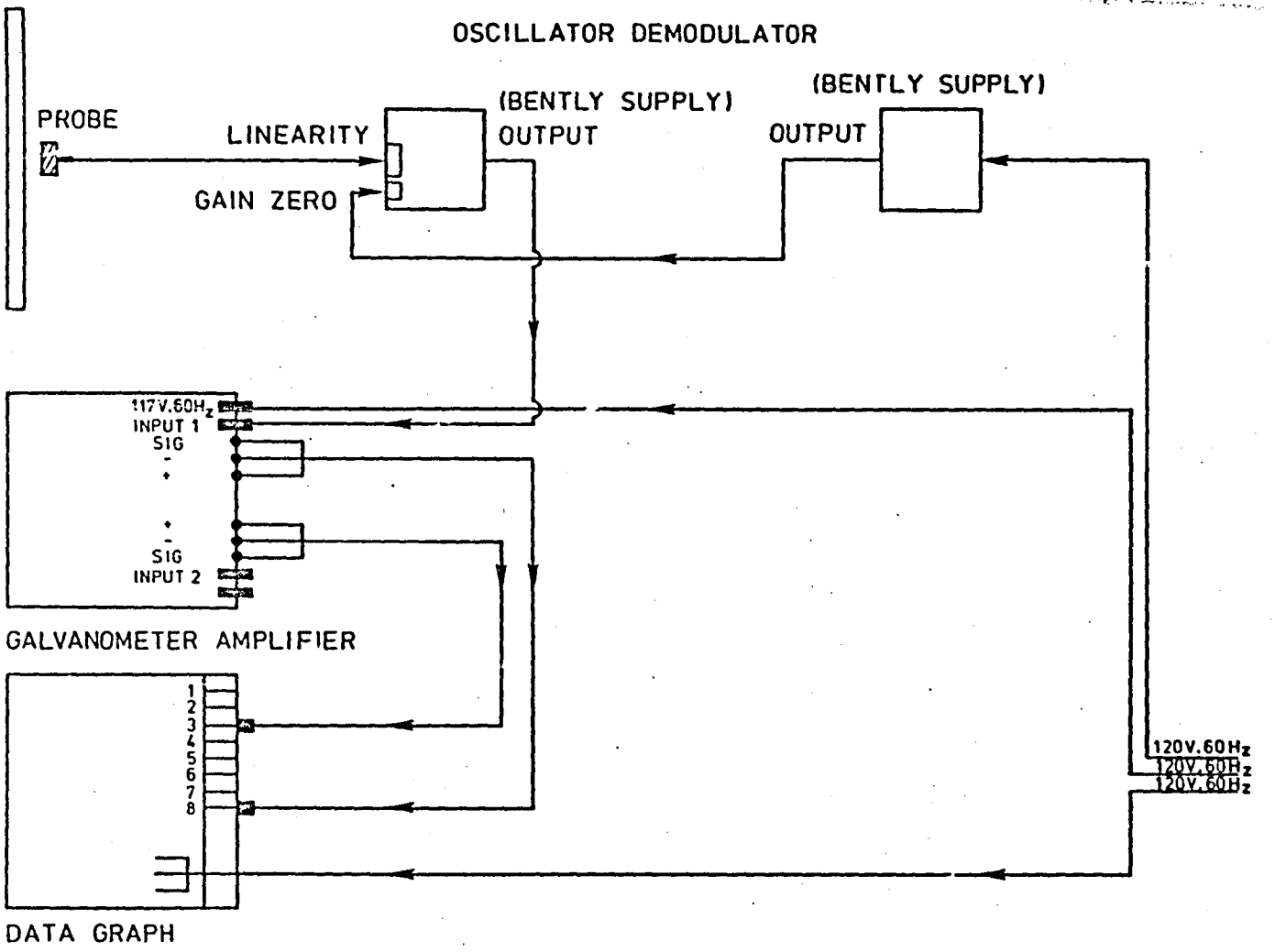

Figure 62. Circuit Diagram.

APPENDIX A

APPENDIX A

Computer Programs

Computer programs were written based on the semi-analytic and the finite-difference procedures described in Chapter II. The following are the input data for the two computer programs given in this appendix and named PARTA," and "Part B," respectively:

M — Number of nodes along the member length = 12,

E — Young's modulus = 30,000 kips/in^2,

MI — Moment of inertia = 0.00213798 in^4,

L — Length of the member = 144.0 in,

K — Rotational stiffness = 2.230 kip-in/rad,

DD — Initial member deflection = 0.366 in,

Rho — Mass per unit length = 651.0 x 10^{-10} kip-sec^2/in^2,

Zeta — Damping Ratio.

Actually the M value is not needed in Part A but is included to keep the input data for both Parts A and B identical. In Part B, the time increment Δt can be adjusted as needed by modifying the statement numbered 121 (T=T+0.001) in which Δt is taken as 0.001 secs. For example, T = T + 0.0005 may also be used. Also, to obtain the Δ-t output for t > 0.5 secs., the fifth statement above the statement numbered 121 may be modified (from DO 7 NN = 0,500,1 for t = 0.5 secs., to say, DO 7 NN = 0,7000,1 for t = 7 secs).

The output for each of the programs is:

Damping ratio

Rotational stiffness

Time and deflection at every 0.005 seconds from the start.

```
CCC                          PART A
CCC              SEMI_ANALYTICAL COMPUTER PROCEDURE
CCC      ::::::::::::::::::::::::::::::::::::::::::::::::::::
CCC      ** PROJECT: DYNAMICS OF A PARTIALLY RESTRAINED COLUMN **
CCC      ********** PROF : DR.ZIA RAZZAQ **********************
CCC      ********** BY : RAJENDRA KUMAR KHELIKAR **************
CCC      ************************************************
CCC
CCC
CCC      DEFINING  OF VARIABLES
CCC
CCC
         DOUBLE PRECISION A(20,400),X(20,1),Y(20),WF(4CCC),SS(150)
         DOUBLE PRECISION CC(500),WJ(20),WK(20),COAM,LAMD,PCR,M
         DOUBLE PRECISION B1,B2,B3,B4,B5,B6,B7,B8,B9,E,MI,ROW
         DOUBLE PRECISION L,DAM1,DAM2,PO,C1,D2,S,Z,WF,WO,P
         DOUBLE PRECISION ZZZ,YYY,PIE,ZETA,K,DD,CC
         DOUBLE PRECISION WG(4C00),R1,R2,R3,LCO,OM
         INTEGER M,I,J,KK,NN,N,IKK
CCC
CCC
CCC      READING OF VARIABLES
CCC
CCC
         DATA M,E,MI,L,K,DD/12,30000.,0.0C214796,144.,2.25,.366/
         DATA ZETA,ROW/0.5000,651.0C87E-10/
CCC
CCC
CCC      CALCULATIONS OF DAMPING COEFF
CCC
CCC
         PIE =3.1415927
         WRITE(22,123)ZETA
123      FORMAT('THE DAMPING COEFFICIENT IS'F8.3)
         WRITE(22,125)K
125      FORMAT('THE ROTATIONAL STIFFNESS IS'F8.3)
         WRITE(22,128)
128      FORMAT('THE TIME AND THE CORRESPONDING DEFLECTIONS ARE')
         DAM1=((12.DO*((PIE*E*MI)**2)*(PIE**2))/L**2)
     *    +(32.DO*E*MI*K*L*((5.DO*(PIE**2)))/(2.DO*L**2))+
     *    (3.DO*((K*L)**2)+4.DO*(PIE**2)/(L**2))
         DAM2=(12.DO*((PIE*E*MI)**2))+(32.DO*E*MI*K*L)
     *    +((9.DO*(K*L)**2)/4.DO)
         LAMD=((PIE/L)**2)*(DAM1/DAM2)
         OM=(E*MI*LAMD/ROW)
         CDAM=2.DO*ZETA*DSQRT(E*MI*RCW*LAMD)
         I=0
         T=0.
         DO 14 I=1,100,1
         ICOUNT=ICOUNT+1
         IF(ICOUNT.GT.2500)ICOUNT=2500
         T=T+.005
         R1=DSQRT(4.DO*OM-(CDAM**2/ROW**2))
         R3=1.DO+((K*L)/(2.DO*E*PIE*MI))
         R2=DO/R3
         WG(I)=DO*(DEXP(-(CDAM*T/(2.DO*ROW))))*(DCOS(R1*T/2.DO)
     *   +((CDAM/(ROW*R1))*DSIN(R1*T/2.DO)))
         WRITE(22,*)T,WG(I)
14       CONTINUE
         STOP
```

ORIGINAL PAGE IS
OF POOR QUALITY

DAMPING RATIO (ZETA) IS 0.500
ROTATIONAL STIFFNESS IS 2.230
TIME AND THE CORRESPONDING DEFLECTIONS ARE

5.000000E-03, 0.36359234245766419
1.000000E-02, 0.35675841937089732
1.500000E-02, 0.34607516684695260
2.000000E-02, 0.33210549126955565
2.500000E-02, 0.31539255379189680
3.000000E-02, 0.29645494226637371
3.500000E-02, 0.27578269234247022
4.000000E-02, 0.25383411381816543
4.500000E-02, 0.23103338186338223
5.000000E-02, 0.20776883146797169
5.500000E-02, 0.18439190347081269
6.000000E-02, 0.16121668308238776
6.500000E-02, 0.13851997143343834
7.000000E-02, 0.11654183037001003
7.500000E-02, 9.5486541208840341E-02
8.000000E-02, 7.5523919371253097E-02
8.500000E-02, 5.6790928634508939E-02
9.000000E-02, 3.9393541085337297E-02
9.500000E-02, 2.3408791642903733E-02
0.1000000, 8.8869791536118727E-03
0.1050000, -4.1460305314922878E-03
0.1100000, -1.5686440478508267E-02
0.1150000, -2.5750134835483353E-02
0.1200000, -3.4370300678196144E-02
0.1250000, -4.1595089157759719E-02
0.1300000, -4.7485342770128493E-02
0.1350000, -5.2112405554311661E-02
0.1400000, -5.5556046438532434E-02
0.1450000, -5.7902498249376428E-02
0.1500000, -5.9242631147522286E-02
0.1550000, -5.9670267907157456E-02
0.1600000, -5.9280647117929573E-02
0.1650000, -5.8169037808137475E-02
0.1700000, -5.6429506647467103E-02
0.1750000, -5.4153836790656145E-02
0.1800000, -5.1430595570203245E-02
0.1850000, -4.8344346633635125E-02
0.1900000, -4.4975000743144337E-02
0.1950000, -4.1397298304452952E-02
0.2000000, -3.7680415757359525E-02
0.2050000, -3.3887687230734003E-02
0.2100000, -3.0076432326551110E-02
0.2150000, -2.6297880536694914E-02
0.2200000, -2.2597182597803331E-02
0.2250000, -1.9013499037981122E-02
0.2300000, -1.5580156249222961E-02
0.2350000, -1.2324860615306887E-02
0.2400000, -9.2699615214163964E-03
0.2450000, -6.4327544538943741E-03
0.2500000, -3.8258158519354138E-03
0.2550000, -1.4573627212199290E-03
0.2600000, 6.6837462999505175E-04
0.2650000, 2.5507643163241710E-03
0.2700000, 4.1923845970754929E-03
0.2750000, 5.5986361422841912E-03
0.2800000, 6.7773606891772667E-03

0.2850000, 7.7384703046350444E-03
0.2900000, 8.4935903668663867E-03
0.2950000, 9.0557227970485300E-03
0.3000000, 9.4389215144204261E-03
0.3050000, 9.6579995606688267E-03
0.3100000, 9.7282518449485841E-03
0.3150000, 9.6652050022535616E-03
0.3200000, 9.4843914370596397E-03
0.3250000, 9.2011482424496712E-03
0.3300000, 8.8304408429123143E-03
0.3350000, 8.3867109067131527E-03
0.3400000, 7.8837478106821786E-03
0.3450000, 7.3345827155084403E-03
0.3500000, 6.7514041218517067E-03
0.3550000, 6.1454936251132054E-03
0.3600000, 5.5271804676211678E-03
0.3650000, 4.9058133991329067E-03
0.3700000, 4.2897482976185574E-03
0.3750000, 3.6863499698399517E-03
0.3800000, 3.1020065427657182E-03
0.3850000, 2.5421548698321568E-03
0.3900000, 2.0113154079338930E-03
0.3950000, 1.5131350693098534E-03
0.4000000, 1.0504366147439888E-03
0.4050000, 6.2527322838021267E-04
0.4100000, 2.3898699772005989E-04
0.4150000, -1.0772988708170953E-04
0.4200000, -4.1477230465601548E-04
0.4250000, -6.8255873529[illegible]1068E-04
0.4300000, -9.1196804477[illegible]58735E-04
0.4350000, -1.1042773073[illegible]26943E-03
0.4400000, -1.2611013551788858E-03
0.4450000, -1.3843346444250337E-03
0.4500000, -1.4760959313828303E-03
0.4550000, -1.5386761632507015E-03
0.4600000, -1.5744899005143024E-03
0.4650000, -1.5860305080444625E-03
0.4700000, -1.5758292770003509E-03
0.4750000, -1.5464185710281397E-03
0.4800000, -1.5002990279892610E-03
0.4850000, -1.4399107926673906E-03
0.4900000, -1.3676087065948787E-03
0.4950000, -1.2856413382286898E-03
0.5000000, -1.1961337000403121E-03

```
CCC                          PART  B
CCC                  FINITE DIFFERENCE COMPUTER PROGRAM
CCC      ::::::::::::::::::::::::::::::::::::::::::::::::::::::::::::
CCC      ** PROJECT: DYNAMICS OF A PARTIALLY RESTRIANED COLUMN **
CCC      ********** PROF : DR.ZIA RAZZAQ **********************
CCC      ********** BY : RAJENDRA KUMAR EKHELIKAR **************
CCC      ************************************************************
CCC
CCC
CCC      DEFINING  OF VARIABLES
CCC
CCC
         DOUBLE PRECISION A(20,400),X(20,1),Y(20),WF(4000),SS(150)
         DOUBLE PRECISION CC(500),WJ(20),WK(20),CDAM,LAMD,PCR,H
         DOUBLE PRECISION B1,B2,B3,B4,B5,B6,B7,B8,B9,E,MI,ROW
         DOUBLE PRECISION L,DAM1,DAM2,PO,C1,D2,S,Z,WR,WO,P
         DOUBLE PRECISION ZZZ,YYY,PIE,ZETA,K,UC,CO
         DOUBLE PRECISION WG(4000),R1,R2,R3,LOU,OM
         INTEGER M,I,J,KK,NN,N,IKK
CCC
CCC
CCC      READING OF VARIABLES
DCC
CCC
         DATA M,E,MI,L,K,DD/12,30000.,0.00214798,144.,2.23,.366/
         DATA ZETA,ROW/0.5000,651.0087E-10/
CCC
CCC
CCC      CALCULATIONS OF DAMPING COEFF
CCC
CCC
         PIE =3.1415927
         DAM1=((12.D0*((PIE*E*MI)**2)*(PIE**2))/L**2)
     *    +(32.D0*E*MI*K*L*((5.D0*(PIE**2)))/(2.D0*L**2))+
     *    (3.D0*((K*L)**2)*4.D0*(PIE**2)/(L**2))
         DAM2=(12.D0*((PIE*E*MI)**2))+(32.D0*E*MI*K*L)
     *    +((9.D0*(K*L)**2)/4.D0)
         LAMD=((PIE/L)**2)*(DAM1/DAM2)
         OM=(E*MI*LAMD/ROW)
         T=0.0
         DT=0.001
         B3=ROW/(DT**2)
         H=L/12.D0
         IKK=0
         B1=E*MI/((H)**4)
         B5=((E*MI/(H))-K/2.D0)/((E*MI/(H))+K/2.D0)
         P=0.
         INN=800-1
        ICOUNT=0
         DO 7 NN=0,500,1
         IF(NN.NE.0)GO TO 121
         T=0.0
         GO TO 10
         TYPE*,NN,T
121      T=T+0.001
         IF (T.EQ.0.001)GO TO 20
         CDAM=2.D0*ZETA*DSQRT(E*MI*ROW*LAMD)
         B4=CDAM/DT
         C1=-1.D0/(B3+B4)
         D2=B3*C1
```

```
CCC
CCC
CCC     CALCULATIONS OF CONSTANTS(B1,B2,B3...)FOR MATRIX
CCC
CCC
        B2=P/(H**2)
        DO 31 IK=1,M-1,1
        A(IK,IK)=0.0
31      CONTINUE
        A(1,1)=6.DO*B1-2.DO*B2-2.DO*B3-B1*B5-B4
        A(M-1,M-1)=A(1,1)
        DO 30 IK=2,M-2,1
        A(IK,IK)=6.DO*B1-2.DO*B2-2.DO*B3-B4
30      CONTINUE
        DO 40 IK=1,M-2,1
        A(IK,IK+1)=B2-4.DO*B1
        A(IK+1,IK)=A(IK,IK+1)
40      CONTINUE
        DO 50 IK=1,M-3,1
        A(IK+2,IK)=B1
        A(IK,IK+2)=A(IK+2,IK)
50      CONTINUE
        IF(T.GT.DT)GO TO 90
CCC
CCC
CCC     CALCULATIONS OF INITIAL DEFLECTION(T=0.0)
CCC
CCC
10      DO  70 I=1,M-1,1
        B8=(K*L)/(4.DO*PIE*E*MI)
        YYY=FLOAT(I)
        ZZZ=FLOAT(M)
        Z=PIE*YYY/ZZZ
        WK(I)=(DD/(1.DO+B8*2.DO))*(DSIN(Z)+B8*(1.DO-DCOS(2*Z)))
70      CONTINUE
        PRINT*,WK(6)
        GO TO 7
CCC
CCC
CCC     CALCULATION OF FIRST  TIME DEFLECTION(T=0.001)
CCC
CCC
20      B5=((E*MI/12.DO)-K/2.DO)/((E*MI/12.DO)+K/2.DO)
        B6=-((DT**2)*E*MI)/(2.DO*ROW*((12.DO)**4))
        B7=-(P*(DT**2))/(2.DO*ROW*(12.DO)**2)
        B8=-(P*(DT**2))/(2.DO*ROW)
        DO 75  I=1,M-1,1
        YYY=FLOAT(I)
        ZZZ=FLOAT(M)
        Z=PIE*YYY/ZZZ
        Y(I)=-DD*((PIE**2)*SIN(Z))/(L**2)
75      CONTINUE
        J=1
        I=1
        WJ(I)=(6.DO*B6-2.DO*B7+1.DO)*WK(1)-4.DO*B6*WK(2)
     *  +(B7*WK(2)+B6*WK(3)+B8*Y(I)-B5*B6*WK(1))
        I=2
        WJ(I)=(6.DO*B6-2.DO*B7+1.DO)*WK(2)+(B7-4.DO*B6)*WK(1)
     *  +(B7-4.DO*B6)*WK(3)+B6*WK(4)+B8*Y(I)
        WJ(11)=WJ(1)
```

```
      WJ(10)=WJ(2)
      DO 80 I=3,M-3,1
      WJ(I)=B6*WK(I-2)+(B7-4.D0*B6)*WK(I-1)+(6.D0*B6-2.D0*B7
     *  +1.D0)*WK(I)+(B7-4.D0*B6)*WK(I+1)+B6*WK(I+2)+B8*Y(I)
80    CONTINUE
      J=0
      WRITE(21,111)K
111   FORMAT('THE ROTATIONAL STIFFNESS IS',F8.3)
      WRITE(21,112)ZETA
112   FORMAT('THE DAMPING COEFFICIENT IS  ',F8.3)
      WRITE(21,113)
113    FORMAT('THE TIME AND THE CORROSPONDING DEFLECTIONS ARE')
      GO TO 7
CCC
CCC
CCC  THE DEFLECTIONS AT TIME GREATER THAN THE FIRST INCREMENT
CCC
CCC
90     IKK=IKK+1
      DO 100 I=1,M-1,1
      YYY=FLOAT(I)
      Y(I)=-DD*((PIE**2)*DSIN(PIE*YYY/12.D0))/20736.D0
      SUM=0.0
      DO 122 KK=1,11
      SUM=SUM+A(I,KK)*WJ(KK)
122   CONTINUE
      WF(I)=C1*SUM+D2*WK(I)+P*C1*Y(I)
100   CONTINUE
      DO 434 I=1,M-1,1
      WK(I)=WJ(I)
      WJ(I)=WF(I)
434   CONTINUE
      IF(IKK.EQ.5)WRITE(21,*)T,WF(6)
      IF(IKK.EQ.5)IKK=IKK-5
7     CONTINUE
      STOP
      END
```

ROTATIONAL STIFFNESS IS 2.230
DAMPING RATIO (ZETA) IS 0.500
TIME AND THE CORROSPONDING DEFLECTIONS ARE

6.000000E-03, 0.36054476463188740
1.100000E-02, 0.34857072755345545
1.600000E-02, 0.33162699151269795
2.100000E-02, 0.31530570391608760
2.600000E-02, 0.30050586557196719
3.100000E-02, 0.28609830892547833
3.600000E-02, 0.27068924323488135
4.100000E-02, 0.25393064779027415
4.600000E-02, 0.23485013350048578
5.100000E-02, 0.21162899446399367
5.600000E-02, 0.18647207550126029
6.100000E-02, 0.16164118546252522
6.600000E-02, 0.13868620961410036
7.100001E-02, 0.11752472410034994
7.600001E-02, 9.9007931338576875E-02
8.100001E-02, 8.3008974406320450E-02
8.600001E-02, 6.7720775151456077E-02
9.100001E-02, 5.1912716058674933E-02
9.600001E-02, 3.5830642709889558E-02
0.1010000, 2.0420828203189287E-02
0.1060000, 5.5902220362889078E-03
0.1110000, -7.6091531849992118E-03
0.1160000, -1.8267619196329048E-02
0.1210000, -2.6108876511530570E-02
0.1260000, -3.2279890773252890E-02
0.1310000, -3.7482539331563384E-02
0.1360000, -4.1784335416689278E-02
0.1410000, -4.5865108240862084E-02
0.1460000, -4.9844546924170027E-02
0.1510000, -5.3389754019614770E-02
0.1560000, -5.5533980915243934E-02
0.1610000, -5.6284231479307660E-02
0.1660000, -5.5840706623869854E-02
0.1710000, -5.4272045119545639E-02
0.1760000, -5.1883400067909164E-02
0.1810000, -4.9319930910300411E-02
0.1860000, -4.7083350805277556E-02
0.1910000, -4.4911758546984864E-02
0.1960000, -4.2636078266074988E-02
0.2010000, -4.0126124717278613E-02
0.2060000, -3.7321025546103294E-02
0.2110000, -3.3904044397488813E-02
0.2160000, -3.0047934972127446E-02
0.2210000, -2.6192254523735046E-02
0.2260000, -2.2563345224884545E-02
0.2310000, -1.9251064694634659E-02
0.2360000, -1.6262909566642753E-02
0.2410000, -1.3726879576359136E-02
0.2460000, -1.1349695836278238E-02
0.2510000, -8.9171810388278820E-03
0.2560000, -6.4150649928605O1E-03
0.2610000, -3.9737740220321239E-03
0.2660000, -1.6511297644617666E-03
0.2710000, 4.9673235270985887E-04
0.2760000, 2.2552525356390655E-03
0.2810000, 3.5855079085586629E-03

0.2860000, 4.5970635743793307E-03
0.2910000, 5.4557387212990898E-03
0.2960000, 6.1707471795620414E-03
0.3009999, 6.8213707394299620E-03
0.3059999, 7.4645525538175598E-03
0.3109999, 8.0553550768267363E-03
0.3159999, 8.4686949717737365E-03
0.3209999, 8.6390865653595872E-03
0.3259999, 8.6312933065495976E-03
0.3309999, 8.4358876112904440E-03
0.3359999, 8.1048616373026998E-03
0.3409999, 7.7148725016753971E-03
0.3459999, 7.3655721062142660E-03
0.3509999, 7.0463235113024418E-03
0.3559999, 6.7035113427910724E-03
0.3609998, 6.3352377532903728E-03
0.3659998, 5.9164013869270539E-03
0.3709998, 5.4190858062857680E-03
0.3759998, 4.8337217997208073E-03
0.3809998, 4.2344126759690297E-03
0.3859998, 3.6657578003130615E-03
0.3909998, 3.1426644653173225E-03
0.3959998, 2.6689783915879129E-03
0.4009998, 2.2597661755809085E-03
0.4059998, 1.8921748153578975E-03
0.4109998, 1.5159370075395461E-03
0.4159998, 1.1294633324869032E-03
0.4209997, 7.4361579156653096E-04
0.4259997, 3.7854482535022735E-04
0.4309997, 3.4678715077558187E-05
0.4359997, -2.5676591223203829E-04
0.4409997, -4.7882110914292085E-04
0.4459997, -6.4849407938908323E-04
0.4509997, -7.8690128760139707E-04
0.4559997, -9.0738161789819987E-04
0.4609997, -1.0110861058975071E-03
0.4659997, -1.1143984379016757E-03
0.4709997, -1.2119705912067364E-03
0.4759996, -1.2866509999497057E-03
0.4809996, -1.3242284279772367E-03
0.4859996, -1.3303860044744655E-03
0.4909996, -1.3095775492935182E-03
0.4959996, -1.2637225988351805E-03

APPENDIX B

APPENDIX B

Instrumentation and Test Setup

A brief description of the instrumentation and test setup used for nducting the vibration experiments described in Chapter III is given here. gure 10 shows a system consisting of a probe, vibration instrumentation, id a deflection-time curve plotter schematically. A brief description of ie system components is described in Section B.1 of this appendix, while he procedure for setting up the test apparatus is outlined in Section B.2.

.1 Instrumentation

The principal components of the instrumentation and their respective unctions are described below:

1. Probe or sensor, and oscillator demodulator.

   This component of the system is manufactured by Kaman Measuring Instruments (Model KD 2300-10C). The probe consists of a variable impedence bridge with an active and a reference coil. The variation of impedence results from the eddy currents induced in nearly conductive surfaces. The probe gives exceptional accuracy for non-contacting measurements of conductive surface motions. It has a high capability for linear calibration within ± 1.0 percent deviation with almost any metal or alloy, whether flat or curved. Adjustment controls are provided such that the output voltage is readily calibrated so that it is directly proportional to the displacement and has a wide frequency response (0.20 KHz, 1db point; and 0.5 KHz, -3dB point).

   The stability is affected by the target material such as a magnetic material. It works very well when the target is near the face of the sensor. The movement of the cable connecting the

sensor and the oscillator demodulator, the dielectric constant, sensitivity to noise, temperature, humidity, and the magnetic field are all greatest when the target is at its full scale displacement. Linearity is not observed when the distance of the target from the sensor is within 10 percent of the full scale displacement. The probe converts the displacement of the conductive surface into an output voltage.

2. Galvanometer amplifier and data graph.

The main function of the galvanometer amplifier is to accept the signal from the transducers, that is, from the probe and the oscillator demodulator which translate mechanical variation into electrical impulses, and is conditioned before sending the signal into the data graph. The amplifier is uniquely designed to facilitate the recording of the signal voltage in a light beam oscillograph. The amplitude of the output signal voltage that can be accommodated by the amplifier ranges from 0.1 to 300 volts with 0.5 to 3 inches peak galvanometer deflection with proper setting of volts/in., gain, and the offset knobs.

The oscillator demodulator removes the carrier frequency from the envelope and extracts only the signal frequency that is to be fed into the galvanometer amplifier.

The data graph consists of five knobs which control the output graph.

a. Power on/off, to be connected to a 230V, 60 Hz power supply.

b. Light intensity knob, to control the intensity of the light from the recording lamp to the galvanometer.

c. Paper speed knob, to control the speed of the photographic film. The speed range is 0.1 to 100 in/sec., selected in steps of 0.1, 0.2, 0.5, 1.0, 2.0, 5.0, 10, 20, 50, and 100 in/sec.

d. Gridline knob, consisting of two push button switches to provide "fine" (0.1 in.) and "coarse" (0.5 in.) gridline spacings, respectively.

e. Transport knob, consisting of two interlocked push buttons to actuate the paper drive. One is a locking type used to activate a continuous run. The other provides a "stop" function as well as a momentary run or "jog" function.

Electrical impulses produced by the transducers may be fed into an amplifier where the signal is conditioned before being introduced into the oscillograph. The signal is then applied to a highly sensitive galvanometer in the oscillograph. Light from a mercury arc or xenon lamp is reflected by the galvanometer mirror through a simple optical system which produces a spot of light on a moving strip of photographic material. By using various combinations of light intensity and record speed, clear legible records are attainable over a wide range of applications.

B.2 Test Setup

The steps given below are followed for setting up the test apparatus:

1. Connect the instruments as shown in the schematic circuit diagram as shown in Fig. 62.
2. A 120V, 60Hz power is supplied to the galvanometer amplifier, datagraph and the oscillator demodulator.
3. Pull the specimen by approximately 0.75 in. from the probe and adjust the three knobs of the galvanometer amplifier such that the

maximum deflection on the datagraph is approximately one-and-a-half inches from the center. Adjust the volts/in and the gain knobs to their maximum values, and the offset knobs at zero to obtain the desired output.

4. Adjust the datagraph knobs by setting the paper speed to 2 in/sec for low frequencies, and select the light intensity to obtain an appropriate thickness of the line describing the Δ-t plot. Fine gridlines are usually preferred for a good quick reference.
5. The specimen is pulled away or towards the probe by means of a nylon string. The specimen is then released by burning the string with a matchstick to induce natural vibration. Before burning the string, the datagraph switch button "run" is pushed to start.
6. The datagraph is made to run for 8-10 seconds or 20 inches of the plotting paper to get the desired output.

END

DATE

FILMED

DEC 5 1985

End of Document